

DEVELOPMENT OF INNOVATIVE MULTICOMPARTMENT
MICROFLUIDIC PLATFORMS TO INVESTIGATE
TRAUMATIC AXONAL INJURY

by

BHASKAR GANESH CHENNURI

A thesis submitted to Johns Hopkins University in conformity with the requirements for
the degree of Master of Science in Engineering.

Baltimore, Maryland

October, 2014

© 2014 Bhaskar Ganesh Chennuri
All Rights Reserved

Abstract

Compartmentalization of cell body from the axon of a neuron is an important aspect in studying the influence of microenvironments. Microenvironment is an integral part of neuronal studies involving traumatic axonal injuries (TAI). While TAI is one of the possible outcomes of various forms of traumatic insults to the central nervous system (CNS) and peripheral nervous system (PNS), many of the mechanistic details are still unknown, it can be agreed that the level of injury often dictates the functional deficit. This motivates the question, what is occurring at both the morphological and biomolecular scale in CNS and PNS axons during and throughout the recovery phase after injury? And, are there any treatment strategies that could be applied to improve the recovery and regeneration of the axons subject to TAI? Motivated by this, I propose to develop novel microfluidic platforms as a part of my master's thesis to allow unprecedented, physiologically relevant focal and graded mechanical injury and observation to both CNS and PNS axons.

My research for this thesis can be broadly classified into two fold. 1) I examined the regenerative effects of the members of the Glial cell line-derived neurotrophic factor (GDNF), a family of neurotrophic factors after axotomy. This work resulted in the discovery of the fact that GDNF is the most potent neurotrophic factor among the family of growth factors for axon regeneration in dorsal root ganglion (DRG) neurons after in vitro axotomy. It was also found that GDNF locally applied to cell body better promotes axonal regeneration in comparison to when applied locally to axons. 2) Development and

refinement of existing axon injury microplatform (AIM) to closely mimic physiological conditions during traumatic injury in CNS neurons. This work was my attempt in improving already existing microfluidic compression platform. I successfully developed a displacement control injury device and demonstrated displacement control as a proof of principle. Further development of these microfluidic platforms will significantly contribute to the field of basic neuroscience, neurobiology, and biomedical engineering.

Primary Reader: Nitish V. Thakor, Ph.D.

Thesis Committee

Nitish Thakor, Ph.D. (primary advisor, reader)

Department of Biomedical Engineering,

Johns Hopkins University

Arun Venkatesan, M.D., Ph.D. (advisor, reader)

Department of Neurology,

Johns Hopkins University

Hai-Quan Mao, Ph.D (reader)

Department of Materials Science and Engineering,

Johns Hopkins University

Acknowledgments

In retrospect, my time as a graduate student at Johns Hopkins has been one of the greatest experiences, a milestone of my life. Hopkins nurtured me, who was once just a naïve and freshly graduated student, into an academic, a leader, a teacher/mentor, a friend, and most importantly as an individual. Hopkins has been the cradle and provided a fantastic fostering environment for my present self and I am forever indebted to this university for aiding in my personal development.

I have to mention about my family here. My existence as an individual today and as the one sharing these views, it is all made possible by my wonderful family. My family is the most important part of my life: my father, mother, sister, and my baby nephew constitute my family. My parents are incredibly knowledgeable, thoughtful, caring, and loving people. They supported me in all my decisions, which are more often than not, whimsical. Never once in my life have I been told I could not achieve something, nor have I ever been talked out of pursuing my dreams. They had to part with and send me half way around the world, across continents and oceans for me to achieve this. This is one amongst the countless and incredible sacrifices they made. They were my anchor when I was sailing through rough waters, and I am sure they will continue to be the same in future. Speaking of my sister, she believes and always considers that her sibling is very knowledgeable, whatever I may be in reality, I will never be able to match her in her empathy in this lifetime. And the newest addition to the family, my baby nephew. He is just adorable and my stress buster. He elevates my mood in a jiffy.

Now I must progress onto Hopkins, so let's start with my advisor. I would like to sincerely thank Prof. Nitish Thakor for considering me as a student under his able guidance. Coming into the program, I was very timid and shy when it came to speaking up or making my presence known. Also there was this cultural shock which pushed me further into a corner. Today, I can say with great confidence that I am very far off from where I have started. The path projected me into a new dimension where I am constantly trying to better myself. This credit goes to Prof. Thakor, he was very patient and understanding when it came to my above mentioned limitations. He was very kind, understanding, and forgiving when I was having troubles even in the personal sphere of my life. Furthermore, I would like to thank him for making me realize the importance of seeing the bigger picture, allowing me to pursue my academic curiosities (often at my own peril), and letting me grow as an individual. Next, I would like to sincerely thank Dr. Arun Venkatesan for taking me in his lab in the Department of Neurology and providing me with all the cell culture techniques I know, and he allowed me to really grasp basic science, to which I am indebted. Johns Hopkins is an incredibly collaborative environment, and as such I have been blessed to be a member of not only Prof. Thakor and Dr. Venkatesan's lab, but also the labs of Dr. Mao, and Dr. Hoke. I am very grateful to have such amazing faculty members that are willing to take time and speak to me about research, life, and anything else I want to bring up. I hope they are happy with the thesis I have written.

Last but not the least, I would like to thank my friends, colleagues, and acquaintances from Hopkins. I have had the pleasure of entering the M.S.E. program with a great class of people and have since met many other fascinating people across different

classes, departments, institutions, and even nationalities. I have made such wonderful friends here and shared many wonderful moments that I wish they last for a lifetime. I would like to specially thank my friends Kalpana Besar, Fozia Ahmed, Maryam Parsaee, Samira Parsaee, Harish Mallidi, Meher, Yeleti, and Vijay Aditya Peddinti. They constituted my family away from home, providing me with immense support. Now let me talk about my colleagues and friends from labs and my acquaintances. As you can imagine, this is an exhaustive list in which I would like to thank: From Dr. Thakor's Lab: Dr. Suneil Hosmane, Dr. Rezina Siddique, Dr. Abhishek Rege, Dr. Heather Benz, Elliot Greenwald, Janaka Senarthana, Cheng Chen, Dr. In Hong Yang, and all the new students; From Dr. Venkatesan's Lab: Labchan Rajbhandari, Dr. Million Tegenge, and Shiva Shrestha. From Dr. Hoke's lab: Aysel. From Dr. Mao's Lab: Kellin Krick, and Markus Tammia. From Dr. Wang's Lab: Dr. Tushar Rane, Helena Zec, and Dong Jin; From K. T. Ramesh's Lab: Dr. Adam Fournier. From Dr. Sarma's lab: Rahul Aggarwal. Academic advisor Samuel Bourne and the Biomedical Engineering Students (too many to count), all the employees of the Biomedical Engineering Program, and Taylor 7 Maintenance Crew. Thank you!

For all her sacrifices and many more to come, I would like to dedicate this thesis to my mother, without her this would have never been a reality.

Contents

Abstract	ii
Acknowledgments	iv
List of Tables	xii
List of Figures	xiii
1 Chapter 1: Introduction	1
1.1 Compartmentalized studies of axons and soma.....	2
1.2 Microtechnology in neurobiology and neuroscience.....	3
1.2.1 Microfluidic platforms for <i>in vivo</i> injury models.....	6
1.2.1.1 Injury mode: Physical.....	6
1.2.2 Microfluidic platforms for <i>in vitro</i> injury models.....	7
1.2.2.1 Injury mode: Physical.....	7
1.2.2.2 Injury mode: Chemical.....	8
1.3 Specific Aims.....	10
1.4 Organization of the Thesis.....	10
2 Chapter 2: Microfluidic Multi-Compartment Chamber Devices in Neuroscience and Neuroengineering	12
2.1 Introduction.....	12
2.2 Fabrication.....	14
2.2.1 Design and Fabrication Techniques.....	15
2.2.2 Modelign and Simulations.....	17
2.3 Multi-compartment Chamber devices in Neuroscience and Neuroengineering.....	23

2.3.1	Multi-compartment Chamber devices for axon guidance.....	25
2.3.2	Multi-compartment Chamber devices for axonal biochemical analysis and assays.....	31
2.3.3	Multi-compartment Chamber devices for Co-culture.....	35
2.3.4	Multi-compartment Chamber device for Injury, Regeneration, and Degeneration.....	37
2.3.5	Multi-compartment Chamber device for Electrical Stimulation and Recording.....	40
2.3.6	Multi-compartment Chamber devices from our group.....	42
2.3.6.1	Circular Compartmentalized co-culture device for axon-glia interactions.....	42
2.3.6.2	Circular Compartmentalized device for microglial phagocytosis of axons.....	50
2.3.6.3	Valve based multi compartmental device for Traumatic Axonal Injuries.....	56
2.4	Discussion and Future Directions.....	62
3	Chapter 3: A compartmentalized culture platform to study axon regeneration and localized effects of GDNF.....	65
3.1	Introduction.....	65
3.2	Materials and Methods.....	67
3.2.1	Cell preparation.....	67
3.2.2	Compartmentalized microfluidic platform (CMP) preparation.....	68
3.2.3	Cell loading.....	69

3.3	Results.....	69
3.3.1	Theoretical Profile of Growth Factor Diffusion.....	69
3.3.2	Computational Simulations to Study Diffusion Patterns of Growth Factors.....	73
3.3.3	Restriction of diffusion analytes.....	74
3.3.4	Axotomy and axonal regeneration by neurotrophic factors.....	75
3.4	Discussions.....	79
3.5	Conclusions.....	81
4	Chapter 4: A Novel 3-Dimensional In Vitro Platform to Study Focal and Repetitive Axonal Injury.....	83
4.1	3D AIM platform.....	83
4.1.1	Introduction.....	83
4.1.2	Materials and Methods.....	87
4.1.2.1	Fabrication of the master template and molds.....	87
4.1.2.2	Fabrication of the gel substrate and establishment of the gradient.....	88
4.1.2.3	Assembly of modified device.....	89
4.1.2.4	Cell preparation and loading.....	90
4.1.3	Results.....	90
4.1.3.1	Establishment of stable soluble gradients in gels in ECM devices.....	90
4.1.3.2	Compatibility between hydrogels and cells.....	92
4.1.3.3	Culture in the modified injury platforms.....	93

4.1.4	Discussions.....	94
4.1.5	Conclusions.....	96
4.2	Displacement control device.....	98
4.2.1	Introduction.....	98
4.2.2	Materials and Methods.....	99
4.2.2.1	Fabrication and assembly of injury platform.....	99
4.2.3	Results.....	100
4.2.3.1	Incorporation of the notch layer in master template.....	100
4.2.3.2	Finite Element Method (FEM) Modeling and notch design.....	101
4.2.3.3	Valve operation, stability, and notches.....	105
4.2.3.4	Imaging neurofilaments and microtubules.....	106
4.2.4	Discussions.....	107
4.2.5	Conclusions.....	110
5	Chapter 5: Conclusions.....	111
5.1	Contributions from Aim 1.....	111
5.1.1	Technical and Scientific Achievements.....	111
5.1.2	Dissemination of original research.....	112
5.2	Contributions from Aim 2.....	112
5.2.1	Technical and Scientific Achievements.....	112
5.2.2	Dissemination of original research.....	114
5.3	Future directions.....	114
5.3.1	Neurotrophic factors and functional nerve regeneration.....	115
5.3.2	Secondary Injury and axonal transportation.....	116

5.3.3 Hybrid and <i>in vivo</i> microfluidic technologies.....	118
A Photolithography Protocol.....	119
B SU8 spin protocols.....	120
C SU8 Dilution.....	121
Bibliography.....	122
Vita.....	144

List of tables

1.1	Microfluidic interfaces for neuroscience and neurobiology research.....	4
3.1	Shows a list of the growth factors we used along with their molecular weights and the calculated diffusion coefficients.....	72
4.1	Experimental conditions the gels were subjected to.....	92
4.2	a. FEM simulations to determine the gap length and pedestal length, b. FEM simulations for degenerative loading for chosen gap and pedestal.....	104
4.3	FEM simulations for various notch clearances for chosen gap and pedestal lengths.....	105

List of figures

2.1	A. Schematic of photolithography technique and micro contact printing (adapted from [64] copyright 2010 Nature Publishing Group), B. Schematic of MIMIC technique (adapted from [67] copyright 1996 American Chemical Society).....	17
2.2	1a & 1b. In vitro reconstruction of a neuronal network using “axonal diodes” in microfluidic culture devices, 1c & 1d. Immunofluorescent images of microfluidic neuronal cultures either on the wide or the narrow side, 1e. Quantification axonal growth polarization (adapted from [89] with permission from The Royal Society of Chemistry), 2a & 2b. Design of the three-channel microfluidic device developed to study neurite turning in 3D scaffolds under a growth factor gradient, 2c, 2d & 2e. Neurite guidance of hippocampal neurons by chemoattractants (adapted from [92] with permission from The Royal Society of Chemistry), 3a. Schematic of micro-jets device with a central open-surface reservoir, 3b & 3c. Neuronal response to netrin (adapted from [93] with permission from The Royal Society of Chemistry), and 4a & 4b. Schematic of the channel design used and diffusion through microfluidic interconnects, 4c & 4d. Traces of neuronal process in gradients and control (adapted from [91] with permission from The Royal Society of Chemistry).....	20
2.3	1a. A schematic of the local perfusion chamber with three-inlet wells, 1b. Stable microenvironments with perfusion, 1c. Labeled neuron following perfusion (adapted from [100] copyright 2010 Elsevier), 2a. Schematic for micropatterning of PLL strip on a substrate and its integration with a compartmentalized microfluidic neuron culture device, 2b. Neurons transfected differentially in different compartments (adapted from [96] copyright 2012 American Chemical Society), and 3a. Schematic	

	of the fabrication of synapse microarray, 3b Synapsin clustering in microwells with HEK293 cells, and 3c. Enlarged view of the box (adapted from [99] copyright 2011 Nature Publishing Group).....	34
2.4	A. Schematic of the co-culture device for sympathetic neurons and cardiomyocytes, 1b SCG neurons in left compartment and 1c. Ventricular myocytes in the right compartment (adapted from [58] with permission from The Royal Society of Chemistry), 2a. Schematic of the multi-compartment neuron–glia co-culture microsystem capable of carrying out multiple localized axon treatments in parallel, 2b, 2c & 2d. Depict axon glia co-culture separated by microchannels, and 2e. Depicts the reproducibility (adapted from [103] with permission from The Royal Society of Chemistry), 3a & 3b. Schematic of device that allows co-culture and separation with valves, 3c & 3d. Neurons in adjacent compartments transfected with different vectors (adapted from [59] copyright Elsevier 2010).....	37
2.5	1a. Microfluidic-based culture platform with illustrations of laser induced axotomy, 1b. Axotomy of 25 μm axon strips with 180 ps laser pulse (adapted from [107] with permission from The Royal Society of Chemistry). 2a. Schematic of the microfluidic device to study chemical injury, 2b & 2c. Chemical influenced degradation of axons with axonal side application of the chemical (adapted from [25] copyright Elsevier 2009), 3a & 3b. Schematic of the microfluidic culture platform for compartmentalization and fluidic isolation of axons from cell body (adapted from [106] copyright Nature Publishing Group 2005).....	40
2.6	1a. Schematic of integrated compartmented culture system, with microfluidic barriers and microelectrode array interfacing with cultured neurons. The multicompart	

divider is aligned to and seated on the microelectrode array. Neurons are then plated in one or more of the compartments, after which they grow into adjacent compartments. Stimulation and recording electrodes on the microelectrode array interface with somal bundles and their processes in all of the compartments, allowing for complicated studies in which both neuronal pharmacology and electrophysiology can be simultaneously studied. (Adapted from [110] copyright Elsevier 2006), 1b. Conceptual sketches of the Artificial Synapse Chip. With an illustration of a single stimulation site and a multiple pixel device shown interfacing the retina. (Adapted from [111] copyright John Wiley and Sons 2003).....42

2.7 3D schematic of the PDMS device with compartments and microchannels in the side to aid visualization (adapted from [16] with permission from The Royal Society of Chemistry).....43

2.8 The device mold was constructed using standard SU-8 photolithography. (A) Beginning with a bare silicon wafer, (B) an initial thin-film resist layer (SU-8 2002; height $\frac{1}{4}$ 2.5 mm) was spun, soft baked, and optically exposed. (C) Subsequently, the substrate was post exposure baked and immersed in developer to define the circular array of microchannels. (D & E) The thick-film resist (SU-8 3050; height $\frac{1}{4}$ 150 mm) was processed similarly to define larger fluidic access ports. After (F) PDMS replication, (G) devices were customized through the use of commercially available dermal biopsy punch tools. (Reproduced from [16] with permission from The Royal Society of Chemistry).....49

2.9 Microfluidic platform enables the study of microglial phagocytosis of axons. **Ai**, A patterning process was used to create 25 μ m-wide PDL stripes interspersed by 25 μ m

gaps. **Aii**, The microfluidic coculture device was aligned and bonded. **Aiii**, **Aiv**, Neurons cultured within the cell body compartment extended axon bundles through the microchannels and into the axon/glial coculture compartment (**Aiii**) where microglia were later cocultured (**Aiv**). **B**. The microfluidic platform was modified by creation of a third compartment. Before addition of wild type or TRIF knock out mouse microglia, a scalpel was used to sever a 10 –20 μm segment of the bundle. (Adapted from [114] copyright 2012 Society For Neuroscience.....55

2.10 Schematic of AIM platform with master template on the left and PDMS device on the rice (adapted from [61] with permission from The Royal Society of Chemistry).....57

3.1 Formulation of the diffusion advection problem.....70

3.2 a. Handling of the groove geometry for computational simulations. Half the groove is meshed for computational solutions of fluid dynamics and diffusion-convection equations. P plot showing the concentration drop along the groove from the axonal side (right side) to the somatic side (left side). The profile along the middle of the groove shows the profile along one of the edges of the groove, b. Computational simulation of diffusion profile of growth factor along microchannel groove. Plot shows the concentration drop along the groove from the axonal side (right side) to the somatic side (left side) within 100 μm of the 500 μm channel. The profile along the middle of the groove shows the profile along one of the edges of the groove.....74

3.3 Analyte restriction maintained for 24 hrs. Diffusion of a small (MW 700) fluorescent analytes were examined under high hydrostatic pressures. Microchannels (region

	between dashed lines) connect compartments of unequal fluid height. Establishment of fluid heights >2 mm prevented entry of dye (solid white lines) into the compartment of higher fluid height. Scale bar 100 μm	75
3.4	Representative axotomy. Images of a single axon within axotomy device a. before, and b. after injury.....	76
3.5	Representative phase contrast images of regenerating axons where neurotrophic factors were administered into cell body compartment. Images were taken every 24 hours for 3 days after injury.....	77
3.6	Axonal regeneration by GDNF, neurturin (NT) and neublastin (NB) after the axotomy. Rate of axonal regeneration induced by the neurotrophic factors over 3 days. ($p < 0.05$).....	78
3.7	Axon regeneration with axonal GDNF application compared with axonal GDNF application concurrently with Cytochalasin D. ($p < 0.05$).....	78
4.1	Master template of ECM layer for the modified AIM platform.....	88
4.2	Illustration of the device assembly.....	90
4.3	a) Fluorescently-labeled GDNF gradients generated simultaneously in four separate channels (channels are arranged from top to bottom). b) Quantification of gradients in the four channels.....	91
4.4	a) Clumping of cells on methacrylated gelatin doped with fibronectin and coated with FITC-PLL on day 2, b) clumping of cells on methacrylated gelatin doped with laminin and coated with FITC-PLL on day 2, c) clumping of cells on methacrylated gelatin doped with both fibronectin and laminin and coated with FITC-PLL on day 2, d) control, e) clumping of cells on methacrylated gelatin washed with HBBS and	

	coated with FITC-PLL on day 2, and f) cells on methacrylated gelatin doped with collagen and treated with HBBS and coated with FITC-PLL on day 2 (scale bar 50 microns).....	93
4.5	a) Dissociated DRG cells seeded in the modified AIM devices can be seen under the channels on methacrylated hydrogels due to the loss of fluidic isolation resulting from the concavity of hydrogel surface, b) healthy DRG cells with no aggregation in the cell body chamber of AIM devices 10 days in culture. (scale bar 50 microns).....	94
4.6	a) On a bare silicon wafer, microchannels were defined in two linear arrays of microchannels, b) a second thicker resist is used to define the overall injury pad clearance, c) on top of this layer a submicron thick layer was coated to define the notch heights, d) finally on top of this the actual layer for injury pad is defined, e & f) depict the top view of the same. (Schematics are not to scale).....	101
4.7	a) Modified compression pads with addition of notches created by gaps of a defined height clearance from glass substrate, b) Modified flow layer master template for the fabrication of displacement control devices.....	103
4.8	a) FEM analysis of modified compression pad of notch device under no compression with 200 μm gap length and 80 μm pedestal length, b) zoomed version of the control condition, c) FEM analysis of modified compression pad of notch device under compression at 7 PSI, pressure needed to barely contact the glass substrate, d) zoomed in version of the compressed condition where one can clearly visualize the buckling.....	103

- 4.9** a) Uncompressed notch valve: the channels were filled with FITC-PLL and incubated overnight to take the images, b) compressed notch valve: valves were compressed prior to flushing the chambers with FITC-PLL, incubated overnight and washed before release of valve. One can clearly visualize the clear zones where the pedestal made contact with glass substrate for the entire duration of coating.....106
- 4.10** a) Confocal images of GFP tagged microtubules (green) with respect to axonal membrane (red) labelled with CMPTx red cell tracker. Microtubules appear to be more localized within the axon with an average diameter around 25nm, b) confocal images of GFP tagged neurofilaments (green) with respect to axonal membrane (red) labelled with CMPTx red cell tracker. Neurofilaments appear to be more dispersed within the axon with an average diameter around 10-12nm. (Axes scale in nm).....107

Chapter 1

Introduction

This work is an effort to understand and elucidate few of the molecular and structural dynamics of axonal injuries and the subsequent fate of axons post injury: to undergo either regeneration or degeneration, and to develop novel microfluidic platforms for neuroscience. This work can further be sub-classified into axonal injuries in Central Nervous System (CNS) and Peripheral Nervous System (PNS). Evidence from literature suggests that axonal regeneration in CNS is non-existent but is a fairly common phenomenon in PNS, given the right conditions. Recently it was found that the CNS axons do not inherently lack the regeneration abilities; rather, it is the environment that they grow and survive in is not conducive of regeneration. This opened new avenues into the research on axonal regeneration in CNS. Though axon regeneration in PNS has been established in the past, those studies are limited by the highly dynamic nature of the events at molecular level *in vivo*.

In vivo animal models of trauma, either to CNS or PNS permits the study of whole organism's response to a multitude of complex variables and behavioral outcome studies. Multiple injury modalities like Instant rotational injury model, Impact acceleration injury model, Lateral fluid percussion injury model, Controlled cortical impact model, Nerve stretch model [1] etc. exist for *in vivo* settings. These models facilitate monitoring of prognosis, and functional outcome to various treatment strategies. Though extremely useful, these models do not shed light on events at single cell and molecular level. To a

reductionist, *in vivo* techniques offer highly complex information leaving with the alternative of *in vitro* techniques. *In vitro* models on the other hand allow the study of biochemical pathways, gene expression levels, and phenotypic changes at single axon resolutions. To attain single axon resolutions *in vitro*, compartmentalization of soma from axons is needed. Attempts towards compartmentalization of neurons *in vitro* started couple of decades ago with the use of neurons with long axons like that of PNS. But those techniques were limited by the size of neurons and their axons rendering them not useful for the study of CNS neurons. Micro electro mechanical device (MEMS) technology integrated with biological applications gave raise to bioMEMS and Lab on Chip (LOC) devices which facilitated the required compartmentalization of axons from soma in these CNS neurons.

1.1 Compartmentalization studies of axons and soma

While neurons have been cultured and studied *in vitro* for decades, the idea of compartmentalized cultures did not become not mainstream until the late 70's. The first attempt at compartmentalization of neurons with segregation of soma and axon into physically distinct and chemically separate compartments was successfully established by Campenot [2, 3]. These chambers were made on a Petri dish by coating a layer of grease on the bottom of the dish and laying a reusable Teflon layer on top of the existing silicone grease layer. The grease layer acts as a hydrophobic barrier which enables the establishment of chemically distinct microenvironments for soma and axon of PNS neurons. These devices were successfully used for several studies ranging from axonal transport to regeneration. Ivins et al. [4] also developed a compartmentalized chamber

using coverslip as a physical barrier in separation of soma and axons in culture. These devices are not versatile for compartmentalized neuronal studies owing to the complexity involved in fabrication and maintenance. Nevertheless, these studies [2-9] pioneered a new era of compartmentalized culture systems in neuroscience and neuroengineering.

1.2 Microtechnology in neurobiology and neuroscience

Effective use of microfluidics in neuroscience started with miniaturization of Campenot chambers. This miniaturized version of Campenot chamber is much needed because of the complexities involved with its fabrication and application for various studies that involve neurons with axons of shorter lengths like in the case of CNS. With an array of parallel microfluidic channels connecting two chambers which otherwise are not connected is developed by Taylor *et al.* [10]. Well established photolithography techniques widely used for MEMS were used to define a master template in silicon wafers which are replica molded in poly(dimethylsiloxane) (PDMS) to make these devices. This started a new avenue for research in neurobiology and neuroscience.

The development of a dual chamber microfluidic device for neuroscience research by Taylor *et al.* [10] spawned interests in further developing various kinds of microfluidic platforms for neuroscience research. Microfluidic platforms and devices for neuroscience can be broadly classified into 1) electrical interfaces, 2) chemical interfaces, 3) physical interfaces, and 4) interface integrating any combination of the other three interfaces[11]. These platforms are being widely applied to culture neurons, manipulate neurons with the

flexibility of manipulating cell body and axons independent of each other, neuronal stem cell differentiation, neuropharmacology, neuroelectrophysiology, neuronal biosensors, and disease models [12, 13]. These microfluidic platforms are also extensively used in studies involving various types of neuronal supporting cells like Schwann cells, astrocytes, oligodendrocytes and even microglia. A brief summary of the microfluidic interfaces and their applications can be found in table 1.1 and a further emphasis on multicompartiment chambers can be found in chapter 2.

Table 1.1: Microfluidic interfaces for neuroscience and neurobiology research

Interface	Applications
Electrical Interfaces	Neuroelectrophysiology, Multi electrode arrays, stimulation, electro-chemical detection etc.
Chemical Interfaces	Neuropharmacology, disease models, fluidic isolation, soluble gradients, chemical guidance etc.
Physical Interfaces	Surface patterning, axon guidance, disease models, stem cell differentiation, neuronal co-culture studies, compartmentalization studies etc.
Combined interfaces	Neuronal biosensors, neuronal co-culture studies, compartmentalization studies, axon regeneration, electrical stimulation, disease models etc.

With this impetus several LOC platforms were developed. LOC devices provide powerful alternatives to existing *in vivo* and *in vitro* techniques in studying Traumatic Axonal Injuries (TAI). Providing platforms to model and study at single cell resolutions with compartmentalization and precise control over cellular microenvironments. They can be automated, require little amount of reagents with a scope for multiplexing, and high throughput[14]. LOC devices have been developed for neuroscience applications ranging from injury settings that can be employed in neuroscience to model and study the injuries and regeneration, synaptic connectivity, and complex live neural networks [15-20] as they can achieve fluidic isolation of the neuronal cell bodies from their axons. Several kinds of microfluidic devices are developed for the applications in neuroscience [12, 21-25].

LOC devices are also broadly employed in neurobiology for neuron cell culture, neuron manipulation, neural stem cell differentiation, neuropharmacology, and neuro-electrophysiology. With respect to axon injury studies, microfluidic platforms are highly compatible with different modes of injuries. Broadly classified, the modes of inducing injuries in neurons on these platforms are: I. Physical, II. Chemical, and III. Both I and II. Physical modes include employing laser ablation techniques [26-28], valve based compression of axons[29], microsurgeries and axotomy. On the other hand chemical injuries are mostly caused by neurotoxins with different modes of action.

1.2.1 Microfluidic platforms for *in vivo* injury models

1.2.1.1 Injury mode: Physical

LOC platforms, a great tool for reductionist approach are also extensively employed to study axon regeneration *in vivo*. Many model organisms like *Aplysia californica*, *Caenorhabditis elegans*, *Drosophila*, and zebrafish are used in the studies of *in vivo* neuron injury and regeneration [26-28, 30-32]. Amongst these, *C. elegans* is a nematode with its genome completely sequenced and with a feasibility of *in vivo* axotomy, offers a powerful model to study *in vivo* nerve injury and regeneration. Immobilizing the worm and subjecting it to axotomy is a critical step in studying the injury and regeneration. Conventional techniques of immobilization employ the use of glue, and anesthetics. Though these modes are typical for immobilizing the worm, they have some drawbacks. These methods can either have unknown toxic effects that are difficult to evaluate or are labor intensive and of low throughput. Microfluidic platforms can be a clever alternative to these problems. Choksi *et al.* [27] has developed microfluidic platforms to immobilize single worms on either a short term or long term basis to characterize their on-chip behavior. Chung *et al.* [26] designed and developed an automated, integrated microfluidic system to perform high-throughput cell microsurgery. Their device is capable of processing multiple worms in parallel without increase in control complexity. The device can be used to simultaneously load worms in one set of channels and perform imaging and laser ablation in the other set. Guo *et al.* [28] has developed a high throughput microfluidic platform for *in vivo* nerve regeneration studies. Their platform enables precise focusing and nano surgery of trapped worms and feeding for recovery of the operated worms in two different modules. The device also incorporates an adjustable trap for immobilization of

worms at various developmental stages. Highly specific laser ablation techniques can be used to injure the worms once they are steadily immobilized. Based on the frequency or the repetition rate of laser, the gaps created in the axotomy vary. With high frequency lasers 2-5 μm gaps are created where as low frequency lasers result in precise 1-2 μm gaps[31, 33]. Other physical modes of causing injury to axons *in vivo* involve needles to transect individual axons, fluid percussion, microelectrodes etc. [34].

1.2.2 Microfluidic platforms for *in vitro* injury models

1.2.2.1 Injury mode: Physical

Stretch induced injury is one of the many modes of physical injury observed *in vivo* during traumatic insult to axons of CNS and PNS. Several groups have modeled and studied these injuries *in vitro*. Stretch-induced injury model [35] on cortical astrocytes (of brain origin) was developed by culturing the cells on deformable membrane which was subjected to deformation by a positive rapid pressure. The system enables to study the extent and degree of injury with precise control over deformation of membrane by varying the amplitude and duration of pressure. Speaking of axons specifically, one of the major hurdles for them to undergo regeneration in an injury setting is the enormous lengths that they would have to grow to bridge established between the proximal extending axon and the distal stump. In bridging these gaps, axons have to circumvent the non-permissive substrates for neurite growth. Myelin of oligodendrocytes is a potent inhibitor for neurite outgrowth in CNS. In addition to this, glial scar formed at the site of an injury acts as both mechanical and biochemical barrier for the growing axons. As the name suggests the scar is often comprised of glial cell types like reactive astrocytes, microglia, oligodendrocyte

precursors, and fibroblasts. It also contains growth inhibitory factors such as semaphorins, ephrins, tenascin and chondroitin sulfate proteoglycans [36]. This non permissiveness can be a kind of negative mechanism involved in enhancing the efficiency of surface recognition process for selective cell and growth cone migration. The non-permissive nature of the myelin and oligodendrocytes can be attributed to membrane proteins of 35 kd and 250 kd, which can be extracted from CNS myelin fractions. Antibodies: IN-1 and IN2 raised against these proteins neutralized the non-permissiveness of the myelin and allowed the axon outgrowth[37]. The growth rate of axon also plays a major role in bridging the gap in regeneration. One of the several strategies to influence a sustained but rapid growth in axons is to apply a continuous mechanical tension. Smith *et al.* [38] developed a device to physically split integrated neuronal cultures into two halves and separate the halves progressively further apart using a microstepper motor system. In doing so they achieved a growth rate of 1mm/day. Transecting axons to induce axonal injury by laser ablation in one of the physical modes [33, 39]. Kim *et al.* [11] developed a neuro-optical microfluidic platform that integrates a microfluidic chip, femtosecond laser for axotomy and mini-incubator to maintain sterile and appropriate microenvironment for long term monitoring of events post injury.

1.2.2.2 Injury mode: Chemical

Traumatic injuries to axons of CNS and PNS can be induced by chemicals like neurotoxins, neurotransmitter in excess (excitotoxicity), and detergents [30, 34]. Injury induced by chemicals in microfluidic platforms aid both the qualitative and quantitative study, as the concentrations can be varied and localized precisely. Several *in vitro* axon

injury models have been developed to study chemically induced injury. Kilinc *et al.*[26] developed a three compartment (cell body, central/proximal, distal compartments) microfluidic device to study simultaneous axonal degeneration and death mechanisms of axons subject to axotomy, with precise spatiotemporal control. The injury was induced by a brief and isolated flux of detergent in the central compartment. They observed rapid Wallerian-like degeneration in the distal axons subject to axotomy. Li *et al.* [22] developed an integrated microfluidic platform to chemically induce axonal injury and study the recovery and regeneration of axon either in co-culture with glial cells in a controllable chamber using valves or treatment with monosialoganglioside, a drug aiding neuronal regeneration.

Other important aspects of the events post injury are survival, recovery and regeneration of the axon. Microfluidic platforms are an excellent choice for studying and understanding the mechanisms involved in regeneration or degeneration post injury, establishment of neural networks. Several strategies to achieve this in microfluidic devices have been devised [40-45]. For example a gradient-generator microfluidic device was developed by Bhattacharjee *et al.* [32]. This device helped to study the neuronal response to a diffusible gradient. This helps to understand the complex mechanisms of axon growth and guidance to chemical gradients. Microfluidic devices have been developed to study synapse formations as they provide a suitable platform to analyze the cellular events underlying the synapse formation [46].

1.3 Specific Aims

The specific aims of my research have the following interests. First, I aimed to study the role of Glial cell line-derived Neurotrophic Factor (GDNF) in the axonal regeneration post injury in simple two chamber microfluidic devices. Second, I aimed at improving the existing microfluidic technologies that allows focal and graded axonal injury to incorporate three dimensional injury models and novel displacement control injury models. Specifically, I have divided the research into the following aims:

Aim 1. To study the role of GDNF as a neurotrophic factor in axonal regeneration post injury of PNS neurons in simple two chambered, open system, microfluidic devices.

Aim 2. To design and optimize three dimensional microfluidic platforms for a focal and graded compressive injury to axons, and to develop microfluidic chambers in a manner compatible with high resolution optical microscopy.

1.4 Organization of the Thesis

This thesis is organized into 5 chapters dealing with the aims presented above. Chapter 1 gives a brief introduction about microtechnologies for axonal injury studies in various settings. Chapter 2 deals with a review of literature in multichambered microfluidic devices in neuroscience with specific applications in axonal injury and regeneration. Chapter 3 and chapter 4 describe the experimental working of aims with brief introductions, materials and methods, results, discussions and conclusions associated with each aim. Chapter 5 consists the conclusions of the work and project some ideas about future possibilities and potential areas of development. Finally, an appendix with protocols

and other miscellaneous details relevant to the experimental settings are provided in the end.

Chapter 2

Microfluidic Multi-Compartment Chamber Devices in Neuroscience and Neuroengineering

2.1 Introduction

Neurons are highly polarized cells with a cell body ‘soma’ and processes ‘axon’ and ‘dendrites’: axon constitutes the majority of protoplasm in a neuron. By this intrinsic nature of polarization, neurons are usually seen extending their axons, often several millimeters into varying microenvironments in their niche. These processes constantly encounter various guidance cues in varying degrees from the surrounding microenvironments in the form of biochemical, and biophysical signals for growth, maintenance and remodeling. These microenvironments encountered by axons in their process of extension more often than not differ in chemical and physical properties in comparison to the microenvironment surrounding soma. Well established and traditional *in vitro* cell culture techniques in petri dish are reliable in elucidating phenomenon affecting on a global scale by bathing soma and axons homogenously in a culture media[47, 48]. But they usually fail about providing invaluable information on much localized phenomenon which are equally powerful in advancing our understanding of neurobiology. And so, it is only imperative to develop novel *in vitro* neuronal culture platforms that can establish and enable tailoring of these varying microenvironments for successful maintenance and study of the cultures in close resemblance to *in vivo* systems. With the advent of and advances in sophisticated photo lithography techniques for semi-conductor industry, a field of study integrating mechanical systems with electrical systems called

MEMS emerged. MEMS further branched out into biological MEMS (BioMEMS) with potential applications in various fields of biology.

BioMEMS integrated with microfluidics emerged as Laboratory-on-a-Chip (LOC) platforms: potential and viable alternatives for existing techniques to conduct various biological studies at micron scales with precise control over the micro environments. The broad spectrum applications of microtechnology has involved engineers[11] in collaboration with biologists to develop several novel LOC devices for various studies[11, 12, 49-53]. These microfluidic systems initiated a new era of studies in biology by efficiently reducing the volume of reagents and samples there by the overall cost incurred[54], and by facilitating spatiotemporal manipulation of a system at cellular dimensions. With the reduction in system size, phenomena like diffusion, surface tension, and viscosity play a prominent role counterintuitive to our experiences with the macroscopic world [55, 56]. These microscale phenomena can be exploited for several practical purposes like establishing and maintaining interfaces, gradients, and even manipulation and processing of droplets in real time for biochemical analysis[57]. Microtechnology also offers potential and viable platforms for investigations in neuroscience. The operation range of neurons fall under the bounds of LOC devices with the possibility of incorporation of electrodes for stimulation and recording, microchannels and other physical barriers for guidance and tailored interactions with other cell types[58-60].

Soft lithography in elastomeric polymer PDMS is one of the most sought after techniques for fabricating LOC devices. Soft lithography encompasses rapid prototyping and replica molding: rapid prototyping of a master template in positive relief is achieved by photo lithography (a commonly used microfabrication technique) and a pre polymer of PDMS is cast and cured on the master template for replica molding. Using this technique, structures and features ranging in sizes from 100 nm to 100 μm can be transferred on to PDMS with great fidelity. Many studies involved the development and use of LOC devices in PDMS consisting of elements like micro channels, pumps, mixers and valves[61]. Several groups have fabricated LOC devices in PDMS for neuroscience studies including neuronal cultures, *in vitro* disease models, and electrophysiology.

We present you in this review, a comprehensive view of recent developments of various multi-compartment LOC devices for neuroscience used across studies involving neuronal cultures, *in vitro* disease models, and electrophysiology. We explore various LOC devices in this review by organizing the discussions in the following way: (1) Fabrication, and (2) Multi-Compartment Chamber Devices.

2.2 Fabrication

Microfluidic devices were conceived as early as 1970s in the form of a miniaturized gas chromatograms[62] serving as an impetus for present day LOC devices. The initial microfluidic devices were developed in silicon and glass, based on then existing technology for MEMS. They were commonly applied in chemical analysis, gradually making their

impact felt in biological applications with the development of BioMEMS. BioMEMS enabled medical and biochemical analysis with increased resolutions, increased density in arrays, massive parallelization, high throughput, and decrease in volume of the reagents being used. BioMEMS combined with the advances in soft lithography spawned LOC devices. The fabrication of these devices is usually done in PDMS elastomer which offers several advantages: PDMS as a material of fabrication is a viable choice because of its low interfacial energy (can be bonded to most surfaces reversibly), chemical and thermal stability (does not react with the surfaces it comes in contact with), permeability to gases (allows gaseous exchange to maintain viable cell cultures), optically transparent down to 230 nm (compatible with imaging), mechanically deformable (for incorporation of valves, pumps), tunable interfaces (hydrophobic/hydrophilic), and of most importance is its inertness and biocompatibility[63].

2.2.1 Design and Fabrication Techniques

Limitations like the cost of operation, compatibility with nonplanar surfaces, suitability for surface chemical modification, and choice of photoresists render the well-established photolithography technique not so useful for LOC applications. In contrast, soft lithography offers to overcome the limitations that are encountered in conventional photolithography. Soft lithography includes photo lithography to create a master template in positive relief by rapid prototyping. First a layout of the device design is developed using Computer Aided Design (CAD) and this CAD file is used to print a high resolution transparency mask (up to a resolution of 5 μm). A 3-4 inch Si wafer is spun with SU8 photoresist to a desired thickness, exposed with the mask and developed. The features left

on the surface of the Si wafer serve as positive relief patterns of the master template in downstream processes as illustrated in figure 2.1 A.

The later part of soft lithography involves developing elastomeric PDMS molds from the master templates by cast molding. The pre-polymer of PDMS is made available in a two part kit comprising of a base and a catalyst/curing agent. The ratio of base to the curing agent can be altered to tune desired mechanical properties of the cross-linked PDMS. A desired mixture of base and curing agent is prepared, degassed and cast on the master template. The cast pre-polymer is then incubated for couple of hours in an incubator for the cross linking reaction: hydrosilylation between the vinyl and hydrosilane groups. The cast is cooled and peeled off from the master template for next cycle of cast molding [64]. The mold produced can be used in various techniques like microcontact printing (μ CP), replica molding, micro-molding in capillaries (MIMIC) and few others [63-67]. In μ CP, the relief structures in PDMS are used as stamps in transferring patterns to the surface of a substrate by contact, resulting in micro patterns and this method has been used often to pattern ECM substrates (figure 2.1). In MIMIC a PDMS mold consisting of parallel grooves is used to create empty channels when in contact with the surface of a substrate. These empty channels act as capillaries and when a liquid of low viscosity is seeded at one end it is taken up across the channels by capillary action. MIMIC is another soft lithography technique to pattern surfaces (figure 2.1 B). These techniques in conjunction with LOC devices are often used in various neuronal studies.

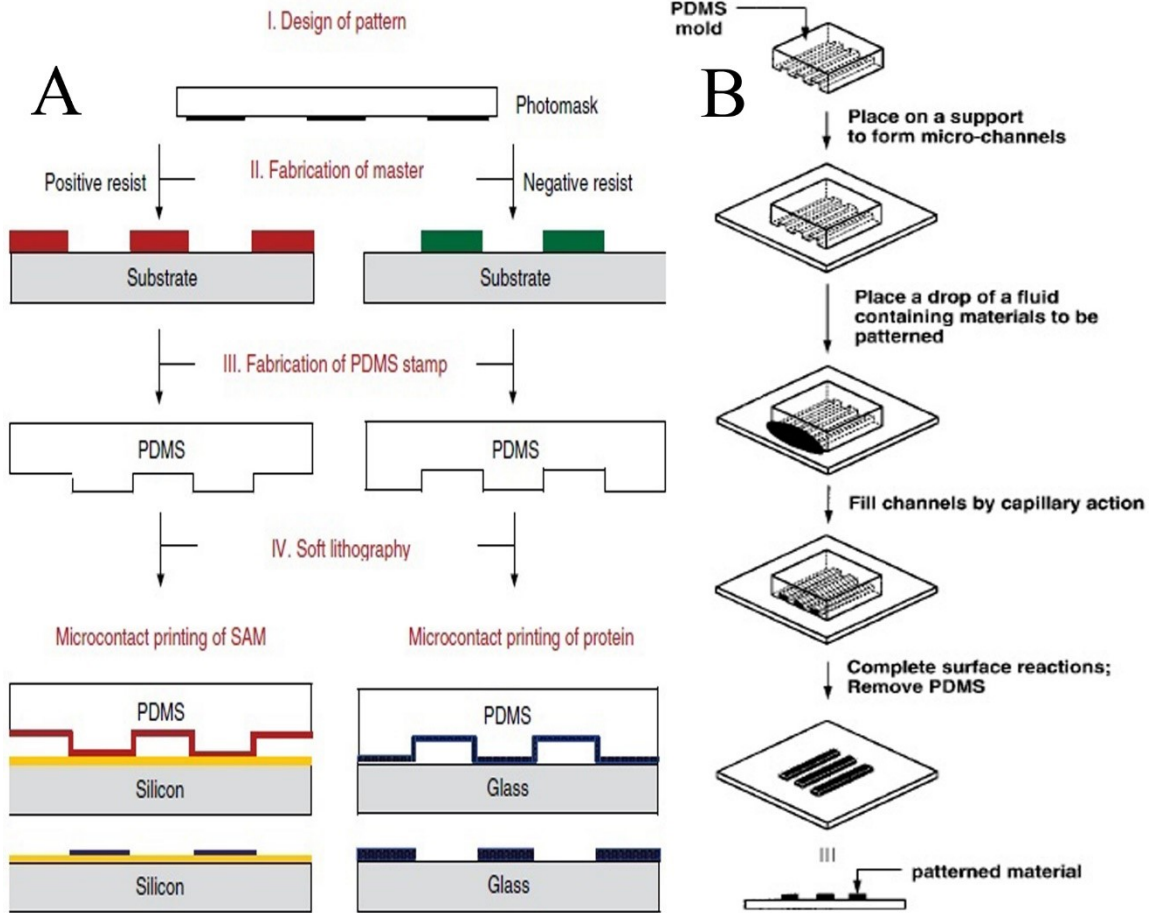


Fig 2.1: A. Schematic of photolithography technique and micro contact printing (adapted from [64] copyright 2010 Nature Publishing Group), B. Schematic of MIMIC technique (adapted from [67] copyright 1996 American Chemical Society).

2.2.2 Modeling and Simulations

The scaling down of neuronal culture system's dimensions to an order of microns not only improves the operation cost and handling, but also allows the precise control of microenvironments with a possibility of compartmentalization. The scaling down of dimensions to micron orders results in significant changes to the physics of fluids that are seldom perceived at macroscopic scales [55-57, 68]. The continuum theory of fluids still holds at micron scales for channel dimensions >100 nm. Often cited paradigm to delineate

the significant deviations in fundamental physical properties at micron scale is mass transport phenomena. Mass transport in microfluidic channels is primarily dominated by viscous forces but not by inertial forces, which are almost negligible resulting in laminar flow profile in the channels. When the microfluidic channel dimensions are further reduced below 100 nm, we enter the regime of nanofluidics. The continuum theory can still be applied here by excluding few layers of molecules adjacent to the channel walls. The physics of nanofluidics further varies significantly from that of microfluidics and this is discussed elsewhere [68-72].

Several non-dimensional numbers are used when describing the physics of microfluidics: Reynolds number, Péclet number, Knudsen number, capillary number etc. In this review we briefly focus on the first three dimensionless numbers which help in understanding the dynamical physical properties of microfluidic neuronal culture systems.

The culture medium is assumed to be a Newtonian fluid and that it obeys Navier-Stokes equations of fluid continuum theory.

$$\rho \left(\frac{\partial \mathbf{u}}{\partial t} + \mathbf{u} \cdot \nabla \mathbf{u} \right) = -\nabla p + \eta \nabla^2 \mathbf{u} + \mathbf{f}$$

ρ – density p – pressure η – coefficient of viscosity

\mathbf{u} – flow velocity vector \mathbf{f} – body force densities

Inertial forces in microfluidic systems are of negligible order compared to viscous forces. This implies that the non-linear term in Navier-Stokes equation, $\mathbf{u} \cdot \nabla \mathbf{u}$ can be neglected. Combined with mass conservation yields the incompressibility condition

$$\nabla \mathbf{u} = \mathbf{0}.$$

The loss of non-linearity in microfluidics results in low Reynolds number (Re) which is defined as the ratio of inertial forces to the viscous forces.

$$Re = \frac{f_i}{f_v} = \frac{\rho u L}{\eta}$$

f_i – inertial force density f_v – viscous force density

ρ – fluid density u – average velocity L – typical length scale

η – coefficient of viscosity

Low Re number flows are not common on macroscopic scales but are frequently encountered in microfluidics. The low Re number in microfluidic devices results in predictable Stokes flow in the channels. The no-slip boundary condition in pressure driven flows ensure that the flow velocity of fluid is zero at walls resulting in a parabolic profile laminar flow. Because of the low Re in microfluidics the flow is deterministic and can be fine-tuned.

The second dimensionless number is the Péclet number. Péclet number signifies the solute transport: the mixing and maintenance of gradients in microfluidic channels. It is defined as the ratio of advective transport to diffusive transport.

$$Pe = \frac{Uw}{D}$$

w – characteristic length U – flow velocity

D – mass diffusion coefficient

Mixing may or may not be desired in the neuronal culture system. In the case of compartmentalization, mixing is not usually desired and a steady gradient of solute molecules, like growth factors are needed to guide axonal growth. Low Pe number results in diffusion dominated mixing which helps maintain a gradient for a long time in culture system.

Another dimensionless number is the Knudsen number. Knudsen number is defined as the ratio of mean free path of molecules to macroscopic length scale. Knudsen number defines the transition of fluid approximation from continuum to discrete molecules. It establishes the validity of continuum Navier-Stokes equations.

$$Kn = \frac{\lambda_f}{L}$$

λ_f – mean free path for collisions L – Characteristic length

The dimensionless numbers mentioned above elucidate the physical phenomena operating in microfluidic systems. They define system performance parameters and help in developing mathematical models to numerically simulate the system. Numerical simulations of microfluidic systems are not only an excellent research tool but also they play a vital role in efficient design, prototype development and optimization. Mathematical models developed for numerical solutions and simulations can easily incorporate the complexities of channel geometry, fluid flow rates, flow profiles, diffusion coefficients, dynamic gradients, their spread in space and time, and possible chemical interactions to great details. An accurate prediction of the behavior of a particular system can be made using the models and simulations which are otherwise elusive on a preliminary examination to our intuition. Mathematical modeling and simulations also further our theoretical understanding of the physics of microfluidic systems which are otherwise hard to realize in experiments and practice.

Mathematical models of these systems are powerful tools or substitute for eliminating the need for laborious experiments to determine optimal conditions by changing any number of parameters on the performance of the device without actually fabricating different devices. But the caveat is that mathematical modeling is an approximation of the physical phenomenon in play (often some physical phenomenon are not accounted for or left out for the sake of simplicity) and the simulations often fail to exactly replicate the experimental observations.

Finite Difference (FD) method, Finite Volume (FV) method and Finite Element Modeling (FEM) are few approaches commonly used to model microfluidic systems. All these methods are relatively similar in that they spatially discretize differential equations over a solution domain[73, 74]. FD method is usually employed in the cases of well-structured grids with simple geometries by converting partial derivatives to numerically solvable differential equations[75, 76]. FV method is similar to FD in the sense that the system is divided into a series of control volume nodes and each node is treated as an independent entity. A system of differential equations are written out for each node, treating the adjacent nodes as unknowns and these equations are numerically integrated [77-79]. The arbitrary geometry of the nodes makes FV more generic over FD but difficulties often arise in establishing the system of governing differential equations and reducing them to a lower order. Also, FV methods are more suitable for systems where viscous forces are negligible, but in the realm of microfluidic systems where viscous forces play a major role, FV method is rendered complex and not feasible. This leaves us with FEM as promising method for simulating microfluidic systems.

Like FV method, FEM has the advantage of dealing with arbitrary and irregular node geometries. FEM begins with discretizing the sample space into finite and spatially distinct series of interconnecting nodes and elements collectively representing the overall geometry of the system. FEM can handle unstructured grids and irregular geometries like linear, triangular, parabolic etc. The partial differential equations for each node is set using techniques in variational calculus. These partial differential equations are then given weights in FEM which are multiplied prior to the integration over the domain. The relative

ease and simplicity with which one can establish even weak formulations and apply boundary conditions makes FEM one of the best sought after method for modeling in microfluidic simulations. Nevertheless, necessary caution is to be taken when applying FEM methods as they suffer from cumbersome numerical computations associated with the irregular and arbitrary geometries. FEM has been not only used to model various flows (non-uniform surfaces, free surfaces, capillary and immiscible flows), mass transfer and mixing (dispersion, gradients), heat transfer (dissipation, gradients), electrophoresis etc., in microchannels [73, 80-83] but its significance is being felt and utilized in modeling gradients in gels established in microchannels , the characterization and optimization of microfluidic device mechanical properties etc. [61, 83, 84] .

2.3 Multi-compartment Chamber devices in Neuroscience and Neuroengineering

While neurons have been cultured and studied *in vitro* for decades the idea of compartmentalized cultures did not become mainstream until the late 70's. The first attempt at compartmentalization of neurons with segregation of soma and axon into physically distinct and chemically separate compartments was successfully established by Campenot [2, 3]. These chambers were made on a Petri dish by coating a layer of grease on the bottom of the dish and laying a reusable Teflon layer on top of the existing silicone grease layer. The grease layer acts as a hydrophobic barrier which enables the establishment of chemically distinct microenvironments for soma and axon. These devices were successfully used for several studies ranging from axonal transport to regeneration. Ivins *et al.* also developed a compartmentalized chamber using coverslip as a physical barrier in separation of soma and axons in culture. These devices are not versatile for

compartmentalized neuronal studies owing to the complexity involved in fabrication and maintenance. Nevertheless, these studies pioneered a new era of compartmentalized culture systems in neuroscience and neuroengineering.

With the development of BioMEMS and LOC devices the compartmentalization of neurons in culture has been achieved with a relative ease compared to the traditional Campenot and Ivans culture systems. Before we discuss any further on the advancements of LOC devices for compartmentalized studies we should address the important question: Why do we need the compartmentalization of neurons? The following reasons listed below should briefly address this question

- a. The neurons in CNS extend over considerable distances through varying extracellular microenvironments to form synapses, the basis of neuronal connectivity.
- b. Etiology of several neurodegenerative diseases and CNS injuries involve axonal damage (for example spinal cord injury and Alzheimer Disease).
- c. Campenot chambers were not successful in culturing CNS neurons involved in the pathology of most neurodegenerative diseases and injuries (for example, cortical, hippocampal, and spinal cord neurons).
- d. Selective isolation of the axonal molecules (for example, axonal mRNA, protein machinery etc.) from mammalian CNS neurons, an achievement not possible by either *in vitro* or *in vivo* methods. (Axonal protein synthesis is important in the development, maintenance, and plasticity of synapses)
- e. To model axonal injury: the ability to selectively lesion axons and biochemically analyze their somata for immediate early gene expression.

- f. Co-culture studies of oligodendrocytes with CNS axons to study the myelination as well as demyelination diseases like MS.
- g. For selective axonal transport studies.

2.3.1 Multi-compartment Chamber devices for axon guidance

The complex circuitry of a human brain involves highly intricate yet structured architecture of connections between individual neurons enabled through functional synapses. The interconnectivity between neurons through functional synapses is often so dense that single neurons are seen networking with several neurons, in the order of hundreds to thousands both in the vicinity and remote areas. A functional connection between two neurons is established via synaptogenesis: a multi-step complex and dynamic process which involves several events at cellular and molecular level like elongation and polarity of neurites, axon path finding/guidance, target recognition and signaling within presynaptic and postsynaptic components. Axon guidance involved in synaptogenesis plays an important role in normal and pathogenic brain development as well as in neurological regenerative and/or degenerative medicine. Several disorders linked with or implicating faulty axon developmental pathways like autism are being discovered and the number is growing [85]. Similarly, neurodegenerative diseases like Alzheimer's, Parkinson's, Huntington's, and prion diseases are associated with synaptic and neuronal dysfunction. Directionality of neuronal pathways in developmental mechanisms of specific connections and degeneration of neuronal networks in mature brains has elicited the interests of several neurobiologists to pursue explorative studies involving molecular processes pertaining to axon guidance, functional synapse formation, maintenance, and

plasticity. *In vivo* methods best preserve the architecture of neuronal connectivity offering realistic and physiological insights into axon guidance, synapse formation and remodeling. However, the sheer number of connections and the complexity associated with mammalian brains serve as road blocks for *in vivo* methods. Resorting to *in vitro culture* techniques offer alternatives to achieve this feat. Nevertheless, traditional *in vitro* techniques with two dimensional dissociated cultures, even with small number of cells result in random connections and three dimensional organotypic culture vary from sample to sample and often the connections are severed in slice preparation. Novel LOC microfluidic platforms are being developed in the recent years to study axon guidance and synapse formation *in vitro* owing to the several advantages they offer over traditional methods.

Traditional *in vitro* culture methods lack the sophistication to conduct studies with spatial compartmentalization of neuronal signals: they do not offer separation of axons from soma to study the local molecular mechanisms involved in axon guidance, and fail to preferentially orient neuronal networks with several neuronal subtypes. Also, they suffer from the lack of complexity in providing a localized plethora of axon guidance cues like canonical guidance cues, morphogens, growth factors, cell adhesion proteins, and the extensive cross talk that is often observed between various guidance pathways. These hinder elucidation of the underpinnings of phenomena involved in complex axon guidance and neuronal networks. With recent technological advancements in microfabrication novel and innovative LOC devices for axon guidance and functional synapse formation studies are being developed. The guidance cues in these devices can be i. Physical [86-89], ii. Chemical [90-93], iii. Or both [86, 92, 93]. Physical cues for guidance often involve

microchannels with various shapes and geometries, which act as conduit for axons to grow and orient. Physical cues can either maintain or realign the current orientation of axons as axons are considered to be stiff and when encountered with barriers they reorient themselves with altering growth rates. Chemical cues can either be growth promoting like neurotrophic factors or growth inhibiting like scar tissue, myelin etc. In order to act as guidance cues these chemical cues are usually presented to the axon growth cone in gradients. The gradients can either be soluble or insoluble, and they can be stable over time or dynamic i.e. the gradients can be spatiotemporally controlled to guide the axonal growth cones.

Takayama *et al.* [86] developed a LOC platform to form a one-way-structured cultured neuronal network that is functionally regulated. Combining microfluidic devices with microcontact printing their device consists of U-shaped array structure for cell trapping in PDMS which is bonded to a previously patterned glass substrate by microcontact printing with areas of cell adhesive and non-adhesive molecules. Once cells were trapped in the device, the cells were exposed to chronic medium flow rates (0.5 $\mu\text{l}/\text{min}$) to study the effects on the direction of neurite elongation. Their study indicates the fact that a chronic medium flow could positively affect the direction of neurite development and can be useful for forming morphologically and functionally regulated cultured neuronal networks. Mahto *et al.* [87] developed a three compartment microfluidic device to study functional synapse formation *in vitro*. The microfluidic device is made up of three parallel compartments, while the middle compartment is narrower and is connected to side compartments with microgrooves that define the directionality of neuritis. The functional

synapses were established by first culturing cells in the side compartments. Once neurites to extend via microgrooves into the middle compartment, fresh cells are seeded into the middle compartment which establish a functional network between the two channels. Pirlo *et al.* [88] a microfluidic system with asymmetric geometries to study neuron-neuron and neuron-glia interactions. They developed a laser cell deposition system to selectively seed cells into a specific microwells interconnected with channels of asymmetric geometry that promote neurite extension and formation of functional synapses. The device geometry permits a unidirectional and functional network formation between neurons and also allows co-culture studies with glial cells. Peyrin *et al.* [89] developed a compartmentalized microfluidic platform called axon diodes for oriented and unidirectional neuronal networks of high complexity. The microfluidic platform consists of two chambers interconnected with funnel shaped asymmetric channels called axon diodes that taper down along the length which ensures that the axons penetrate only in one direction resulting in the unidirectionality of the network established. Functional and highly oriented binary neuronal networks between different types of neurons can be easily established with this device.

Shi *et al.* [90] developed a compartmentalized microfluidic chamber with multicomponent, protein-micropatterned surfaces to investigate local crosstalk between N-cadherin and fibroblast growth factor receptor in axon guidance. The chamber design, a microchannel barrier overhang on the cell side suits aggregate cultures like explants or embryoid bodies better than dissociated cell cultures. Millet *et al.* [91] developed a multicompartment microfluidic device to pattern tunable surfaces for axon guidance. The

device design consists of three parallel channels with the middle channel interconnected to the two peripheral channels via microchannels, allowing establishment of biologically more relevant substrate diffusion gradients in combination with more tunable and dynamic fluid-phase laminar flow gradients. Using this device they established differential substrate patterns of stable, surface-bound gradients of laminin and Texas Red-conjugated bovine serum albumin (TR_BSA) perpendicular to binary FITC-PLL lines for preferential neuronal polarity and axon guidance. Kothapalli *et al.* [92] designed and fabricated a microfluidic device to study axon guidance. The device design permits the study of 3D neuronal culture closely evoking native cell responses. The microfluidic device is a multicompartment device with a T-shaped gel region at the intersection of three microfluidic channels: media, cell, and guidance channels. Stable soluble gradients of guidance cues were established across the gel, orthogonal to the direction of neurite growth in as little as 30 min and maintained stable over a period of 48 hours, impervious to external perturbations. Bhattacharjee *et al.* [93] conceptualized and implemented a neuron-benign gradient-generator multicompartment, microfluidic device to study axon guidance. The device design incorporates a large, central open reservoir for cells with parallel source and sink microchannels on sides, interconnected orthogonally by smaller microchannels called microjets. This design ensures negligible flow in the open reservoir resulting in minimal shear-stress to the cells and thereby improving the viability of cultures, hence neuro-benign. Stable gradients of guidance cues are established across the source, reservoir and sink by laminar flow of media with a certain concentration guidance cue in the source microchannel while the media flowing in sink microchannel carries no guidance cue. Stable diffusible surface gradients are established between the two boundary concentrations

within 2-5 min and are stable up to 6 hours, the shear-force to which the neurons are exposed due to the flow in gradient creation is negligible.

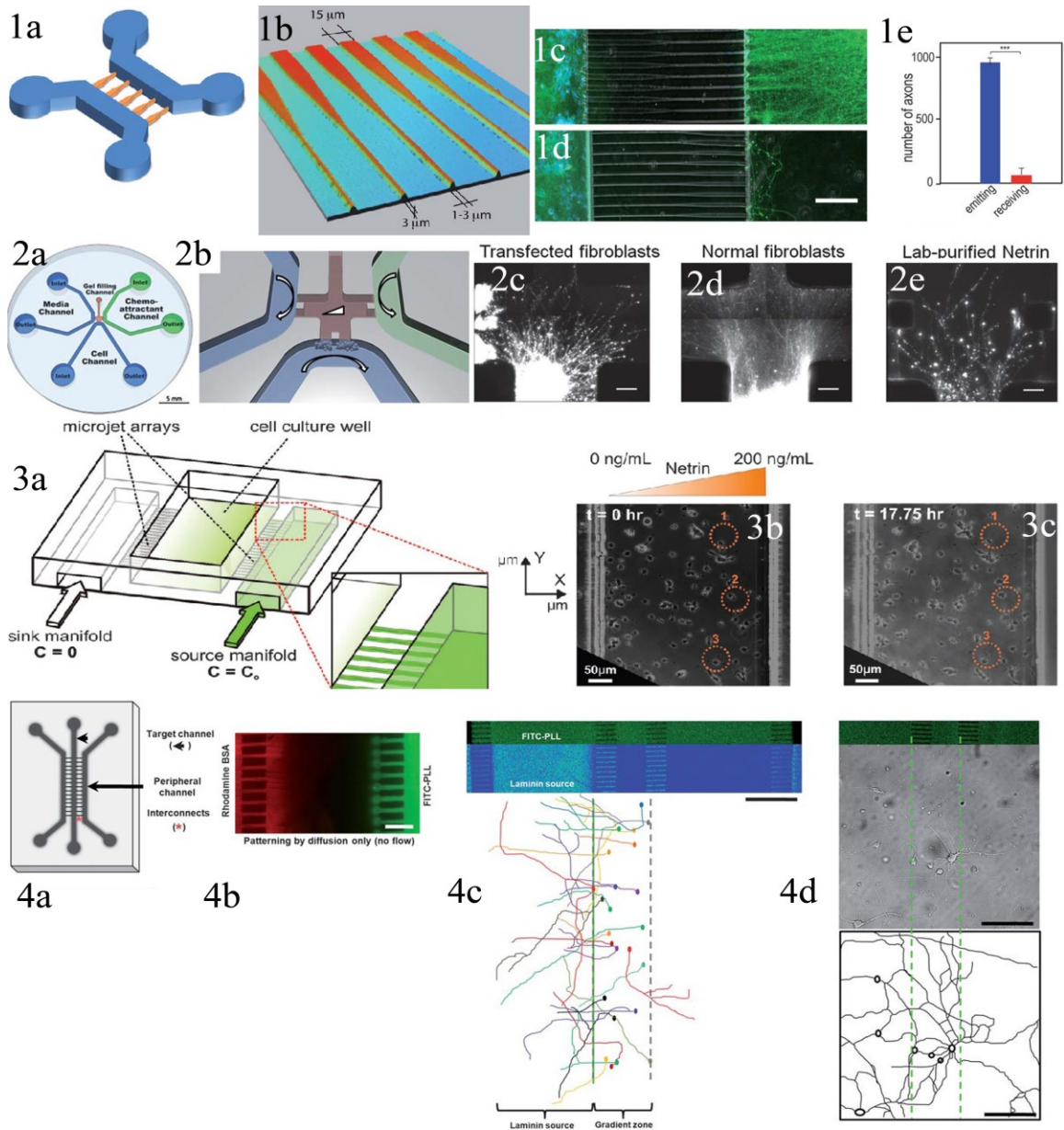


Fig 2.2: 1a & 1b. In vitro reconstruction of a neuronal network using “axonal diodes” in microfluidic culture devices, 1c & 1d. Immunofluorescent images of microfluidic neuronal cultures either on the wide or the narrow side, 1e. Quantification axonal growth polarization (adapted from [89] with permission from The Royal Society of Chemistry), 2a & 2b. Design of the three-channel microfluidic device developed to study neurite turning in 3D scaffolds under a growth factor gradient, 2c, 2d & 2e. Neurite guidance of hippocampal neurons by chemoattractants (adapted from [92] with permission from The Royal Society of Chemistry), 3a. Schematic of micro-jets device with a central open-surface reservoir, 3b & 3c. Neuronal response to netrin (adapted from [93] with permission from The Royal Society of Chemistry), and 4a & 4b. Schematic of the channel design used and diffusion through microfluidic interconnects, 4c & 4d. Traces of neuronal process in gradients and control (adapted from [91] with permission from The Royal Society of Chemistry).

2.3.2 Multi-compartment Chamber devices for axonal biochemical analysis and assays

The characteristic polarity of a neuron with soma, dendrites, and an axon(s) enables formation of complex circuitry with highly defined directionality in chemical communication between neurons, information processing, storage, and retrieval. Earlier, it was thought that axons were devoid of protein synthesis machinery for biosynthesis of proteins and other molecules, and that the synthesis occurs solely in soma and the finished products are translocated either actively or passively to axon [94]. The selective transport of synthesized proteins in soma only to axons undergoing synaptic changes is hard to explain without local protein synthesis in axons. Recent evidences supporting local protein synthesis in axons [95] are increasing in number indicating the necessity to selectively study the mechanisms of proteins synthesis and transport in axons with no interference from soma. Disruption of axonal transport is observed in pathology of several neurodegenerative disorders like Alzheimer's, Huntington's, and Parkinson's. Also, axonal degeneration and neuronal apoptosis is closely linked with mitochondrial transport. All these evidence points to the fact that the analysis of axonal transport, mRNA pool, protein synthesis etc. sans somal counterparts is paramount.

Traditional neuronal culture techniques involved culturing of either dissociated neurons or explants in petri dishes. The sense of compartmentalization and fluidic isolation is not maintained in these cultures and it was extremely hard to isolate and study the biochemical processes in axons. Identified solely by the morphology, axons were randomly oriented in all directions and often entangled. Often the sense, i.e. retrograde or anterograde

is extremely hard and painstaking to identify in these cultures. They are not high-throughput, scaling up is labor intensive and often difficult. Microfluidics and LOC devices are right up the alley and address several of these issues in neuroscience and neuroengineering. The dimensions of these devices are similar to that of neurons *in vivo* and they provide compartmentalization and fluidic isolation. This enables the study of localized axonal mechanisms without even the slightest interference from somal compartment. Several groups have developed novel LOC devices to study transport, protein synthesis and biochemical analysis in axons and functional synaptic junctions [96-102].

Millet *et al.* [97] developed multicompartiment microfluidic devices, both with open and closed channel systems to study the microenvironments of neurons in culture at low densities. Ability to culture neurons at low densities enables one to specifically isolate the microenvironments of axons for biochemical analysis. With the option to perfuse, collection of samples from the microenvironment is spatiotemporally controlled. Noo Li Jeon group [96, 98, 101, 102] developed several variations of multicompartiment microfluidic devices to study various aspects of axonal transport, axonal mRNA and axonal translates. The basic device design consists of two microfluidic compartments one each for soma and axon interconnected by microchannels. Hydrostatic pressure driven fluidic isolation can be achieved for a period of 48 hours in these devices which permits the collection of axonal fraction without and interference from the cell body compartment. In some cases, to increase the axonal fraction output, the closed soma chamber was made open to achieve high density cultures and the device length was increased 5 fold. Axonal

fraction was mainly collected by shear forces: rapid perfusion by micropipette causes disruption of axons by huge shear forces. The device design was further modified into a three chamber design to study mitochondrial transport in healthy and injured axons and integrated with automated tracking system. Shi *et al.* [99] developed a high-throughput microfluidic platform, synapse microarray for ultra-sensitive, large scale assays and quantitative screening of synaptic proteins involved in synaptogenesis. The synapse array design consists of two compartments one each for soma and axon connected by microchannels to isolate axons from soma. Axonal compartment is covered by a PDMS membrane (80 μm thick) with a clearance of 3 μm , providing no hindrance to axonal outgrowth. The purpose of this membrane is to contain genetically modified cells expressing synaptic membrane proteins in microwells defined in the membrane. Cells so contained in these microwells are evenly spaced out at defined densities and maintain good contact with axons to induce protein synthesis relevant to synaptogenesis in axons. This platform is a powerful tool to study molecules involved in synaptogenesis in a high-throughput fashion with great degree of control in experimental parameters. Taylor *et al.* [100] developed a multicompartment microfluidic platform for visualization, manipulation, and biochemical analysis of synapses. The device design consists of three parallel chambers, two peripheral chambers for distinct neuronal populations and a middle chamber for perfusion. The two peripheral chambers are connected to the middle perfusion chamber with microchannels of unequal lengths. This unequal lengths in the design permits formation of functional, oriented, and unidirectional synapses between the two populations of neurons. The perfusion chamber has three inlets with the two peripheral inlets are for fluidic focusing. This fluidic focusing allows for precise collection of either presynaptic or

synaptic or post synaptic fractions for biochemical analysis. This device offers collection of fractions with a great order of spatiotemporal precision for synaptogenesis analysis.

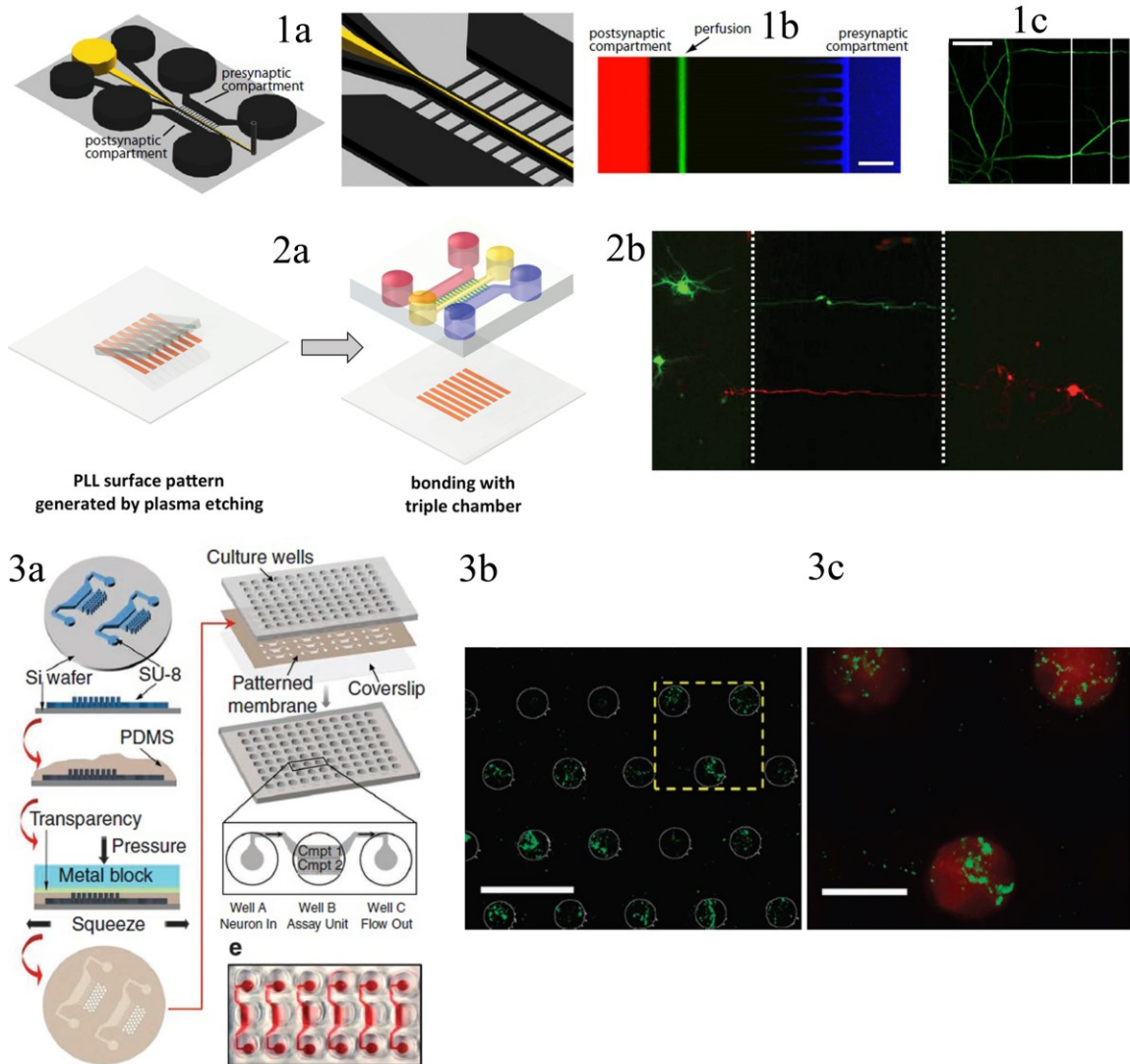


Fig 2.3: 1a. A schematic of the local perfusion chamber with three-inlet wells, 1b. Stable microenvironments with perfusion, 1c. Labeled neuron following perfusion (adapted from [100] copyright 2010 Elsevier), 2a. Schematic for micropatterning of PLL strip on a substrate and its integration with a compartmentalized microfluidic neuron culture device, 2b. Neurons transfected differentially in different compartments (adapted from [96] copyright 2012 American Chemical Society), and 3a. Schematic of the fabrication of synapse microarray, 3b Synapsin clustering in microwells with HEK293 cells, and 3c. Enlarged view of the box (adapted from [99] copyright 2011 Nature Publishing Group)

2.3.3 Multi-compartment Chamber devices for Co-Culture

Vertebrate nervous system is made up of several types of cells: neurons, astrocytes, oligodendrocytes, microglia in CNS, and neurons, Schwann cell in PNS. To effectively study the organization of nervous system, apart from studying individual populations one needs to study the interactions between several types of cells that make up the system. It is the only way to elucidate the emergent properties of the system which consists of paracrine signaling, action potential conduction, and pathologies associated with several neurodegenerative diseases like Multiple Sclerosis, Alzheimer's, Parkinson's etc. Nervous system also exchanges information with several other physiological systems in the body of an organism which makes it imperative to study the interactions between different types of cells. Typically, a cell co-culture platform should be able to (1) incorporate cells of various types in distinct regions, (2) self-sustain and provide optimal culture conditions, (3) selectively address, manipulate, and maintain each cell type without influencing the rest, (4) and control cell-cell interactions. Microfluidic platforms have the potential to meet all these requirements and several groups have taken up this aspect of microfluidics in co-culture studies for neuroscience.

Park *et al.* [103] developed a multi-compartment microfluidic platform for co-culture studies of neurons and glia. The device design consists of an inner circular compartment for cell body isolation and an outer concentric circular array of 6 axonal compartments that are interspaced evenly at 400 μm . Each axonal compartment is connected to the central cell body reservoir by high fluidic resistance microchannels. They developed Micro-macro Hybrid Soft-lithography Master fabrication (MMHSM) technique

to enable the co-existence of both microscale and macroscale structures in single PDMS master molds. They studied parallel and localized biomolecular treatment capability of the device and myelination of axons by oligodendrocyte progenitor cells. Majumdar *et al.* [59] developed a microfluidic platform for neuron-glia co-culture which incorporates a valve, that when compressed enables complete isolation between the two types of cells acting as a physical barrier unlike in other devices where the fluidic isolation is achieved by hydrostatic pressure difference. In this device, the incorporation of valve completely eliminates interactions of any kind, even the smallest diffusions that may occur in hydrostatic fluidic isolation. The device design consists of two chambers one each for each cell type: neurons, and glia which are connected by microchannels and completely isolated by a pneumatically controlled valve. Gao *et al.* [60] further modified the device to mimic 3D cell culture system by using gels sandwiched between the two sides of a modified valve. Takeuchi *et al.* [58] assembled a multielectrode-array with a microfluidic platform to co-culture cells from different systems: neurological and cardiovascular. Their device enables investigation of relations between cardiac fibrillation and sympathetic nervous system.

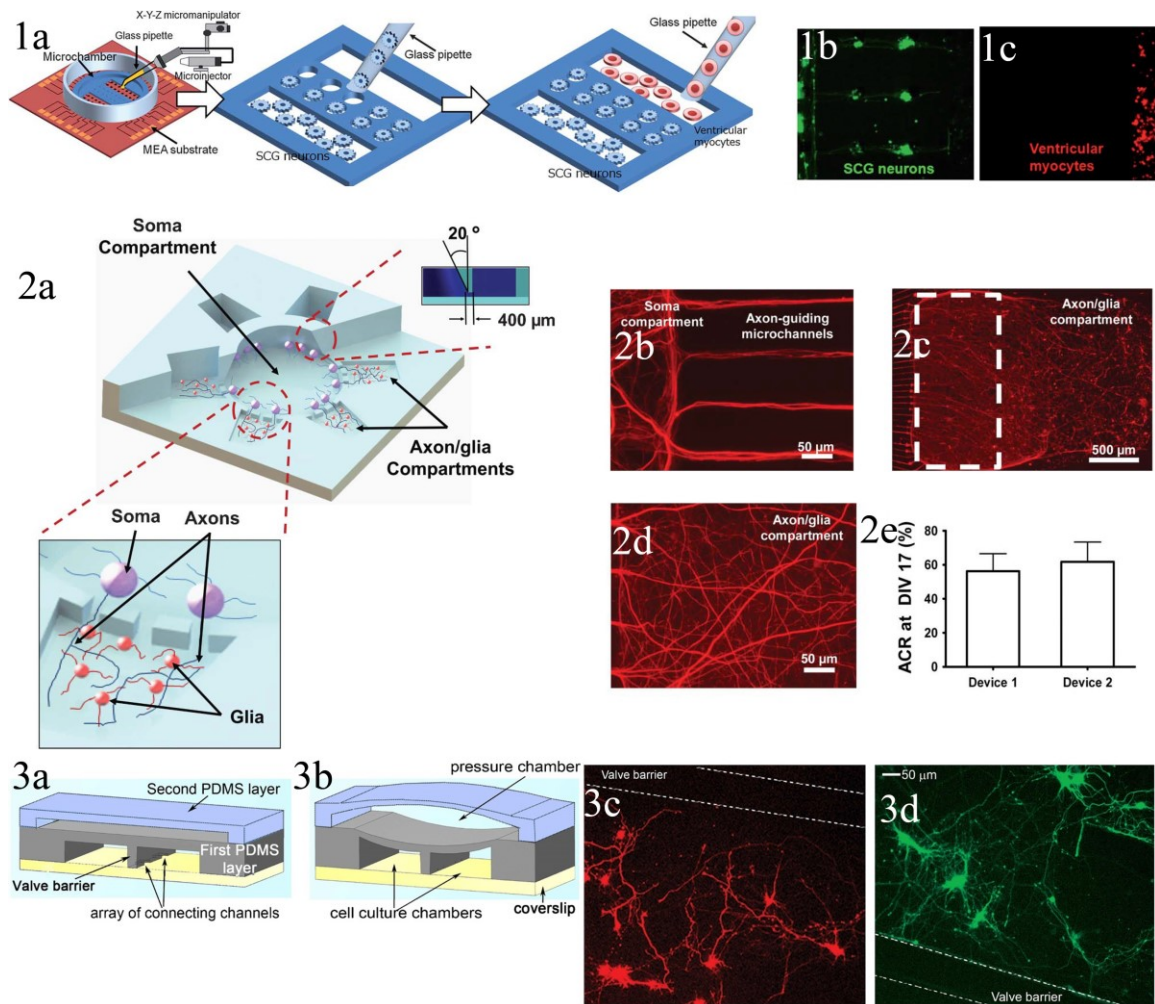


Fig 2.4: A. Schematic of the co-culture device for sympathetic neurons and cardiomyocytes, 1b SCG neurons in left compartment and 1c. Ventricular myocytes in the right compartment (adapted from [58] with permission from The Royal Society of Chemistry), 2a. Schematic of the multi-compartment neuron-glia co-culture microsystem capable of carrying out multiple localized axon treatments in parallel, 2b, 2c & 2d. Depict axon-glia co-culture separated by microchannels, and 2e. Depicts the reproducibility (adapted from [103] with permission from The Royal Society of Chemistry), 3a & 3b. Schematic of device that allows co-culture and separation with valves, 3c & 3d. Neurons in adjacent compartments transfected with different vectors (adapted from [59] copyright Elsevier 2010).

2.3.4 Multi-compartment Chamber device for Injury, Regeneration, and Degeneration

Focal or multifocal abuse to the axons in the white matter tracts of Central Nervous System (CNS) during Traumatic Brain Injury (TBI) and or Spinal Cord Injury (SCI) leads to Traumatic Axonal Injury (TAI). These injuries often lead to irreversible damage

resulting in permanent loss of function. Modeling studies help to understand the biological mechanisms of nerve regeneration and degeneration and play a role in developing new therapeutic strategies. There are several modes of experimental setups: *in vivo*, *in vitro*, and *in silico* models to study injury. *In vivo* animal models of trauma permit the study of whole organism's response to a multitude of complex variables and permit behavioral outcome studies. Though these models are useful, they are highly complex, of low reproducibility, involve large number of parameters, labor intensive, need specific skills, very time consuming, and most important of all, *in vivo* models lack tools to monitor events post injury and axonal regeneration in real time. *In vitro* models on the other hand allow the study of biochemical pathways, gene expression levels, and phenotypic changes to the level of a single axon. *In vitro* models also facilitate the study of different types of traumatic injuries like transection, compression, stretch, and shear[104].

Microfluidics provide a powerful alternative to the existing *in vivo* and *in vitro* methods to model and study the axon injuries. They provide platforms: to model and study at single cell resolutions, that can be automated, with scope for multiplexing and high throughput[14]. Broadly classified, the modes of inducing injuries in neurons on these platforms are: (1) Physical, (2) and Chemical. Physical modes include employing laser ablation techniques [26-28], valve based compression of axons[61], microsurgeries and axotomy, are amongst the several to name. On the other hand chemical injuries are mostly caused by neurotoxins with different modes of action [105].

Taylor *et al.* [106] pioneered in developing a multicompartment microfluidic platform to study CNS axon injury, regeneration and transport. The device design consists of two identical compartments physically separated by microchannels. Using this device platform they successfully isolated CNS axonal mRNA, and studied somal transcription activity in response to axotomy by vacuum aspiration in axonal compartment. Hellman *et al.* [107] developed a microfluidic platform integrated with picosecond lasers to study axonal injury and regeneration. Microfluidic injury platform combines MIMIC for surface patterning: alternating strips of Chondroitin Sulfate Proteoglycans (CSPG) and poly-L-lysine were laid. The platform enables study of events after a partial or complete transection of axon. Kim *et al.* [108] developed a neuro-optical microfluidic platform integrating femtos second laser with microfluidic platform to study single axon injury and regeneration. The device model resembles that of Taylor *et al.* [106] with longer channels up to 5 mm in length. Yang *et al.* [25] developed a compartmentalized open chamber microfluidic device to study the toxicity of chemotherapeutic drug paclitaxel.

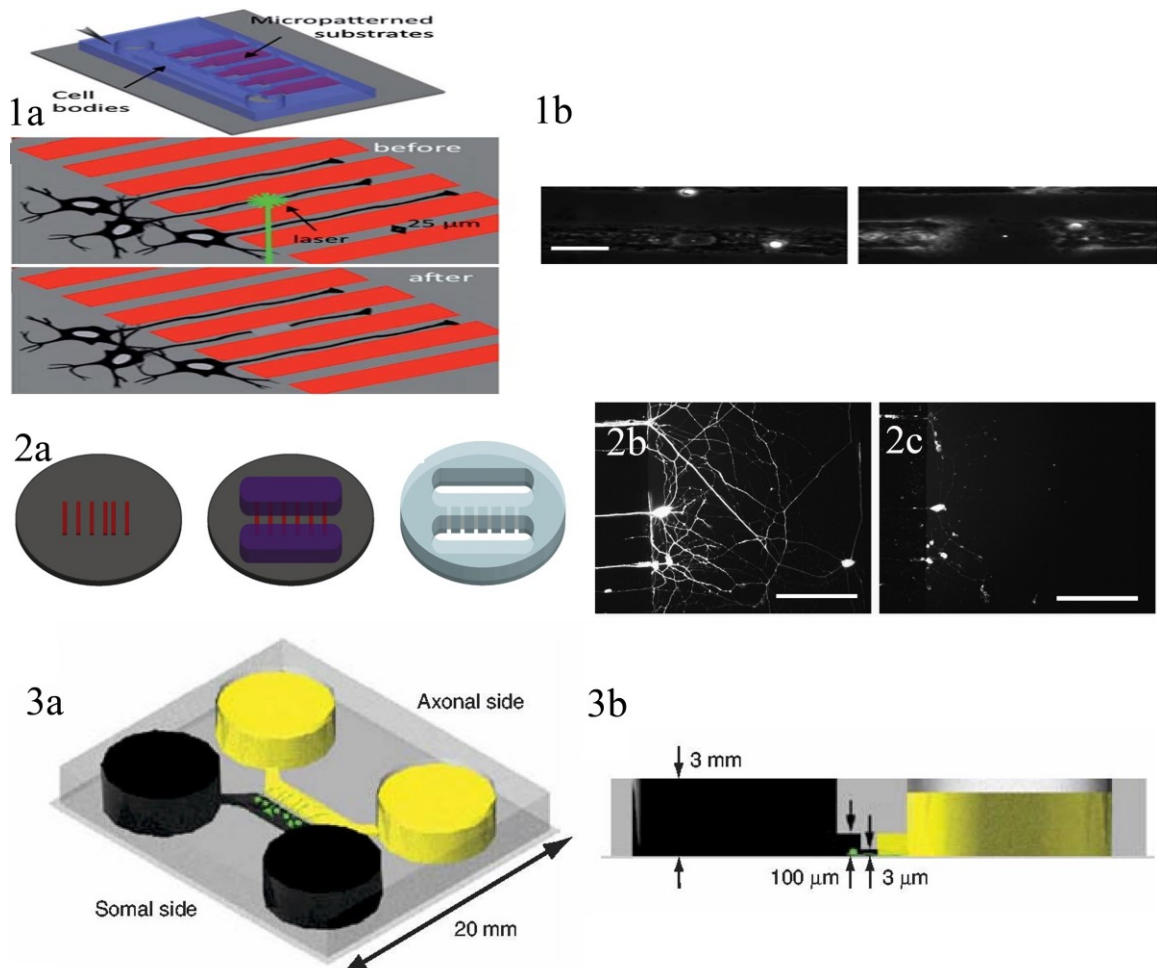


Fig 2.5: 1a. Microfluidic-based culture platform with illustrations of laser induced axotomy, 1b. Axotomy of 25 μm axon strips with 180 ps laser pulse (adapted from [107] with permission from The Royal Society of Chemistry). 2a. Schematic of the microfluidic device to study chemical injury, 2b & 2c. Chemical influenced degradation of axons with axonal side application of the chemical (adapted from [25] copyright Elsevier 2009), 3a & 3b. Schematic of the microfluidic culture platform for compartmentalization and fluidic isolation of axons from cell body (adapted from [106] copyright Nature Publishing Group 2005)

2.3.5 Multi-compartment Chamber device for Electrical Stimulation and Recording

Neuronal organization as complex circuits and networks involve communication between neurons via chemical signaling. To determine the state and activity of a circuit or network one could either track the real time metabolic activity of each and every neuron involved or monitor fluctuations of the extra cellular field potential in the vicinity of the

neurons involved. In a reductionist approach, one is more interested in the activity of a single neuron and ion channels involved. Based on the scale that the neurons operate, LOC offers great potential for developing novel platforms to record as well as stimulate activity in individual neurons. Kathryn *et al.* [109] developed soft material based PDMS electrode arrays to measure activity in individual neurons. These microfabricated soft electrodes are highly reproducible and allow high-resistance seal with cell membranes. Ravula *et al.* [110] microfabricated compartmented culture system to study neurons by established fluidic isolation. The axon were guided by tracks of collagen on glass substrate containing multi electrode arrays. This platform allows studying the effects of drugs on neurons with compartmentalization and selectively observe the electrical activity. Peterman *et al* [111] developed the artificial synapse chip, a high-resolution physiological retinal interface which incorporates MEMS techniques of micro-patterning of cells, and localized chemical stimulations with flexible and biocompatible materials. The incorporation of MEMS techniques in developing potential retinal interfaces is an advancement that is welcome in addressing issues with exiting interfaces. MEMS can be used for stimulating retinal cells at great complexities with maintaining the integrity of a retina.

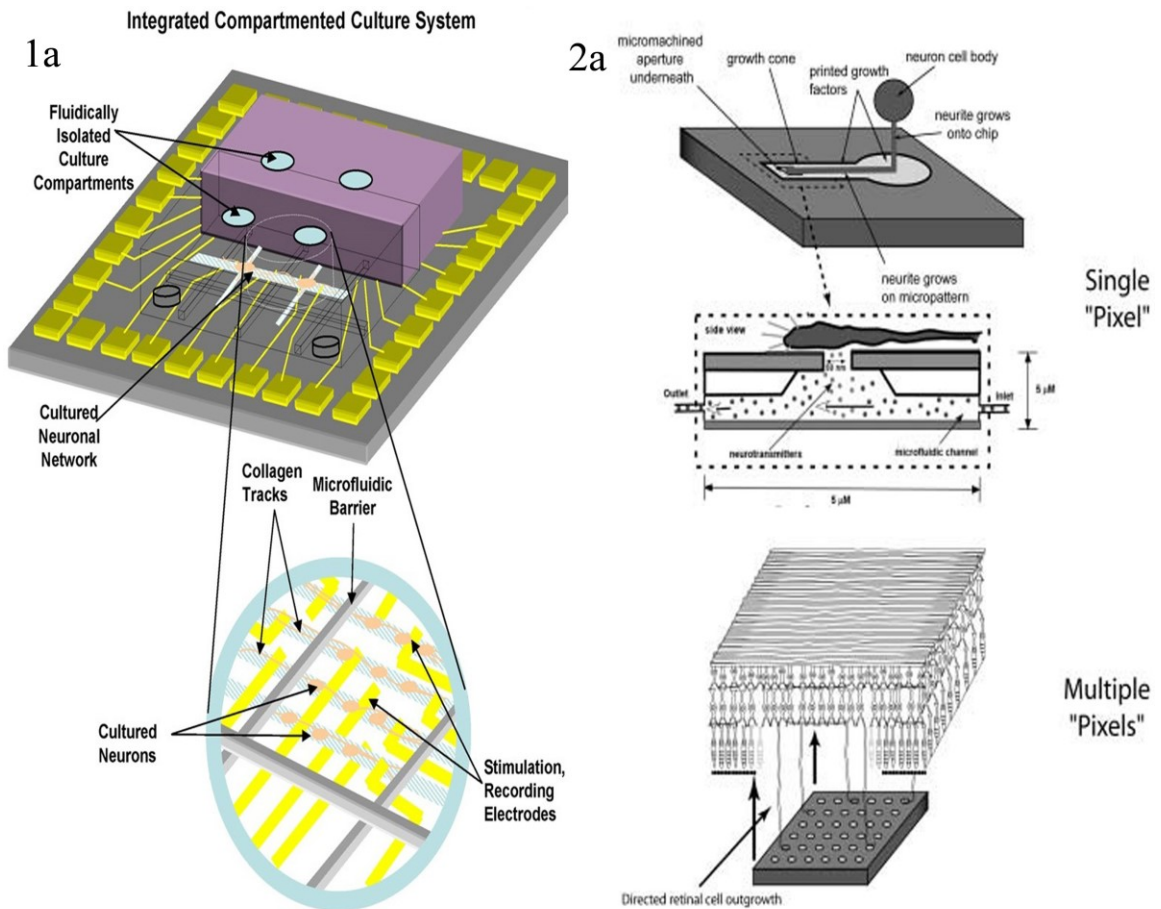


Fig 2.6: 1a. Schematic of integrated compartmented culture system, with microfluidic barriers and microelectrode array interfacing with cultured neurons. The multicompartment divider is aligned to and seated on the microelectrode array. Neurons are then plated in one or more of the compartments, after which they grow into adjacent compartments. Stimulation and recording electrodes on the microelectrode array interface with somal bundles and their processes in all of the compartments, allowing for complicated studies in which both neuronal pharmacology and electrophysiology can be simultaneously studied. (Adapted from [110] copyright Elsevier 2006), 1b. Conceptual sketches of the Artificial Synapse Chip. With an illustration of a single stimulation site and a multiple pixel device shown interfacing the retina. (Adapted from [111] copyright John Wiley and Sons 2003)

2.3.6 Multi-compartment Chamber devices from our group

2.3.6.1 Circular Compartmentalized co-culture device for axon-glia interactions

A circular compartmentalized LOC platform was developed in the lab to co-culture neurons with glial cells and study axon-glia interactions[24]. The rationale behind developing such a platform is that several neuroinflammatory and neurodegenerative

diseases strongly imply specific interactions between axons and glia [112, 113]. Then existing culture techniques did not support precise placement of cells and control of cell body and axonal microenvironments; this device is developed to address these issues. The developed LOC platform has two concentric arrays of multiple independent compartments which are interconnected by several microchannels between the inner circular and outer circular compartments in a one on one mapping. The circular geometry of the device allows for ready merging of adjacent compartments allowing to maintain independent cell bodies or axons in either distinct or uniform microenvironments. The circular geometry of the device also enables the enhancement of axonal output through microchannels by centrifugation. It also enables use of patterned microstencils to directly place glial cells within areas of interest in the axonal compartment.

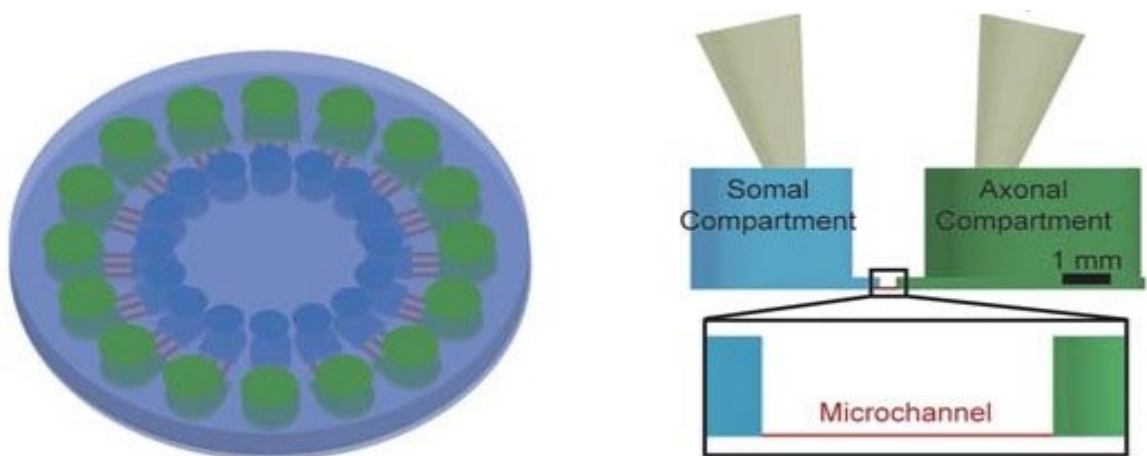


Fig 2.7: 3D schematic of the PDMS device with compartments and microchannels in the side to aid visualization (adapted from [16] with permission from The Royal Society of Chemistry).

MATERIALS

REAGENTS

Poly-D-lysine (PDL) (100 $\mu\text{g ml}^{-1}$, Sigma)

Sodium tetraborate, (99%, 100 g, Sigma)

Boric acid, (99.5%, 100 g, Sigma)

PDMS (Sylgard 184, Dow Corning)

Neurobasal media (Invitrogen)

Disposable plastic weigh boats for mixing PDMS

Disposable plastic stir rods

40 mm glass bottom petri dishes (Willco Wells, Netherlands)

Razor blades

Sharpened stainless steel punch

Transparency mask (CAD/Art service)

Photoresists, SU-8 2002 and SU-8 3050 (Microchem)

SU-8 photoresist developer (Microchem)

4 inch silicon wafer (WRS Materials, CA)

EQUIPMENT

Digital balance

Laboratory oven for curing PDMS

Vacuum desiccator for degassing PDMS

Plasma cleaner (Harrick Plasma, NY)

REAGENT SETUP

Neuron culture media: Neurobasal media.

Borate buffer solution: Prepare 0.1M borate buffer solution (1.24 g boric acid, 1.9 g sodium tetraborate, 400 ml Nanopure water, pH 8.5).

PDL solution: Dissolve 400mg of PDL (1 mg ml^{-1}) in borate buffer solution by stirring for 30 min. Sterilize the solution by filtration with 0.2 μm filter. PDL solution can be stored at $-20 \text{ }^\circ\text{C}$ for future use.

PROCEDURE

Fabrication of master template TIMING 9 h

1. Dehydration Bake: Clean a 4-inch Si wafer with compressed N_2 gas and place it on a hot plate set at $200 \text{ }^\circ\text{C}$ for 10 minutes for dehydration bake. (If the relative humidity is $>10\%$ you may have to increase the duration of the bake.)
2. Plasma treatment: Plasma treat the dehydrated Si wafer with O_2 plasma at 350 mtorr pressure and 250 W power for 3 minutes to clean the wafer surface and improve surface roughness for better adhesion to photoresist.
3. Photo resist coating: Flood SU-8 2002 photoresist on a plasma treated 4-inch Si wafer and spin at 1,000 rpm for 30 s ($2.5\text{-}3 \text{ }\mu\text{m}$ thick).
4. Soft bake: Bake the photo resist coated wafer for 2 min at $95 \text{ }^\circ\text{C}$ on a leveled hot plate.
5. Exposure: Expose the soft baked wafer through a high-resolution transparency mask (20,000 dpi, CAD/Art, OR) containing a circular array of 1500 microchannels of width $8\text{-}10 \text{ }\mu\text{m}$ and length $500 \text{ }\mu\text{m}$ evenly spaced at $15\text{-}25 \text{ }\mu\text{m}$ at 100 mJ/cm^2 .
6. Post exposure bake: After exposure, bake the wafer at $95 \text{ }^\circ\text{C}$ for 4 min on a hot plate.

7. Development: Develop with SU-8 developer (photoresist developer) by spraying the developer on the wafer until all of the unexposed photoresist is stripped off.
8. Rinse with isopropyl alcohol two or three times to check the development, if it leaves white streaks on the wafer use the developer again.
9. Spin dry the wafer to remove excess developer and or isopropyl alcohol.
10. Heat the developed wafer on hot plate at 95 °C for 10 min to remove any residual fluid to improve adhesion for the second layer of photo resist on wafer.
11. Photo resist coating: Spin a second layer of photoresist, SU-8 3050, at 1,000 rpm for 30 s (150 μm thick).
12. Soft bake: Bake the second layer of photo resist for 45 min at 95 °C on a leveled hot plate.
13. Mask alignment: Align a high-resolution transparency mask (CAD/Art, OR) containing an outer circular array of axon ports (4 mm in diameter) and an inner circular array of soma ports (3 mm in diameter) with the alignment cues on the soft baked wafer from the first layer of photoresist.
14. Exposure: Expose the soft baked wafer through the aligned high-resolution transparency mask for the second layer at 250 mJ/cm².
15. Post exposure bake: After exposure, bake the wafer at 95 °C for 5 min on a hot plate.
16. Development: Develop with SU-8 developer (photoresist developer) by spraying the developer on the wafer until all of the unexposed photoresist is stripped off.
17. Rinse with isopropyl alcohol two or three times to check the development, if it leaves white streaks on the wafer use the developer again.
18. Spin dry the wafer to remove excess developer and or isopropyl alcohol.

19. Hard bake: Bake the wafer at 150 °C on a hot plate at least for 6 hours.

Fabrication of PDMS devices by replica molding TIMING 4 h

20. Weigh out a 10:1 ratio (50 g + 5 g) of PDMS base to cross-linker into a disposable weigh boat and mix thoroughly for 5–10 min.

CRITICAL STEP: If PDMS is not mixed thoroughly or the amount of catalyst is not adequate, PDMS will not cure completely and will make the master mold unusable.

21. Place the PDMS mixture in a vacuum desiccator and degas the bubbles formed during mixing for 30-60 min.

22. Passivate the Si wafer by silane treatment for 10 – 15 min (usually longer, 45-60 min during first use).

23. Place the master template wafer in a plastic weigh boat and while gently pressing on it with a Q-tip slowly pour the PDMS mixture over it to achieve a thickness of 5-7 mm. Let the PDMS spread out and settle evenly for 10 min. If there are any bubbles in the region of interests pop them with sterile pipette tips or a clean razor blade.

24. Place the weigh boat in a leveled laboratory oven and cure for 60 min at 80 °C. The PDMS mixture will solidify and become transparent when fully cross-linked or cured.

25. Cut the plastic weigh boat to remove the cured PDMS mold with master. Carefully remove the PDMS mold from the master wafer applying gentle pressure in order to not to break the wafer.

26. Using a steel circular punch excise out the devices from the cured PDMS replica of master mold.

27. Punch out the somal ports using 3 mm biopsy punches and punch out the axonal ports using 4 mm biopsy punches with the channel side up. Clean both the surfaces by using a Scotch tape to remove any debris resulted during the excision.
28. Further sonicate the cleaned devices in 100% ethanol for 5 min with feature side down to remove any residual debris. Once sonicated, clean the devices with compressed air to remove PDMS debris and other surface contaminants.

Cleaning the glass bottoms and bonding with the devices TIMING 30 min

29. Sonicate the 40 mm glass bottom petri dishes in 100% ethanol for 5 min with the bonding side down. Once sonicated, clean the glass bottoms with compressed air to remove surface contaminants.

CRITICAL STEP Debris removal on both the bonding surfaces is paramount for a leak free and tight seal. Small particles resulting during punching can act as barriers when bonding PDMS to glass substrate.

30. For a reversible seal bring into contact the cleaned devices (with features side down) and cleaned glassed bottoms which seal reversibly upon contact.
31. For a tighter seal, treat both the device and the glass bottom surfaces with oxygen plasma at 45 W for 1 min and bring into contact the feature side surface of the device to the glass bottom and gently press on the device against the glass bottom for a tight seal.

CRITICAL STEP: When sealing the PDMS to substrate, do not press around the channels region, as they can collapse and may be blocked when excessive pressure is applied.

Coating the assembled devices with PDL TIMING 13-14 h

32. Sterilize the devices with 70% ethanol and wash the device thrice with doubly deionized water to remove excess ethanol under a sterile laminar hood.

33. Coat the devices with PDL by adding PDL only to one of the two ports of the device and let the PDL flow. Once the PDL flow is established, top both the ports with PDL and set the devices aside for overnight coating at 37 °C in a humidified incubator.

CRITICAL STEP Make sure that no air bubbles are trapped to ensure uniform coating of PDL.

34. Remove the PDL from all the ports and wash off excess PDL in 3 rinses with doubly deionized water.

35. Add the Neurobasal media in the ports and store the device at 37 °C until needed for experimentation.

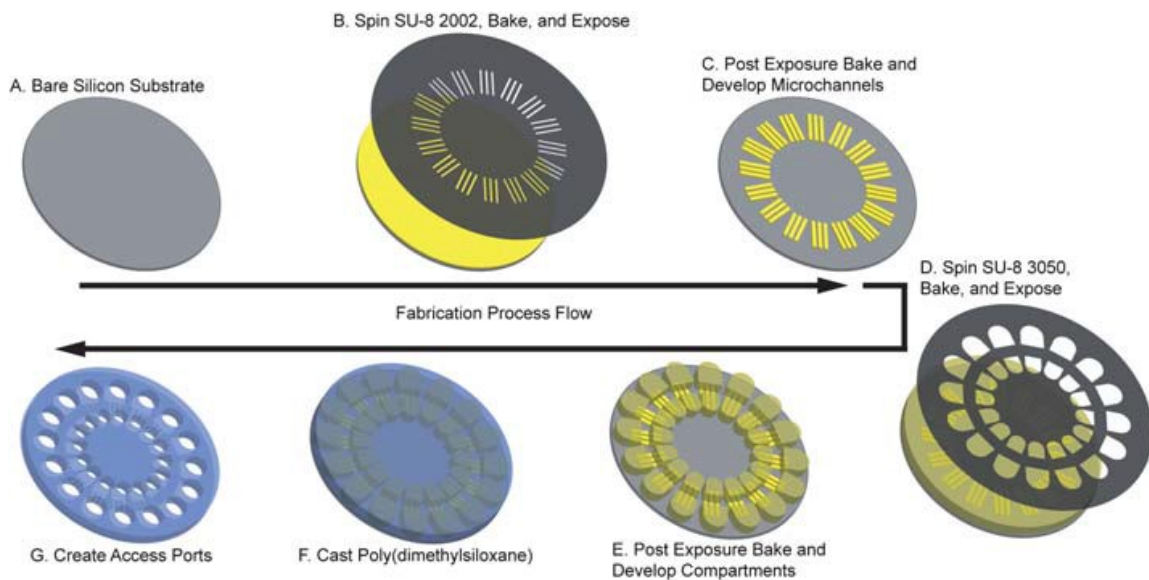


Fig 2.8: The device mold was constructed using standard SU-8 photolithography. (A) Beginning with a bare silicon wafer, (B) an initial thin-film resist layer (SU-8 2002; height $\frac{1}{4}$ 2.5 mm) was spun, soft baked, and optically exposed. (C) Subsequently, the substrate was post exposure baked and immersed in developer to define the circular array of microchannels. (D & E) The thick-film resist (SU-8 3050; height $\frac{1}{4}$ 150 mm) was processed similarly to define larger fluidic access ports. After (F) PDMS replication, (G) devices were customized through the use of commercially available dermal biopsy punch tools. (Reproduced from [16] with permission from The Royal Society of Chemistry)

The circular compartmentalized microfluidic neuron culture device offers a novel method to integrate large access ports in close proximity to (a) microchannels providing straightforward loading of cells near microchannels, (b) increase the cell density near the entrance of microchannels with optimized platform geometry so that centrifugal forces can be quickly applied to manipulate neuronal cell distribution, (c) manipulate co-culture conditions using micropatterning techniques, (d) study axon micro glial interactions, (e) study differential microglial response to injured axons, and (f) establish hydrostatic pressure to achieve fluidic isolation. The other advantages that the circular geometry of the device confers is that the external forces required to enhance cell placement at the end of the microchannels are minimal which has a direct implication in maximizing the cell viability and perpetuating axon-glia co-culture. This microfluidic device can serve as an *in vitro* model for CNS injury. We utilized this platform to demonstrate preferential accumulation of microglia specifically to injure as compared to healthy axons, serving as a foundation to elucidate mechanisms of axon–glia interactions in neurological disease maintenance and progression. Overall, this novel multi-compartment co-culture platform enables distinct modes of axon–glia co-culture and provides experimental versatility to investigate axon-specific and axon–glia-specific cellular and molecular events implicated in neurobiological disease.

2.3.6.2 Circular Compartmentalized device for microglial phagocytosis of axons

A novel circular compartmentalized LOC platform was developed in the lab to co-culture neurons with microglial cells to investigate mechanisms of microglial phagocytosis of bundled axons [114]. The rationale behind developing such a platform is that the

persistence of endogenous debris in mammalian CNS is one of the foremost barriers to regeneration after injury [115, 116]. A critical insight into the microglial debris clearance mechanism in CNS opens new avenues for CNS repair strategies. Then existing culture techniques did not support precise placement of microglia and control of cell body and axonal microenvironments. The current device is developed to address these issues. The developed LOC platform uses an extra cellular matrix (ECM) patterning device to create 25 μm wide tracks of PDL for the axons to grow along and bundle in a circular arrangement. These tracks are evenly spaced with a gap of 25 μm in between them facilitating the attachment of microglia. Once the ECM tracks are laid a similar circular LOC device with microchannels is aligned on the tracks. The ECM patterning facilitates that the axon bundles remain spatially distinct and localized from microglia once emerging from the microchannels. This spatial demarcation enables quantification of axonal debris by microglia.

MATERIALS

REAGENTS

Poly-D-lysine (PDL) (200 $\mu\text{g ml}^{-1}$, Sigma)

Sodium tetraborate, (99%, 100 g, Sigma)

Boric acid, (99.5%, 100 g, Sigma)

PDMS (Sylgard 184, Dow Corning)

Neurobasal media (Invitrogen)

Disposable plastic weigh boats for mixing PDMS

Disposable plastic stir rods

40 mm glass bottom petri dishes (Willco Wells, Netherlands)

Razor blades

Sharpened stainless steel punch

Transparency mask (CAD/Art service)

Photoresists, SU-8 2002 and SU-8 3050 (Microchem)

SU-8 photoresist developer (Microchem)

4 inch silicon wafer (WRS Materials, CA)

EQUIPMENT

Digital balance

Laboratory oven for curing PDMS

Vacuum desiccator for degassing PDMS

Plasma cleaner (Harrick Plasma, NY)

REAGENT SETUP

Neuron culture media: Neurobasal media.

Borate buffer solution: Prepare 0.1M borate buffer solution (1.24 g boric acid, 1.9 g sodium tetraborate, 400 ml Nanopure water, pH 8.5).

PDL solution: Dissolve 400mg of PDL (1 mg ml^{-1}) in borate buffer solution by stirring for 30 min. Sterilize the solution by filtration with 0.2 mm filter. PDL solution can be stored at $-20 \text{ }^{\circ}\text{C}$ for future use.

PROCEDURE

Fabrication of master template TIMING 9 h

- a. The master template of ECM patterning device consists of only one layer of photoresist defining the height of channels for ECM tracks. The fabrication of which is similar to the one described in the previous section in following steps: 1-10 & 19.

- b. The master template for the co-culture device consists of two layers of photoresist defining the height of channels and the height of chambers. The fabrication of which is similar to the one described in previous section in following steps: 1-19

Fabrication of PDMS devices by replica molding TIMING 4 h

- a. Fabrication of ECM patterning device by replica molding is similar to the one described in the previous section in following steps: 20-28
- b. Fabrication of co-culture device by replica molding is similar to the one described in the previous section in following steps: 20-28

Cleaning the glass bottoms and bonding with the devices TIMING 30 min

1. Sonicate the 40 mm glass bottom petri dishes in 100% ethanol for 5 min with the bonding side down. Once sonicated the glass bottoms are cleaned with compressed air to remove surface contaminants.

CRITICAL STEP Debris removal on both the bonding surfaces is paramount for a leak free and tight seal. Small particles resulting during punching can act as barriers when bonding PDMS to glass substrate.

2. For a reversible seal bring into contact the cleaned devices (with features side down) and cleaned glassed bottoms which seal reversibly upon contact.
3. For a tighter seal, treat both the device and the glass bottom surfaces with oxygen plasma at 45 W for 1 min and bring into contact the feature side surface of the device to the glass bottom and gently press on the device against the glass bottom for a tight seal.

CRITICAL STEP: When sealing the PDMS to substrate, do not press around the channels region, as they can collapse and may be blocked when excessive pressure is applied.

Coating the assembled devices with PDL TIMING 13-14 h

4. Sterilize the devices with 70% ethanol and wash the device thrice with doubly deionized water to remove excess ethanol under a sterile laminar hood.
5. Coat the devices with PDL by adding PDL only to one of the two ports of the device and let the PDL flow. Once the PDL flow is established, top all the ports with PDL and set the devices aside for overnight coating at 37 °C in a humidified incubator.

CRITICAL STEP Make sure that no air bubbles are trapped to ensure uniform coating of PDL.

6. Remove the PDL from both the ports and wash off excess PDL in 3 rinses with doubly deionized water.
7. Add the Neurobasal media in the ports and store the device at 37 °C until needed for experimentation.

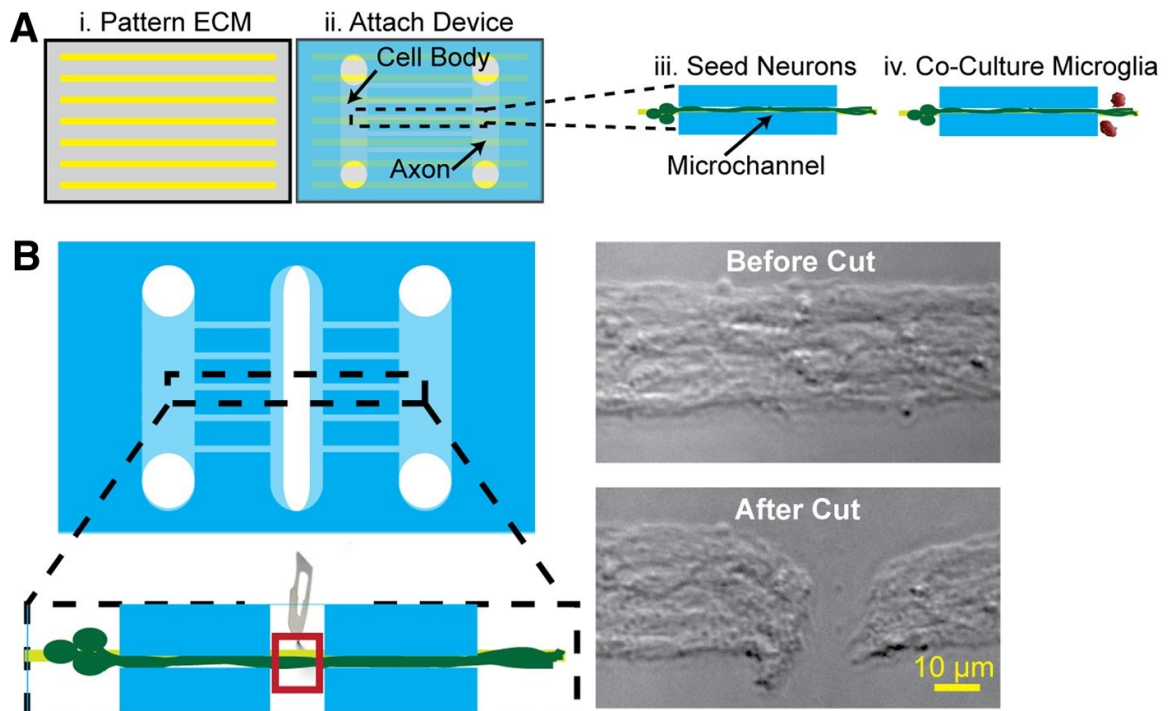


Fig 2.9: Microfluidic platform enables the study of microglial phagocytosis of axons. **Ai**, A patterning process was used to create 25 μm -wide PDL stripes interspersed by 25 μm gaps. **Aii**, The microfluidic coculture device was aligned and bonded. **Aiii**, **Aiv**, Neurons cultured within the cell body compartment extended axon bundles through the microchannels and into the axon/glial coculture compartment (**Aiii**) where microglia were later cocultured (**Aiv**). **B**, The microfluidic platform was modified by creation of a third compartment. Before addition of wild type or TRIF knock out mouse microglia, a scalpel was used to sever a 10 –20 μm segment of the bundle. (Adapted from [114] copyright 2012 Society For Neuroscience)

The circular compartmentalized microfluidic neuron culture device offers novel methods to integrate large access ports in close proximity to (a) microchannels providing straightforward loading of cells near microchannels, (b) increase the cell density near the entrance of microchannels with optimized platform geometry so that centrifugal forces can be quickly applied to manipulate neuronal cell distribution, (c) manipulate co-culture conditions using micropatterning techniques, (d) study axon micro glial interactions, (e) study differential microglial response to injured axons, and (f) establish hydrostatic pressure to achieve fluidic isolation. The other advantages that the circular geometry of the device confers is that the external forces required to enhance cell placement at the end of

the microchannels are minimal which has a direct implication in maximizing the cell viability and perpetuating axon-glia co-culture. This microfluidic device can serve as an *in vitro* model for CNS injury. Hosmane *et al.* [114] utilized this platform to demonstrate preferential accumulation of microglia specifically to injure as compared to healthy axons, serving as a foundation to elucidate mechanisms of axon–glia interactions in neurological disease maintenance and progression. Overall, this novel multi-compartment co-culture platform enables distinct modes of axon–glia co-culture and provides experimental versatility to investigate axon-specific and axon–glia-specific cellular and molecular events implicated in neurobiological disease.

2.3.6.3 Valve based multi compartmental device for Traumatic Axonal Injuries

A novel microfluidic compression platform called axon injury micro-compression (AIM) platform to study traumatic axonal injuries (TAI) at single axonal resolution was developed in the lab [61]. The active component in inflicting a focal and graded injury to a single axon is a compressible valve that can be pushed down on to the axons with varying forces. This device when combined with time-lapse microscopy allows monitoring the fate of axons during the time course of an injury. Existing devices had shortcomings in delivering focal and graded compression injuries to the axons, and studying the time course of injury [117]. The device design consists of two layers: (1) fluid layer, that contacts glass substrate, and (2) control layer, that defines compression and subsequent deflection of valve by fluid. Fluid layer in contact with the glass substrate defines three distinct compartments: (1) cell body, (2) injury, and (3) axonal. This compartmentalization enable

the study of TAI independent from cell bodies and the injured axons can be subject to differential treatment with respect to the cell bodies.

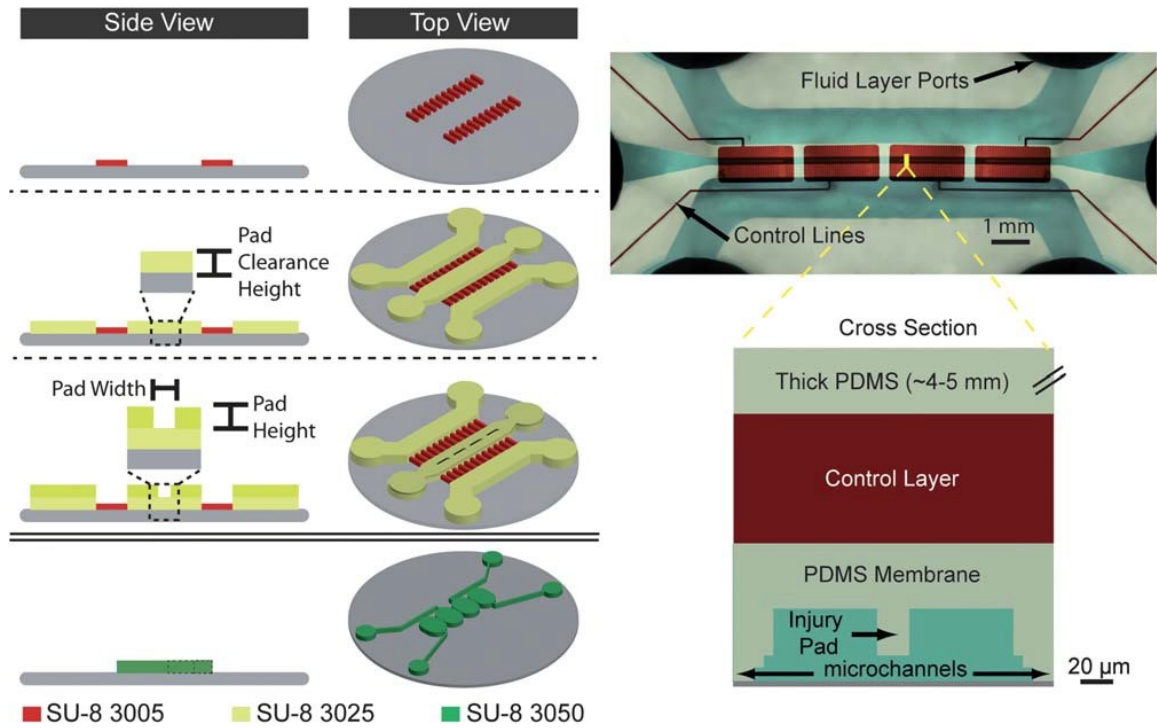


Fig 2.10: Schematic of AIM platform with master template on the left and PDMS device on the right (adapted from [61] with permission from The Royal Society of Chemistry).

MATERIALS

REAGENTS

Poly-D-lysine (PDL) ($200 \mu\text{g ml}^{-1}$, Sigma)

Sodium tetraborate, (99%, 100 g, Sigma)

Boric acid, (99.5%, 100 g, Sigma)

PDMS (Sylgard 184, Dow Corning)

Neurobasal media (Invitrogen)

Disposable plastic weigh boats for mixing PDMS

Disposable plastic stir rods

40 mm glass bottom petri dishes (Willco Wells, Netherlands)

Razor blades

Sharpened stainless steel punch

Transparency mask (CAD/Art service)

Photoresists, SU-8 3005, SU-8 3025, and SU-8 3050 (Microchem)

SU-8 photoresist developer (Microchem)

4 inch silicon wafer (WRS Materials, CA)

EQUIPMENT

Digital balance

Laboratory oven for curing PDMS

Vacuum desiccator for degassing PDMS

Spin coater

Plasma cleaner (Harrick Plasma, NY)

REAGENT SETUP

Neuron culture media: Neurobasal media.

Borate buffer solution: Prepare 0.1M borate buffer solution (1.24 g boric acid, 1.9 g sodium tetraborate, 400 ml Nanopure water, pH 8.5).

PDL solution: Dissolve 400mg of PDL (1 mg ml^{-1}) in borate buffer solution by stirring for 30 min. Sterilize the solution by filtration with 0.2 mm filter. PDL solution can be stored at $-20 \text{ }^{\circ}\text{C}$ for future use.

PROCEDURE

Fabrication of master template TIMING 9 h

- c. The master template of AIM device consists of three layers of photoresist defining the height of channels, clearance for the injury pad, and the chambers respectively. The fabrication of which is similar to the one described in the previous section in following steps: 1-18 for the first two layers and then 10-19 for the third layer.

Fabrication of PDMS devices by replica molding TIMING 4 h

1. Weigh out a 10:1 ratio of PDMS base to cross-linker into a disposable weigh boat and mix thoroughly for 5–10 min. 50 g + 5 g for control layer, and 10 g + 1 g flow layer.

CRITICAL STEP: If PDMS is not mixed thoroughly or the amount of catalyst is not adequate, PDMS will not cure completely and will make the master mold unusable.

2. Place the PDMS mixture in a vacuum dessicator and degass the bubbles formed during mixing for 30-60 min.
3. Passivate the Si wafers (control layer and flow layer) by silane treatment for 10 – 15 min (usually longer, 45-60 min during first use).
4. For the control layer, place the master template wafer in a plastic weigh boat and while gently pressing on it with a Q-tip slowly pour the PDMS mixture over it to achieve a thickness of 5-7 mm. Let the PDMS spread out and settle evenly for 10 min. If there are any bubbles in the region of interests pop them with sterile pipette tips or a clean razor blade.

For the flow layer, place the master template on a spin coater and hold it in place under vacuum. Pour the PDMS over the wafer so that atleast $\frac{1}{4}$ of the wafer is covered and spin at 800 rpm for 1.5 min.

5. Place the weigh boats in a leveled laboratory oven and cure for 20 min at 80 °C. The PDMS mixture will solidify and become transparent when fully crosslinked or cured.
CRITICAL STEP The PDMS cross-linking should be controlled in a careful manner to establish good bonding between control and flow layer. The curing step should neither be too long nor too short. The PDMS should be lightly sticky but not tacky.
6. Cut the plastic weigh boat to remove the cured PDMS control mold and master. Carefully remove the PDMS control mold from the master wafer applying gentle pressure in order to not to break the wafer. Punch the gas inlets with sharpened gauge #23 needles in each device and punch out the devices from the mold. Clean the bonding surface with scotch tape to remove debris from punching.
7. Plasma treat both the flow layer and punched control layer devices at 45 W power for 1 min. Align the control layer devices to flow layer with the help of cues on both the layers. Once aligned cure the bonded device at 80 °C overnight in the incubator.
8. Excise the devices from flow layer master template and punch ports using 3 mm biopsy punches. Clean both the surfaces by using a Scotch tape to remove any debris resulted during the excision and punching.
9. Further sonicate the cleaned devices in 100% ethanol for 5 min with feature side down to remove any residual debris. Once sonicated clean the devices with compressed air to remove PDMS debris and other surface contaminants.

Cleaning the glass bottoms and bonding with the devices TIMING 30 min

10. Sonicate the 40 mm glass bottom petri dishes in 100% ethanol for 5 min with the bonding side down. Once sonicated, clean the glass bottoms with compressed air to remove surface contaminants.

CRITICAL STEP Debris removal on both the bonding surfaces is paramount for a leak free, and tight seal. Small particles resulting during punching can act as barriers when bonding PDMS to glass substrate.

11. For a reversible seal bring into contact the cleaned devices (with features side down) and cleaned glassed bottoms which seal reversibly upon contact.

12. For a tighter seal, treat both the device and the glass bottom surfaces with oxygen plasma at 45 W for 1 min and bring into contact the feature side surface of the device to the glass bottom and gently press on the device against the glass bottom for a tight seal.

CRITICAL STEP: When sealing the PDMS to substrate, do not press around the channel region, as they can collapse and may be blocked when excessive pressure is applied.

Coating the assembled devices with PDL TIMING 13-14 h

13. Sterilize the devices with 70% ethanol and wash the device thrice with doubly deionized water to remove excess ethanol under a sterile laminar hood.

14. Coat the devices with PDL by adding PDL first to one of the two injury ports followed by cell body port and distal port on the same side of the device and let the PDL flow. Once the PDL flow is established, top all the ports with PDL and set the devices aside for overnight coating at 37 °C in a humidified incubator.

CRITICAL STEP Make sure that no air bubbles are trapped to ensure uniform coating of PDL.

15. Remove the PDL from all the ports and wash off excess PDL in 3 rinses with doubly deionized water.

16. Add the Neurobasal media in the ports and store the device at 37 °C until needed for experimentation.

With the AIM platform we could successfully establish injury thresholds for different axon responses in primary rat embryonic CNS cells and this is for the first time that a valve structure was used to injure axons in a microfluidic setting. This AIM platform can also be extended to study the secondary injury aspects in a traumatic axonal injury, like cytoskeletal changes, transport disruption, calcium fluctuations, mitochondrial fate etc. The advantages with this platform is that single axons can be isolated and a focal graded injury can be delivered in a controlled way. The time course of injured axon can be easily tracked for its fate which further enables one to conduct drug screening studies.

2.4 Discussions & Future Directions

Several practical issues as delineated earlier with *in vivo* systems in the study of neuroscience prompts one to adopt *in vitro* approaches. To reiterate, traditional *in vitro* approaches to neuroscience has its own limitations like: (1) Simulating varying extracellular microenvironment along the length of neurons, (2) Independent and interference free study of axons which has implications in neurodegenerative diseases, injuries, axonal damage, isolation of the axonal biomolecules, axonal transport studies, and (3) Co-culture studies of neurons with various cell types. To address these limitations MEMS and microfluidics are being extensively employed. Though the concept of MEMS was developed in the 70's, initially intended for chemical analysis, the presence in biology and subsequently neuroscience is being felt in the last decade. This primarily is due to the

fact that integration of MEMS technology with biology needed development of technology in its infancy to a state where it can address the complex needs of biological systems in parallel to the biology and neuroscience itself. People started realizing the potential in MEMS and developed several LOC devices for neuroscience ranging from injury studies, electrophysiology, co-culture, synaptogenesis, learning and memory, disease and therapeutic strategies etc.

Though being applied in a wide spectrum of neurobiological studies, MEMS technology is still in its early developmental phase. Majority of the existing LOC platforms are 2D systems restricting the study to a plane, and because of this current studies are limited to dissociated and organotypic cultures. In their native state, the organization of tissues and organs is 3D and neurons are no exception. Cellular organization at tissue and organ scale is non homogenous and it implies a necessity for co-culture studies. Though there are LOC platforms currently available for co-culture studies they are not sophisticated enough to perform network level studies. With the advancement in technology these may soon be addressed.

The future of LOC devices for neuroscience can be envisioned as highly modular, versatile, and programmable on similar scales of semi-conductor industry. The first generation of computers occupied huge spaces and performed limited tasks. Current generation of computers are small enough to be carried in pockets and perform a multitude of tasks simultaneousl. On a similar note, it is not exaggerating when one imagines a future

of MEMS and LOC devices with highly customizable and modular units which can be programmed to a wide and highly specific array of needs in neuroscience. Also the wide spread use of LOC platforms will enable their commercialization and use in day to day lives of people, requiring limited skills from their end.

Chapter 3

A compartmentalized culture platform to study axon regeneration and localized effects of GDNF

3.1 Introduction

Use of compartmentalized cell culture devices for neuroscience is commonplace nowadays. Conceptualized and realized as Campenot chamber in late 1970's, it is the earliest attempt at maintaining compartmentalized neuronal cell cultures. The Campenot chamber was used to isolate axons from neuronal cell bodies in studying the role of retrograde transport of neurotrophic factors in neuronal cell survival [118]. Owing to limitations like low efficiency & throughput, and cumbersome fabrication & maintenance of silicone grease barrier led to the replacement of Campenot chamber with better alternatives like bioMEMS and LOC devices. MEMS technology is being explored extensively for biological applications, part of which deals with neuronal cultures to separate somal and axonal compartments with precise control. MEMS technology being used in fabrication of LOC devices involves soft lithography for replica molding. Polydimethylsiloxane (PDMS) is the material widely chosen for several physical properties which render it useful for neuronal culture purposes both in CNS and PNS neurons [24, 25, 119]. These LOC devices have two isolated chambers physically interconnected by array of parallel microchannels. This setup enables fluidic isolation between the two chambers by establishing hydrostatic pressure differences which is maintained over extended periods of time due to high resistance of microchannels [120, 121]. Once the cells are seeded, the

proximity to the channels determines the fate of neurons to extend axons through microchannels, and application of hydrostatic pressure difference across microchannels induces fluidic isolation between axon and neuronal cell body allowing a researcher to manipulate each cellular compartment independently of each other. Despite the potential for fluidic isolation in LOC devices, no critical appraisal of separation of soluble factors has been carried out.

The purpose of this study is twofold: 1) to examine the critical parameters of microfluidic device that facilitates stable fluidic separation of somal and axonal compartments over extended periods time, and 2) to examine the site of action of three neurotrophic factors in an in vitro axotomy model of sensory axonal regeneration. We chose to use three members of the Glial cell line-derived neurotrophic factor (GDNF) family of neurotrophic factors which are previously known to play important roles in neural development and various neurological diseases [122-127]. In particular, they have been shown to promote survival and differentiation of dopaminergic neurons, motor neurons and dorsal root ganglion (DRG) sensory neurons [128-131]. Due to its therapeutic potential, a number of studies have evaluated the role of GDNF in the nervous system in the setting of disease and traumatic injury [132-134]. In addition to GDNF, other members include neurturin, neublastin, and persephin [135]. In clinical trials and animal experiments, GDNF has been shown to enhance myelination [136-138] and enhance survival of motor neurons in models of amyotrophic lateral sclerosis [139-141], and dopaminergic neurons in models of Parkinson's disease [142, 143]. Similarly, neurturin showed increased survival of motor and dopaminergic neurons [144-146] and neublastin

was effective in reducing neuropathic pain [147-149]. In addition, all members of the GDNF family showed enhancement of axon outgrowth after axotomy [150-152]. However, the biological site of action of GDNF family members in axon regeneration is not well characterized. Traditional *in vitro* settings for neuronal cultures do not facilitate compartmentalization of axons from neuronal cell bodies, thus making it difficult to delineate axon-specific mechanisms. Using the compartmentalized microfluidic chamber system we examined the parameters critical to diffusion of neurotrophic factors between the chambers and tested the regenerative potential of GDNF, neurturin and neublastin. Similar to previous publications, GDNF was most potent but its potency was most noticeable when the neurotrophic factor was applied to the neuronal cell bodies directly. To examine if the regrowth enhancement effect with axon application of GDNF was real, we applied a retrograde transport blocker, Cytochalasin D, concurrently with GDNF. We demonstrated that this effect is lowered in the presence of a transport blocker, indicating that GDNF may need to be transported to the cell body or systemically in order to see optimum growth. These results help to further elucidate GDNF's role in regeneration following injury as well allow for further factors for consideration in its potential use as a therapeutic treatment.

3.2 Materials and Methods

3.2.1 Cell preparation

All experiments involving animals were conducted according to protocols approved by the Animal Care and Use Committee of the Johns Hopkins University School of Medicine. Unless otherwise noted, tissue culture supplies were obtained from Invitrogen

(Carlsbed, CA). Dorsal root ganglia (DRG) neuronal cultures were prepared as previously described [136]. Briefly, DRGs were dissected from decapitated embryonic age day 15 rats. Once obtained, cells were enzymatically dissociated with 0.25% Trypsin in L15 medium and then suspended in media. The DRGs were maintained in Neurobasal medium containing 10% fetal bovine serum, 20% glucose, 1 % penicillin/streptomycin, B-27 supplement, 2 M L-glutamine, and 10 ng/ml glial derived nerve growth factor (GDNF). Two days after seeding cells, neurobasal media containing 10 μ M of Cytosine arabinoside was added to the cultures in order to decrease the amount of glial cells.

3.2.2 Compartmentalized microfluidic platform (CMP) preparation

A two-step photolithographic process was utilized to create the master mold. Silicon wafers (University Wafer, MA) were coated with SU-8 2002 (Microchem; MA), spun, and soft baked using parameters specified by the manufacturer to yield a resist thickness of 2.5 μ m. An array of microchannels, each with dimensions: width = 10 μ m, length = 500 μ m, were defined by UV light exposure through a high resolution DPI transparency (Cad/Art, OR). The exposed substrate was once again baked, to enhance polymer cross-linking post exposure, and developed as stated in the resist technical sheet to fully define the microchannels. The process was immediately repeated with SU-8 3050 (Microchem; MA) to define the fluidic reservoirs with dimensions: width = 3 mm, length = 13 mm. The master mold was then treated with trichlorosilane (United Chemical Technologies; PA) for 30 minutes to create a nonstick surface for subsequent processing. Standard soft lithography was performed using Sylgard 184 polydimethylsiloxane (PDMS) (Dow Corning, MI) as described previously (Ng, et al., 2003). After curing, the PDMS was

carefully removed from the master and access ports were created using a suite of dermal biopsy punch tools (8 mm) (Huot Instruments, WI).

3.2.3 Cell loading

DRG neurons were loaded into the soma side of devices and grown for 5 days to allow axons sufficient time to grow through channels and into the axonal side. Using a glass pipette, axons were transected at the base of the microchannels and neurotrophic factors were applied to axonal or neuronal cell body compartments at a concentration of 100 ng/ml, a commonly used peak concentration for various neurotrophic factors. Regeneration of axons was monitored by daily imaging of the axonal side and measuring the length of longest axon coming from each microchannel. A minimum of 10 axons per experimental condition was measured and experiments were done in triplicates.

3.3 Results

3.3.1 Theoretical Profile of Growth Factor Diffusion

In order to identify whether growth factors can diffuse from the axonal to cell body compartment during the treatment of growth factors in the axonal compartment, we developed models to simulate this experimental setup. The central idea behind the compartmentalized platform is to have fluidic connectivity between microchannel-connected compartments. If the microchannels contain a small cross-sectional area ($< 30\mu\text{m}^2$), this device paradigm allows axons to grow from one compartment into another but attenuates the diffusion of molecules from the compartment of lower hydrostatic

pressure to the compartment of higher. In our experiment a small differential pressure gradient was established with a higher pressure in the axonal compartment as compared to the cell body compartment. As a result, a low velocity retrograde flow was created in the microchannels to prevent molecular anterograde diffusion. We show theoretically, through computational simulations, that chemical isolations are achieved when working with the aforementioned parameters (Figure 3.1).

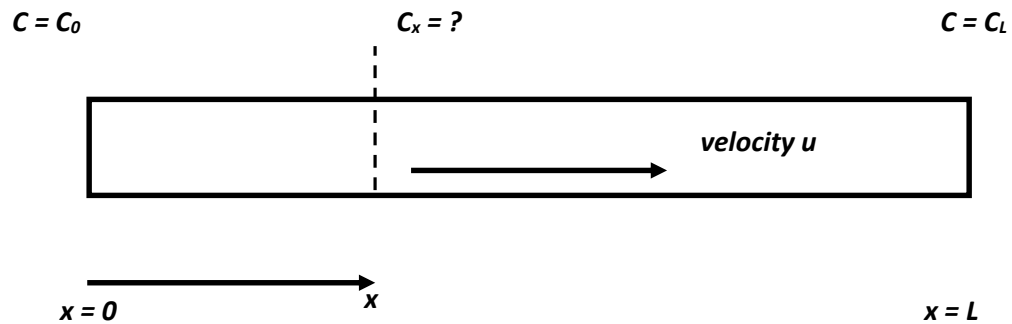


Fig. 3.1: Formulation of the diffusion advection problem.

The diffusion of any molecule in a fluid medium is governed by the diffusion-convection equation. The first term including spatial derivatives of concentration describes passive diffusion while the second term including the velocity of the medium describes active diffusion (or the convective element).

$$\frac{\partial C}{\partial t} = D \cdot \nabla^2 C - \vec{v} \cdot \nabla C$$

Where C is the concentration at a point (x,y,z) at time t

D is the coefficient of diffusion

\vec{v} is the velocity vector at the point (x,y,z) at time t

The pressure and concentration gradients driving the dynamics are mainly along the groove (x-axis) and hence, this can be approximated as a one-dimensional problem. Steady state is achieved when

$$D \frac{d^2 C}{dx^2} = u \frac{dC}{dx}$$

Where u is the x-component of the velocity

Solving this with appropriate boundary conditions yields the following solution.

$$C_x = C_L \cdot e^{-\frac{u}{D}(L-x)}$$

$$C_0 = C_L \cdot e^{-\frac{uL}{D}}$$

For pressure (gravity) driven flows, C_0 can be expressed as

$$C_0 = C_L \cdot e^{-\frac{\rho g \cdot \Delta h \cdot a^2}{16\eta D}}$$

Where Δh is the height difference of water column at inlet and outlet (leading to the pressure difference which drives the flow), ρ is the density and η is the viscosity of water (saline) and a is the channel height (the most critical dimension for laminar flow).

Due to the geometry of the system,

Δh is limited to about 2mm,

a is $2.5\mu\text{m}$ (height of the groove)

The other constants used are

$$g=9.81\text{m/s}^2,$$

$$\eta= 0.00089 \text{ m}^2/\text{s}$$

$$\rho= 1000 \text{ kg/m}^3$$

The diffusion coefficient D is calculated indirectly from its inverse dependence on the square root of molecular weight of the diffusing species. D_{oxygen} is known to be $2 \times 10^{-9} \text{ m}^2/\text{s}$. The mol. wt. of oxygen (M_{oxygen}) is 16 Daltons.

$$D_{\text{growthfactor}} = D_{\text{oxygen}} \cdot \sqrt{\frac{M_{\text{oxygen}}}{M_{\text{growthfactor}}}}$$

Table 3.1 shows a list of the growth factors we used along with their molecular weights and the calculated diffusion coefficients.

Name of Growth Factor	Molecular Weight (Daltons)	Calculated Diffusion Coefficient (m^2/s)
Human GDNF	21 kDa [153]	$5.5 \times 10^{-11} \text{ m}^2/\text{s}$
Rat Neurturin	19.5 kDa [145]	$5.7 \times 10^{-11} \text{ m}^2/\text{s}$
Rat Neublabin	4.5 kDa [154]	$1.2 \times 10^{-10} \text{ m}^2/\text{s}$

It suffices to work with a mol. wt. of 4.5 kDa as it is the smallest molecule we use, with the highest tendencies to diffuse. Or, stated otherwise, the amount of growth factor

diffusing to the somatic compartment will also be less than the amount of rat neublastin diffusing to the somatic compartment. So, considering the diffusion of rat neublastin,

$$\frac{C_0}{C_L} = e^{-\frac{1000 \times 9.81 \times 0.002 \times (2.5 \times 10^{-6})^2}{16 \times 0.00089 \times 1.2 \times 10^{-10}}} = 6.8 \times 10^{-32}$$

Thus, there is negligible diffusion from the axonal compartment to the somatic compartment at steady state. Care must be taken that while doing the experiments, the height difference in the two compartments must be achieved before adding the growth factor to the axonal compartment so that there is always an anterograde flow preventing diffusion of species in the retrograde direction.

3.3.2 Computational Simulations to Study Diffusion Patterns of Growth Factors

Simulations were done in COMSOL Multiphysics (Formerly called FEMLAB; COMSOL Inc., MA), a finite element-modeling package. The complex nature of the geometry was simplified to study the diffusion pattern in only one of the microchannel grooves. Each microchannel has a plane of symmetry passing through the middle (a plane going from floor to ceiling all along the length halfway between the two vertical walls). Further simplification of the geometry was done using such symmetric considerations and only half a microchannel needed to be simulated (Figure. 3.2a). Simulation consisted of meshing the architecture into a grid of smaller elements. The aspect ratio of such finite elements was tailored to suit the aspect ratio of the microchannel, that is, elements were longer along the length (x-axis) than along the width or height (y and z axes respectively).

The geometry was first solved for fluidic parameters such as velocity and pressures at all points. This was done by solving the continuity and Navier-Stokes equations for the microchannel. While all three cases were simulated as described above, we present the results of rat neublastin (the smallest molecule we used) diffusion (figure 3.2b). This suffices to demonstrate the paucity of small molecule diffusion through a microchannel feature.

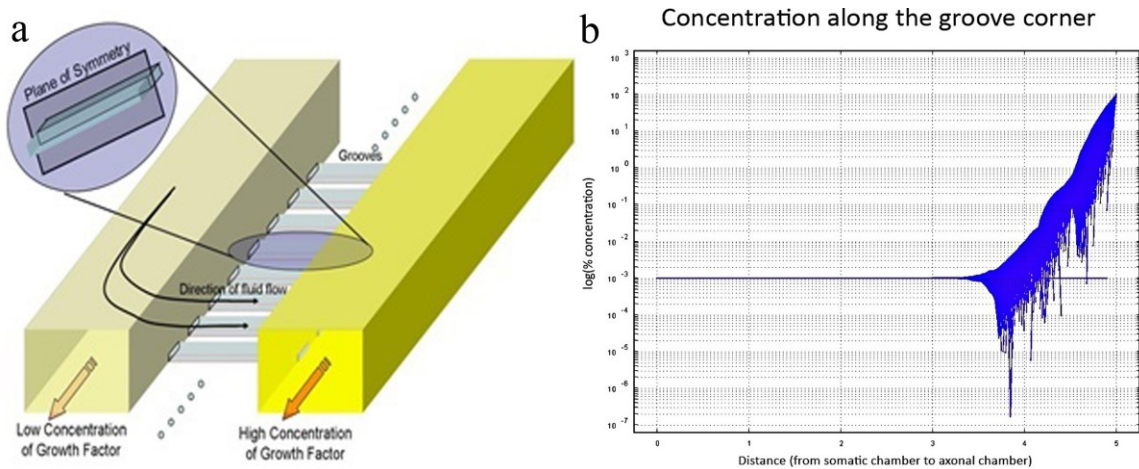


Fig 3.2: a. Handling of the groove geometry for computational simulations. Half the groove is meshed for computational solutions of fluid dynamics and diffusion-convection equations. P plot showing the concentration drop along the groove from the axonal side (right side) to the somatic side (left side). The profile along the middle of the groove shows the profile along one of the edges of the groove, b. Computational simulation of diffusion profile of growth factor along microchannel groove. Plot shows the concentration drop along the groove from the axonal side (right side) to the somatic side (left side) within 100 μm of the 500 μm channel. The profile along the middle of the groove shows the profile along one of the edges of the groove.

3.3.3 Restriction of diffusing analytes

Fluid volumes were modified such that the somal compartment was of lower fluidic height than the axonal compartment. By doing so, a hydrostatic pressure was established between these microchannel-connected compartments, thereby creating a small flow to counteract diffusive forces. A 1 microliter bolus of fluorescein isothiocyanate (FITC; Sigma, MO) dye was introduced to the somal compartment and was imaged over the course

of 24 hrs. Empirically, a fluid height difference ≥ 2 mm was sufficient to prevent the diffusion of a low-molecular weight (MW 700 Da) analyte to the axonal compartment for at least 24 hrs (Figure 3.3). Continued maintenance of the height differential by adding 5 microliters of media to the higher volume compartment daily allowed for restriction of small analytes.



Fig 3.3: Analyte restriction maintained for 24 hrs. Diffusion of a small (MW 700) fluorescent analytes were examined under high hydrostatic pressures. Microchannels (region between dashed lines) connect compartments of unequal fluid height. Establishment of fluid heights >2 mm prevented entry of dye (solid white lines) into the compartment of higher fluid height. Scale bar $100 \mu\text{m}$.

3.3.4 Axotomy and axonal regeneration by neurotrophic factors

In order to identify the regrowth of axotomized axons, we allowed neuronal processes to grow into the axonal chamber and then transected axons using a glass pipette or metal syringe. The representative figure (figure 3.4) to visualize single axons, before and after axotomy in a case where the seeding density is low. We observed some retraction

and degeneration of axons when they are cut slightly farther from the microchannel opening.

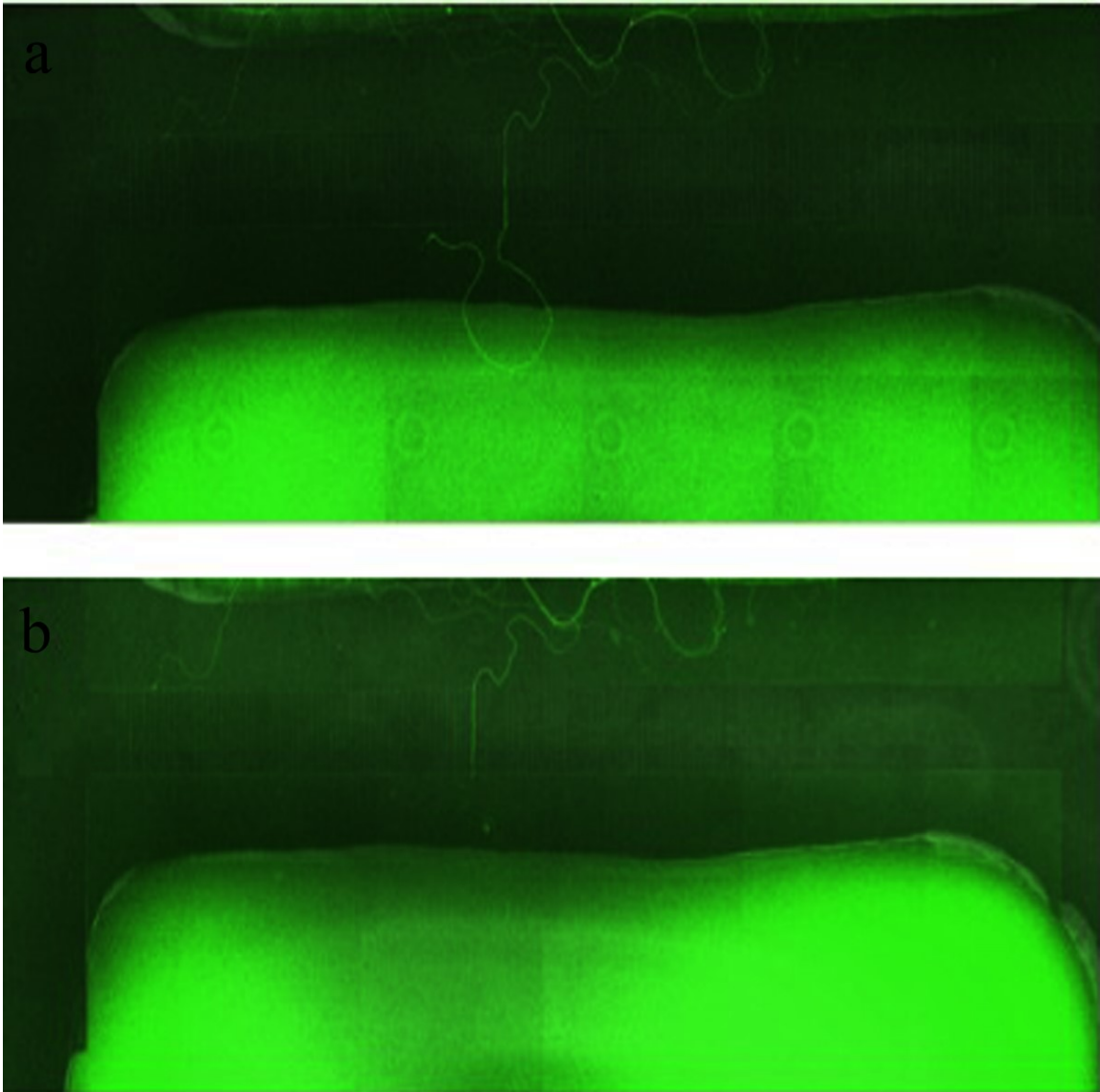


Fig 3.4: Representative axotomy. Images of a single axon within axotomy device a. before, and b. after injury.

Then, we added recombinant GDNF, neublastin, or neurturin to either axon or cell body compartments of cultured DRG neurons for 72hours. Multiple images of the axons were captured using phase contrast microscopy and we used ImageJ (NIH; Bethesda, MD)

to calculate percent changes in axon lengths before and after axotomy in the presence or absence of growth factors. In figure. 3.5, we see representative images of the DRGs before and after different neurotrophic factor treatments, all taken at the same magnification. In these images, we see the axons exiting channels and traversing into the axonal compartment on the right.

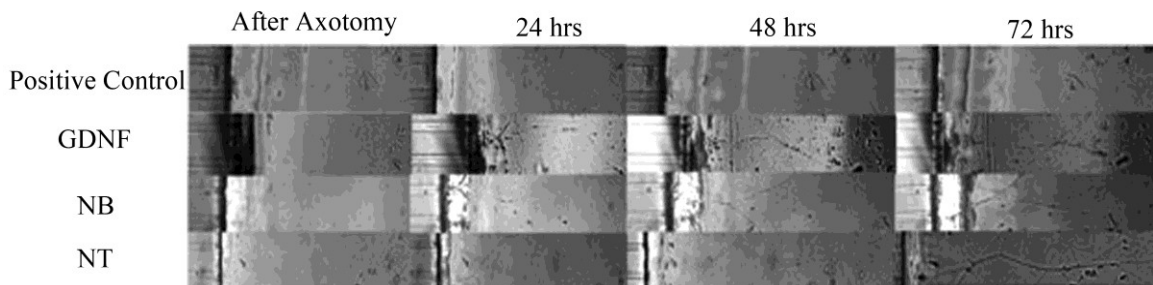


Fig 3.5: Representative phase contrast images of regenerating axons where neurotrophic factors were administered into cell body compartment. Images were taken every 24 hours for 3 days after injury.

As summarized in figure 3.6, all of the neurotrophic factors induced enhanced axonal regeneration whether they were applied to the axonal or somal compartments but GDNF was most potent. Furthermore, there was a slight benefit to applying GDNF to the somal compartment. In order to determine if the enhancement effect of adding GDNF to the axonal compartment was real, we carried out experiments with concurrent application of GDNF and Cytochalasin D. In figure 3.7, we can see that the results indicate that this enhancement is diminished with the application of retrograde transport blocker, indicating a need for GDNF to be transported into the cell.

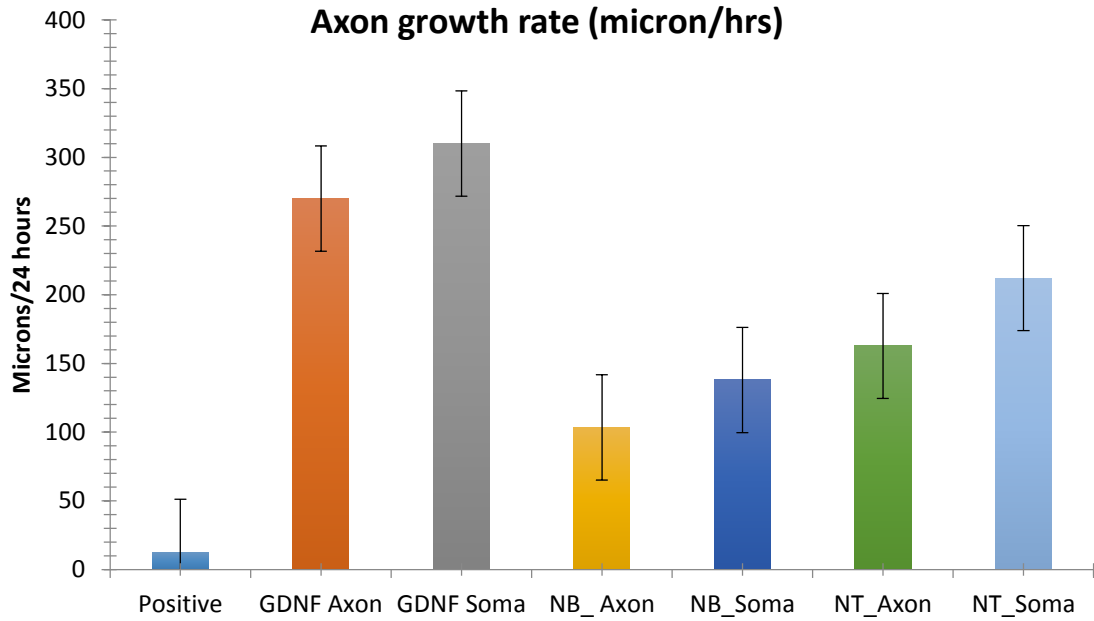


Fig 3.6: Axonal regeneration by GDNF, neurturin (NT) and neublastin (NB) after the axotomy. Rate of axonal regeneration induced by the neurotrophic factors over 3 days. ($p < 0.05$)

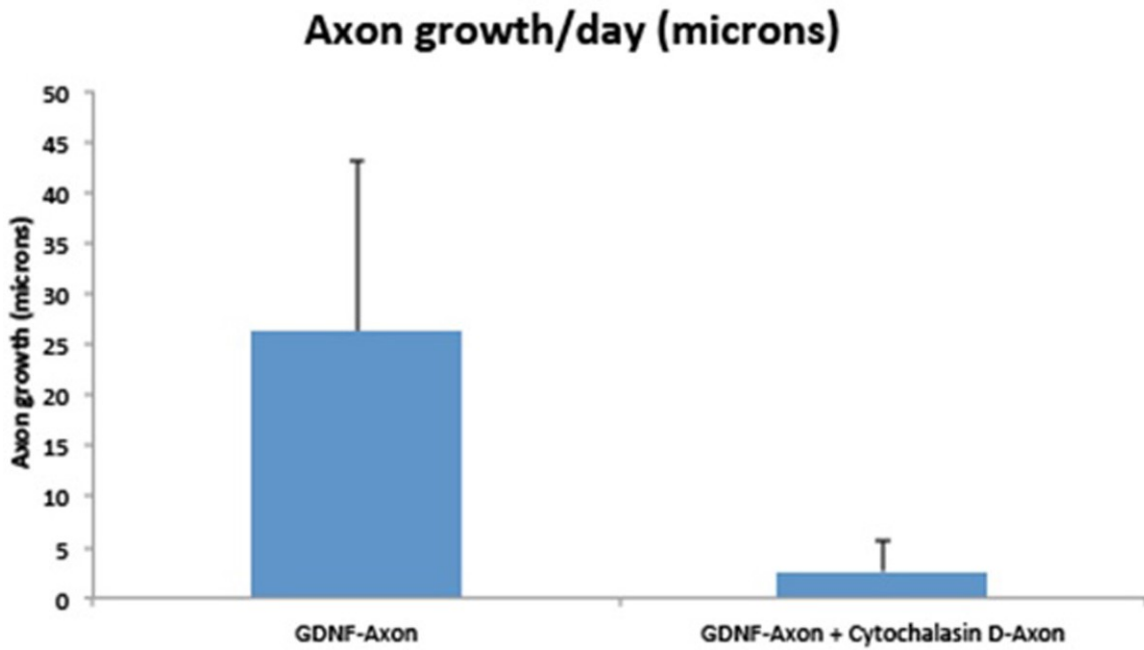


Fig 3.7: Axon regeneration with axonal GDNF application compared with axonal GDNF application concurrently with Cytochalasin D. ($p < 0.05$)

3.4 Discussions

Compartmentalized microfluidic culture systems have been utilized in a variety of neuronal studies, from examining the effects of toxins and neuroprotectants on axons versus soma, to enhancing spatial and temporal control of neurons and other cultures, and performing axon-glia co-culture studies [25, 155-157]. Several injury systems have been incorporated within microfluidic culture devices in order to investigate axon-specific mechanisms in injury and regeneration. These systems include simple aspiration of the distal compartment, two-photon laser ablation, and hydrodynamic shear based axotomy [158, 159]. In the current study, through modification of the device into an open system, we were able to transect axons simply and easily by scratching the surface of the glass with a sharp glass pipette or metal syringe.

As compartmentalized microfluidic culture devices have become ubiquitous, appropriate characterization of the diffusion properties within the devices would not only be beneficial but necessary. This study demonstrates a potential pitfall in designing and carrying out microfluidic experiments with neuronal cultures. Unless a proper hydrostatic pressure is maintained, there is no true fluidic separation of the axonal and neuronal cell body compartments. Experiments studying the effects of individual local manipulations of axons and neuronal cell bodies will have to take these observations into consideration. This is especially true for small molecular manipulations as they are more likely to diffuse through the microchannels and confound the findings of an experiment.

Neurotrophins have traditionally been known to play integral roles in neuronal survival during development, but only relatively recently has their function in regeneration been explored. [160] GDNF and its family of growth factors, neurturin, artemin, and persephin, represent a class of novel neurotrophic factors. These growth factors signal through a two-receptor complex consisting of rearranged during transfection (RET) Trk and a glycosylphosphatidylinositol (GPI)-linked GFR- α . The growth factors GDNF, neurturin, artemin, and persephin preferentially bind to bind to GFR- α 1, GFR- α 2, GFR- α 3, and GFR- α 4, respectively. GDNF has been shown to provide neuroprotection and promote axonal regeneration, but the role of the other family members is not as clear.

Injury to peripheral nerve reactivates its intrinsic growth capacity, and the retrograde transport of injury signals has been suggested to be one of the essential mechanisms for regeneration [161]. The retrograde transport of GDNF has been postulated to act as a positive injury signal for induction of regeneration.[162] The enhancement of regeneration by GDNF within our in vitro system is consistent with previous studies. It has previously been demonstrated that GDNF selectively promotes regeneration of injury primed sensory neurons, both in vitro where GDNF caused enhancement of neurite outgrowth in preconditioned DRG neurons, and in vivo where GDNF administered directly to cell bodies in lesioned spinal cord facilitated the preconditioning effect and enhanced regeneration further. [163]

3.5 Conclusions

In our study we found that GDNF acts as a more potent inducer of regeneration than the other GDNF family growth factors (neurturin, neublastin) which we examined. GDNF and its receptor GFR- α 1 are upregulated in the distal denervated segment of injured nerve, suggesting that GDNF may provide trophic support for injured peripheral neurons. No analogous upregulation of neurturin, persephin, and artemin or their receptors was found following injury [164]. However, it is note-worthy that we do see enhancement of regeneration at all if this is the case.

The finding that GDNF administered to cell bodies produced better results than GDNF administered to distal axonal compartments is interesting which further led to explore the role of retrograde axonal transport/relay of GDNF signal to cell body which maybe a reason for the observation. A previous study utilized compartmentalized cell culture devices to study the role of GDNF as a retrograde survival factor and its ability to promote survival over long distances to cell bodies [165]. In this study, it was found that GDNF promoted survival of DRG neurons equally well from either distal axon or cell body application. However, this study was not done within an injury model, and the DRG neurons were relatively healthy, and thus the reason for this discrepancy in the potency of GDNF depending on location of application may be due to the fact that we are using injured DRG neurons. It is important to note that the mechanism of action of GDNF may be different in these two systems, indicating the need to study the role of growth factors in both injury and developmental systems separately. It has been demonstrated that GDNF and GFR- α 1 are retrogradely transported in peripheral axons, but these studies were also

done in relatively healthy neurons.[166] Axonal injury may have an impact on protein turnover and retrograde transport, and this may impair some of the retrograde pathways for GDNF transport, making the application of GDNF directly to the cell bodies more effective. Our experiments comparing axonal GDNF application alone and together with Cytochalasin D demonstrate the important role of retrograde transport of GDNF as well as indicate that the enhanced regeneration effect may be cell body specific rather than at the localized axon.

Neurotrophic factors are a promising area of research for understanding regeneration. Their role in providing trophic support during development and in maintenance of neurons has long been known, but elucidating their roles in regeneration may prove fruitful in the development of therapies for overcoming neural degeneration and for enhancing regeneration post injury. Understanding axon specific or cell body specific effects of growth factors and being able to distinguish between local effects and retrograde signaling will be necessary for any future therapies. Compartmentalized microfluidic culture devices may be instrumental in these studies, but caution must be exercised to better characterize the devices to ensure true microfluidic separation of chambers.

Chapter 4

A Novel 3-Dimensional In Vitro Platform to Study Focal and Repetitive Axonal Injury

4.1 3D AIM platform

4.1.1 Introduction

Traumatic injuries and insults in various modes to Central Nervous System (CNS) often transgress as Traumatic Axonal Injuries (TAI). TAI involve focal to multi-focal damage of axons within the white matter tracts of the brain, and based on the degree and extent of TAI, the effects are often debilitating with a complete loss of function [167]. The functional restoration is greatly limited by the fact that CNS environment is not conducive of axonal regeneration [168, 169]. In spite of the gravity of TAI, many mechanistic details involved remain unknown and the individuals who suffer mild to medium brain injuries continue their activities only to succumb to devastating compounded injuries far worse than each of their isolated insults.

Primary insult to axons in TAI leads to secondary insults which might be even more severe and degenerative than the primary alone. The primary insult can be of various forms: mechanical forces arising from stretch, compression, shear or in combination of any of these lead to secondary insults. Secondary insults involve changes at morphological and biomolecular scales: disruption of cytoskeleton, axonal transport, axonal protein synthesis,

mitochondrial structural changes [170-173]. Recent evidence suggests that mild axonal trauma, on the other hand, may cause subtle axonal injury that is often reversible. However, long-lasting changes may become encoded within the axon- a form of traumatic “memory”- rendering the axon far more vulnerable to future traumatic insults predisposing them to a more severe secondary insult. Therefore, it is of critical importance to understand the mechanisms and consequences of focal axon injury and to correlate injury with the degree and nature of forces exerted upon the axon.

The modeling and study of complex dynamics involved in the settings of traumatic injuries in CNS and PNS provide valuable mechanistic insights about these injuries that are often irreversible resulting in permanent loss of function. The modeling studies help understand the biological destiny of injured nerves and axons, regeneration or degeneration and play a role in developing new therapeutic strategies. There are several experimental setups like *in vivo*, *in vitro*, and *in silico* models to study the injury [1, 26-28, 35]. *In vivo* animal models of trauma enable the study of whole organism’s response to a multitude of complex variables and even facilitating behavioral studies. *In vivo* models encompass Instant rotational injury model, Impact acceleration injury model, Lateral fluid percussion injury model, Controlled cortical impact model, Nerve stretch model, complete transaction model, and complete contusion model [1, 174]. Though *in vivo* models are useful, they do not permit study at single cell resolution, highly complex to operate, low reproducibility, large number of parameters to model, labor intensive, need specific set of skills, and are very time consuming. Also, they are limited by technological advancements to study time

course of degeneration following an injury, response to graded injuries, and changes in biochemical pathways along the time course of an injury challenging.

In vitro models, on the other hand, allow the study of biochemical pathways, gene expression levels, and phenotypic changes at single axon resolutions. *In vitro* models also facilitate the study of different types of traumatic injuries like transection, compression, stretch, and shear [1, 35, 174]. Microfluidics provides a powerful alternative to the existing *in vivo* and *in vitro* methods to model and study the axon injuries. They provide platforms: to model and study at single cell resolutions, compartmentalization and precise control over cellular microenvironments, can be automated, require little amount of reagents, scope for multiplexing and high throughput [49, 175, 176]. Several kinds of microfluidic devices are developed for the applications in neuroscience as these devices' settings can be broadly employed for neuron cell culture, neuron manipulation, neural stem cell differentiation, neuropharmacology, neuro-electrophysiology and neuron biosensors. [11-13, 21, 53, 177].

Development of microfluidic platforms for neuronal studies is propelled by following limitations to traditional *in vivo* and *in vitro* studies: (1) like in the case of *in vivo*, compartmentalization of the axon from soma is absent. A detailed investigation of sub-cellular events during injury isolated to either axons or soma is desired and hence the distinction between axon-specific and cell body-specific events; (2) lack of accuracy and precision in delivering spatiotemporally controlled injury to axons; (3) lack of high resolution imaging modality pre, during, and post axonal injury, and (4) lack of a tools to

measure the magnitude of various forces acting on axons during the injury. The issue of compartmentalization to study axons independent from cell body in peripheral nervous system (PNS) is first addressed by developing the Campenot chamber in 70s [3]. This chamber uses Teflon partition on a glass petri dish which divides and creates fluidic isolation between three chambers by the application of silicon grease. However, Campenot chamber is not suitable for CNS applications as the CNS neurons are far smaller in size, the reproducibility of silicon grease seal between glass and Teflon is low, and is very laborious. To circumvent these existing issues with traditional platforms in several lab-on-chip (LOC) approaches emerged to the study CNS neuronal cultures [10, 11, 97, 119, 175, 176, 178-180]

One of key the aspects of TAI is focal and graded axonal injury [117, 167], and LOC platforms to study focal and graded TAI in CNS axons were developed [61, 107, 108]. Hosmane *et al.* [61] developed an axonal injury micro-compression (AIM) platform with active valve components created from deformable biocompatible elastomeric material, poly (dimethylsiloxane) (PDMS). This platform integrates microfluidic valve technology with compartmentalization of CNS axons from their neuronal cell bodies. By pushing down the valve on an axon segment, a focal and graded compressive injury can be imparted. The study revealed a trimodal response to the graded injuries. Though the study elucidated new aspects of injury dynamics they do not precisely mimic *in vitro* conditions: (1) axons were subject to injury on a glass substrate which is of several order magnitude stiffer compared to biological tissues, and (2) does not combine the study of compression and stretch based injuries which are more likely to happen, in combination.

Motivated by this, I developed an add-on to the already existing AIM platform to substitute the glass substrate with a soft gel substrate whose material stiffness can be tuned. The combined novel microfluidic platform allows observation of focal and graded mechanical injury to CNS axons as a combination of compression and stretch. Fabrication of microfluidic platforms to allow a focal, graded mechanical injury to isolated CNS axons in a manner compatible with high resolution optical microscopy and spatiotemporal tracking. The developed platform potentially allows: (1) incorporation of a methacrylated gelatin gel substrate to allow complex injury modalities mimicking *in vivo* injury models to single CNS axons, (2) development of finite element models to characterize the mechanical load applied to the axons during injury setting, (3) experimental identification of stress thresholds for modal responses both in the settings of reversible and irreversible axonal injuries, and (4) determine sub-cellular spatiotemporal fluctuations of Ca^{2+} flux and cytoskeletal rearrangements at the site of injury, an early indicator of injury severity.

4.1.2 Materials and Methods

4.1.2.1 Fabrication of the master template and molds

The third layer of the assembled device, the substrate layer of AIM device was fabricated in PDMS. The master template for the substrate layer was created using single layer photolithography process. 4 inch silicon wafers (University Wafer, MA) were spin coated with 150 μm thick SU-8 3050 (Microchem, MA) and exposed to UV radiation with transparency mask (CAD/Art, OR) to define 4 parallel chambers (figure 4.1) for gel substrates. Each of these four chambers runs along the width of three parallel compartments in the AIM device. Once the master template is fabricated, substrate layer molds were prepared in PDMS. PDMS pre-polymer was mixed in 5:1 ratio (w/w) of base to curing

agent so that excess cross-linker results in better bonding with the second (fluid) layer of AIM platform. Secondly, the stiffness of the mold can be increased such that a thin, strong layer of it could be created to fit the entire 3 layered assembly in a petri dish without any contact with the lid there by avoiding potential contaminations.

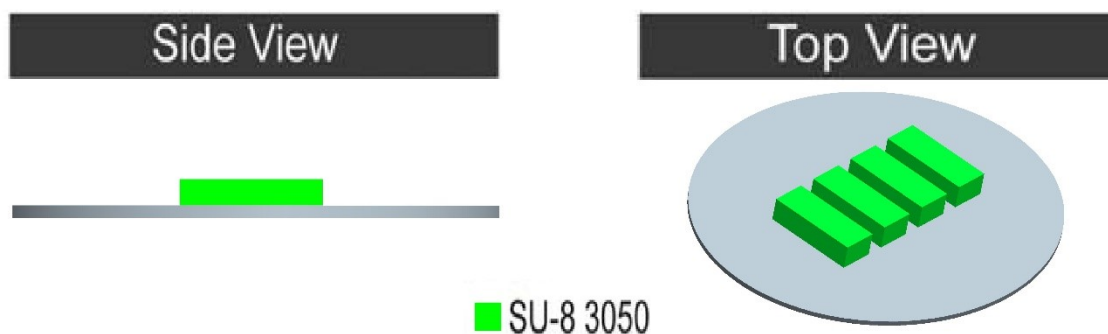


Fig 4.1: Master template of ECM layer for the modified AIM platform.

4.1.2.2 Fabrication of the gel substrate and establishment of the gradient

Methacrylated gelatin gel is a photo-crosslinked hydrogel that is biocompatible. Gelatin is chemically modified with the incorporation of methacrylate to amine groups in gelatin to form methacrylated gelatin. Methacrylated gelatin was synthesized as described previously [181]: Type A porcine skin gelatin was dissolved in Dulbecco's phosphate buffered saline (DPBS) at 60 °C and methacrylic anhydride was added to this solution in required ratio to control the degree of cross-linking. The solution was constantly stirred at 50 °C and allowed to react for 1 h and lyophilized. Photoinitiator 2-hydroxy-1-(4-(hydroxyethoxy)phenyl)-2-methyl-1-propanone (Irgacure 2959) was added to the

macromer in 0.5% (w/v) DPBS. The dissolved solution was injected into the ECM mold channels using a pipette and crosslinked via strong UV irradiation for 2 min.

Linear diffusible gradients of glial cell-derived neurotrophic factor (GDNF) were generated in methacrylated gelatin hydrogels that were established in channels using a surface tension driven, single channel microfluidics gradient generation method previously described in [182]. Methacrylated gelatin hydrogels were established in the channels of the ECM device and FITC-GDNF in DPBS was placed at the output of the channel as a drop. A smaller (in volume) drop of FITC-GDNF was placed at the input. Due to the surface tension a forward flow is established and a gradient is created.

4.1.2.3 Assembly of modified device

Methacrylated gelatin gels were established in the ECM devices using a plain a PDMS block for planar surface. The devices were peeled off from the PDMS block and cleaned carefully with scotch tape. AIM device fabricated using the method described in [61] was plasma treated and was placed on top of the ECM device, aligned and bonded. The whole assembly was placed in a 30 mm glass bottom petri dish and subjected to plasma treatment to flow media in the channels (figure 4.2).

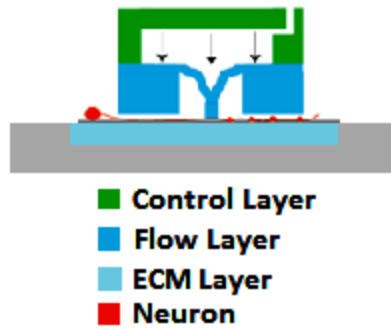


Fig 4.2: Illustration of the device assembly

4.1.2.4 Cell Preparation and loading

Devices were coated with $200 \mu\text{g ml}^{-1}$ PDL (Sigma, MO) as an extra cellular matrix (ECM) layer prior to cell seeding. The devices were left overnight at 37°C , washed 3X next day with ddH₂O, and filled with neuro basal/B27 [24] media and stored in standard humidified incubator (Thermo Scientific, MA) at 37°C with 5% CO₂ until used. Rat embryonic day 17 (E17) primary hippocampal neurons were derived as previously mentioned in [183] and used for this studies. E17 cells derived were seeded at low densities (150-450 neurons/device) and media was replenished every 3 to 4 days to maintain neuronal viability.

4.1.3 Results

4.1.3.1 Establishment of stable soluble gradients in gels in ECM devices

ECM layer design of the device incorporates establishment of stable and soluble gradients of neurotrophic factors in the methacrylated gelatin gels. The dimensions for each of the 4 lanes for gels (one for each injury pad) are chosen such that the cell bodies are not exposed to chemical cues in the gels. In doing so, we could essentially study the

regeneration of axons post injury solely under the influence of growth cone's response to cues in the proximal part of axon.

Methacrylated gelatin solution was first loaded in the channels and cross-linked with UV irradiation to form gels in the lanes. Once the gels were formed from cross-linking a concentrated drop of fluorescently-labelled GDNF was introduced at the input ports. Due to surface tension and capillary action a gradient of GDNF is established in the channels (figure 4.3). The initial bump in the concentration of GDNF is due to the fact that there is a sudden increase in the cross section between the input ports and the lanes. This step change in cross section leads to dead zones at the corners where there is no CGDNF and hence low concentration.

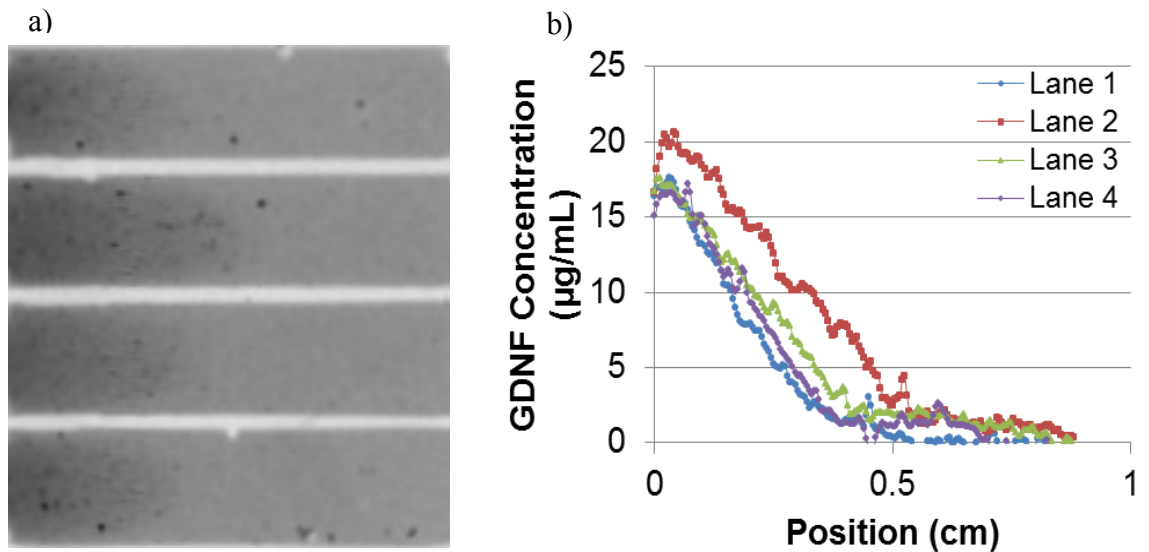


Fig 4.3: a) Fluorescently-labeled GDNF gradients generated simultaneously in four separate channels (channels are arranged from top to bottom). b) Quantification of gradients in the four channels

4.1.3.2 Compatibility between hydrogels and cells

Before cultures could be established in the modified platforms the compatibility of rat E17 1^o hippocampal cells with methacrylated gelatin gels has to be checked. Hence, methacrylated gelating gels were established in 96 well culture plates and the gel surfaces were modified with various conditions to investigate the compatibility. The gels were treated with the conditions mentioned in table 4.1. Inspection of cells under microscope right after and an hour into seeding revealed considerable aggregation, an indicator of poor health and compatibility of cells with methacrylated gelatin gels. The gels were then doped with other ECMs like collagen, laminin, and fibronectin to improve the compatibility with. To verify that the ECM coating is proper on the gels, fluorescently-labelled PLL (FITC-PLL) was used (figure 4.4). Though FITC-PLL revealed proper coating on gels inside the wells, no improvement in compatibility was observed. Methacrylate group being acidic, we suspected the presence of any uncross-linked residue from synthesis of methacrylated gelatin could decrease the pH of hydrogel. Accordingly the gels were washed with either HBBS or DPBS 3x times before further ECM coating. All these modifications were futile and seemed not to improve the compatibility between methacrylated hydrogels and cells.

Table 4.1: Experimental conditions the gels were subjected to

S. No	Experimental Conditions	Concentration of dopants ($\mu\text{g ml}^{-1}$)	Notes
1	Mgelatin + PDL	25, 50, 75, 100, 200	Media turns yellow
2	Mgelating + Collagen	0.5	Media turns yellow
3	Mgelatin + Fibronectin	0.5	Media turns yellow
4	Mgelatin + Laminin	0.5	Media turns yellow
5	Mgelatin + Fibronectin + Laminin	0.5, 0.5	Media turns yellow
6	Mgelatin + PDL + Collagen/Laminin/Fibronectin	75, 0.5	Media turns yellow

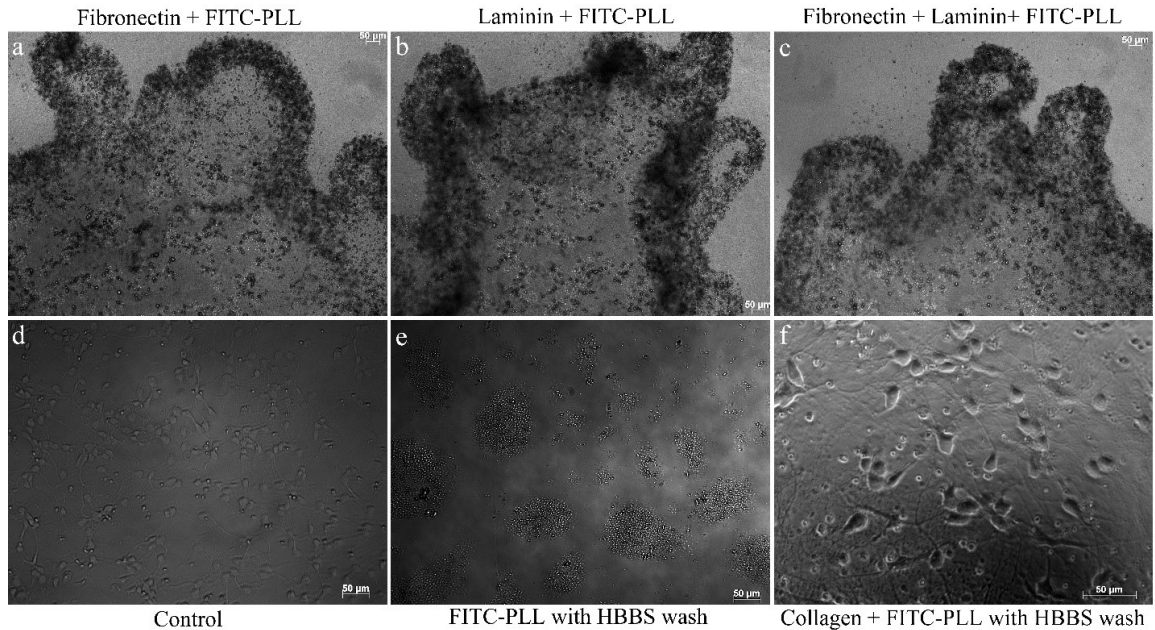


Fig 4.4: a) Clumping of cells on methacrylated gelatin doped with fibronectin and coated with FITC-PLL on day 2, b) clumping of cells on methacrylated gelatin doped with laminin and coated with FITC-PLL on day 2, c) clumping of cells on methacrylated gelatin doped with both fibronectin and laminin and coated with FITC-PLL on day 2, d) control, e) clumping of cells on methacrylated gelatin washed with HBBS and coated with FITC-PLL on day 2, and f) cells on methacrylated gelatin doped with collagen and treated with HBBS and coated with FITC-PLL on day 2 (scale bar 50 microns)

4.1.3.3 Cultures in the modified injury platforms

ECM layers were aligned and assembled with the AIM devices to form a single 3D TAI compressive injury platform. Methacrylated gels in ECM layer were often not planar and this resulted in failure of fluidic isolation between chambers of AIM device. This can be due to surface tension forces in the hydrogels resulting from rehydration with media. Nevertheless, to estimate the initial performance of the device rat E17 1^o hippocampal cells were used. As seen in the figure, due to the lack of fluidic isolation cell could be seen in all the compartments. Also, gels were not compatible to the cells and the cells started aggregating as early as 20 min post seeding in the devices. Mice dissociated DRG neurons were used instead of rat E17 1^o hippocampal cells to check whether they can be limited to

the cell body chamber due to their size in spite of the lack of fluidic isolation. To eliminate the chances of cell dispersion in all chambers cells were seeded directly on top of the gels instead of conventional loading through the cell loading ports. Though the DRGs extended their axons and remained healthy (figure 4.5), these results could not be reproduced.

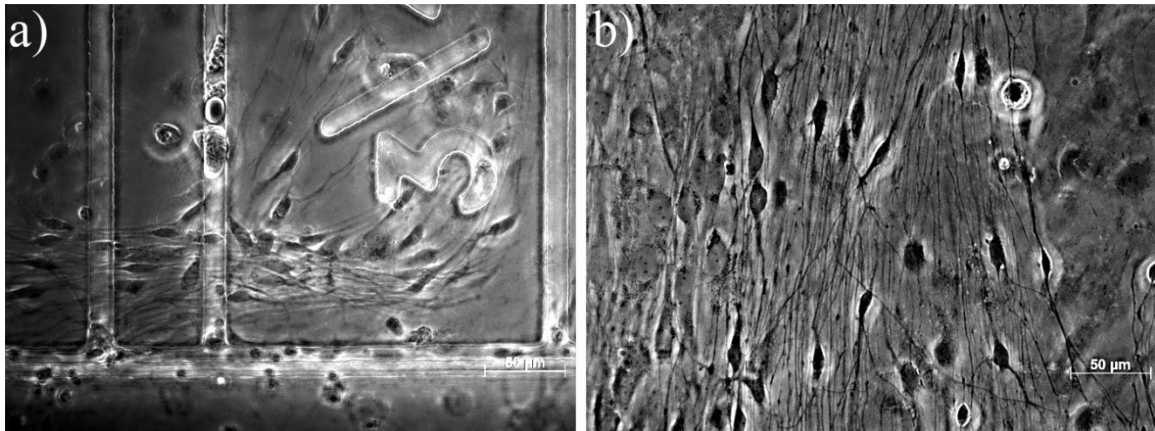


Fig 4.5: a) Dissociated DRG cells seeded in the modified AIM devices can be seen under the channels on methacrylated hydrogels due to the loss of fluidic isolation resulting from the concavity of hydrogel surface, b) healthy DRG cells with no aggregation in the cell body chamber of AIM devices 10 days in culture. (scale bar 50 microns)

4.1.4 Discussions

TAI occurring in the settings of traumatic brain injury and spinal cord injury can be result of insults of various kinds. Amongst those various modes of insults compression is one. TAI resulting from compression injury was earlier established and studied in giant squid axons. Giant squid axons are rendered easy to handle because of their large size (>0.5 mm in diameter). Initial experiments with these axons gave insights into the compression injuries in axons but these studies cannot shed light on the mechanical characteristics of CNS cells. Also, CNS axons are very small in comparison to giant squid axons and very delicate to handle with.

In order to study compression injury in CNS axons, each axon should be addressed individually to track down the post injury cellular sequences. To achieve this techniques should be developed to handle each axon independently. Existing techniques like laser ablation achieves the job but they are qualitative, they do not present information about the stress being directly applied to the axon. It is important to study the stress directly being applied to an axon because based on the degree of strain the injury outcome and cellular response changes. Current TAI platform is intended to address the issue of obtaining quantitative information from the insults to axons.

TAI platform is a LOC device that incorporates MEMS and soft lithography technologies to mold a device in PDMS. To quantitatively study the stress on axon the device incorporated a valve that deflects under a pressure which can be controlled. Using this device previous study found out that axons have a trimodal response post injury based on the input pressure to the valve. Though this outcome gave new insights into the extents of axonal regeneration after injury the study did not reflect the physiological conditions which may be different from what has been observed. In order to improve the device and make it closer to mimic physiological conditions the hard glass substrate is exchanged with soft ECM layer.

An ECM layer was developed as add on to the existing TAI platform to replace the current hard glass substrate with a soft ECM layer molded in PDMS. For ECM methacrylated gelatin gels were chosen as the stiffness of the gel can be fine-tuned based

on the cross linker in the pre polymer mixture. The whole assembly doesn't modify design and mechanism of TAI platform which eliminates the optimizations usually involved with new designs. Though the TAI platform is kept intact the ECM layer has to be optimized.

Developed ECM layer has optimization issues that are to be worked out before any further experiments. First and foremost the compatibility of the gels with rat primary E17 hippocampal cells has to be improved. Currently the gels are acidic as can be seen when neurobasal media is added to the gels. The pH indicator turns yellow indicating that the pH of gels is acidic which maybe a reason for the incompatibility. Then there is the issue of the concavity of gel surfaces that disturb the fluidic isolation meant to be achieved by the microchannels. This could be altered by changing the surface tension of the gels or modifying gels such that they expand after cross-linking or rehydration to fill the gaps established between the gels and microchannels. Once these issues could be optimized the stiffness of gels can be varied and gradients can be established. By varying the gel stiffness one could study the post injury response of axons to varying stiffness in the gels.

4.1.5 **Conclusions**

This study aims at improving the physiological relevance of the TAI device by incorporating soft substrate for the axons to grow on and to be injured. This is a very simple modification to the existing device by adding a layer of PDMS to incorporate soft substrates under the channels. Rat dissociated DRG neurons were successfully cultured in the devices but could not be injured due to the lack of fluidic isolation. Rat 1^o E17 hippocampal cells survived on the gels only once amongst several trials. If the gels could

be made more compatible the device would give great insights into the post injury axonal response based on the stiffness of the substrate.

4.2 Displacement control device

4.2.1 Introduction

The dynamics of TAI are still elusive and not yet completely deciphered. In the settings of a TAI it is the secondary insult, an outcome of the primary injury which is more debilitating. The cytoskeletal disruption and reorganization due to these repeated secondary insults often do not present any observable symptoms. It has been widely accepted that changes to the cytoskeletal structure within axons are the primary means for axonal collapse following injury. Actin filaments, intermediate (neuro-) filaments, microtubules, and cross-linking proteins collectively are responsible for the structural properties of the neuronal axon. While the cytoskeletal network contribution has been accepted, the mechanisms by which this structure degrades and the contribution of each cytoskeletal components is not understood. Insight into the structural mechanics of these alterations will lead to a more complete comprehension of neural axon cellular integrity.

Previous studies of axonal injury in the giant squid axon [184] have yielded generalized descriptions of morphological outcomes to graded mechanical loading resulting in distinct types of responses including continued maintenance, slow/fast retraction, and wallerian degeneration of the axon. The large size ($> 1\text{mm}$) of the giant squid axon permits physical manipulation of the tissue, however the far smaller sizes of mammalian CNS axons have precluded them from similar experimental manipulations. Therefore, to date, there has been little quantitative correlation between applied stress and the injury response of CNS axons. Apart from a recent study investigating the mechanical role of microtubules in stretch injury to the axon [185], previous studies have either focused

on stress application to the whole neuron, thereby masking axon-specific effects, or have looked at stress levels that induce complete axon transection [106].

Importantly, spatiotemporal tracking of cellular and sub-cellular changes in the axon has been one of the greatest challenges to understanding the primary and secondary injuries in the setting of traumatic insult to the CNS. Our aim is to develop a microfluidic platform by utilizing the previously established AIM platform technologies proposed in [61] with rigorous computational modeling, we could potentially achieve a fundamental understanding of the dynamics of a) axon morphology, b) calcium flux, and c) membrane and cytoskeletal rearrangements and “injury memory” as functions of graded compressive and tensile strain. In this study, we will seek to understand mechanisms by which forces causing mild reversible injury may lead to irreversible axonal damage when applied repetitively. We plan to achieve these by modifying the injury pad in AIM device by introducing notches along the length of the pad. The notches would permit the compression of axon to varying degrees based on the pre-defined clearance heights of the notches from the substrate from which the axons grow when compressed.

4.2.2 Material and Methods

4.2.2.1 Fabrication and assembly of injury platform

The axon injury micro-compression (AIM) platform previously described in [61] is modified in the valve design to incorporate the notches. The earlier design was a three layer fabrication process and the current design incorporates an additional layer in between layer

2 and layer 3. This additional layer defines the notch clearance from the glass substrate below which is usually in sub-micron sizes. This new layer 3 was defined by using SU8 2000.5 (Microchem, MA). The spinning protocols were followed as given by the manufacturer.

4.2.3 Results

4.2.3.1 Incorporation of the notch layer in master template

Master template of the device is defined on a 4 inch silicon wafer in positive relief. The fabrication of the master template involves 4 layer photolithography process. The layers are stacked progressively on top of each other, and each layer is designed in such a way that the features of the layer above are projected onto the layer below along with its own features. While stacking the layers, the features on the layer that is being stacked are always confined within the area of the features defined below. This is to ensure that the features do not collapse during replica molding in PDMS. The first layer (bottom to top) defines the microchannels for axons, the second layer defines the clearance for the valve, the third later defines the height of the notches, and the final layer defines the height of compartments.

Thickness of the third layer which defines the height of the notches is less than a micron and is at least 20 times less compared to other layers. This submicron thickness poses a challenge and the protocol has to be modified in defining this layer. Low viscosity of the photoresist and an inhomogeneous surface smoothness (due to the presence of exposed areas) results in improper distribution of photoresist during the spin coating of the

third layer. This results in the absence of well-defined features and in order to improve the adhesion between layer 2 and layer 3, layer 2 is subject to plasma treatment which increases surface roughness. Layer 2 is subject to plasma etching for 100 watts and 30 seconds at 600 mtorr, higher pressure results in lesser etching of the surface.

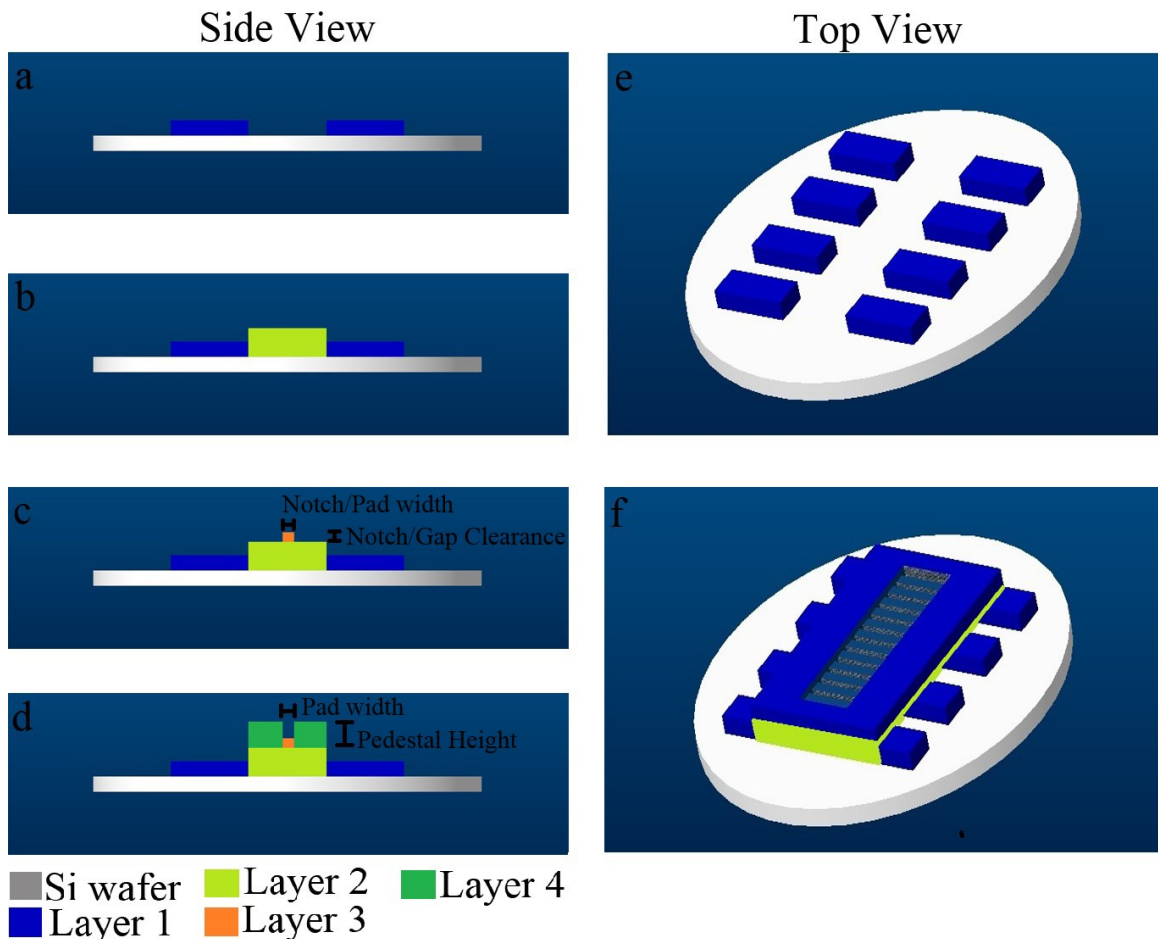


Fig 4.6: a) On a bare silicon wafer, microchannels were defined in two linear arrays of microchannels, b) a second thicker resist is used to define the overall injury pad clearance, c) on top of this layer a submicron thick layer was coated to define the notch heights, d) finally on top of this the actual layer for injury pad is defined, e & f) depict the top view of the same. (Schematics are not to scale)

4.2.3.2 Finite Element Method (FEM) modeling and notch design

The valve structure defined by Hosmane *et.al.*[61] was modified to incorporate discrete patterns of notches with predefined height clearance from the bottom of the glass

surface (figure 4.7). The clearance was introduced such that upon compression the axons traversing under the notches are subject to partial compression which will alter the fabric of cytoskeleton in the axon. The length of notches are defined as gaps and the spacing or interspersion between them as pedestals, which actually make the contact with glass substrate, when subject to pressure. Starting with an iteration of 200 μm gap and 80 μm pedestal lengths, devices were fabricated in PDMS and the valves were subject to compression under compressed CO_2 gas. The integrity of the modified valve is compromised and it started collapsing under pressures 10-20% higher than the minimum required for a contact with the glass substrate. The loss of structural integrity in the valve defeats the purpose of having a control over the degree of compression of an isolated axon. Hence FEM was employed to model and define pedestal and gap lengths to modify the structural and mechanical integrity of valve in action.

For FEM analysis, all the modeling parameters were borrowed from the model previously defined in [61]. FEM simulations with 200 μm gap length and 80 μm pedestal lengths resulted in buckling and collapse of pedestals at pressures as little as 7 psi (figure 4.8). In order to find optimal gap and pedestal lengths FEM simulations were first run to check response at 7 psi and then the degenerate loading response at 55-95 kPa (table 4.2). A gap distance of 10 μm and a pedestal distance of 20 μm were found to be optimal with a 77 % clearance intact when a notch height of 910 nm was considered. Further FEM simulations were run to determine of range of notch heights for the devices. All the simulations were performed to study the degenerate loading response (applied load 55-95

kPa) at 10 psi. The simulations yielded a minimum height of 400 μm to work with and anything below it collapses (table 4.3).

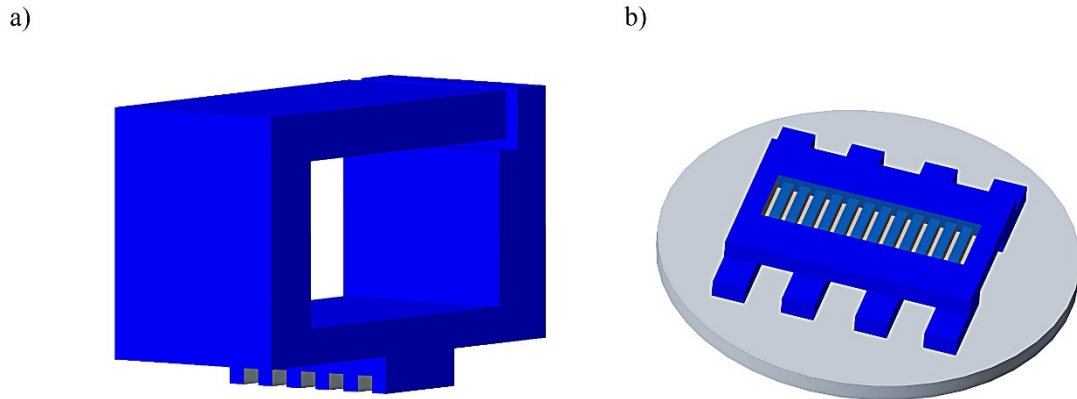


Fig 4.7: a) Modified compression pads with addition of notches created by gaps of a defined height clearance from glass substrate, b) Modified flow layer master template for the fabrication of displacement control devices.

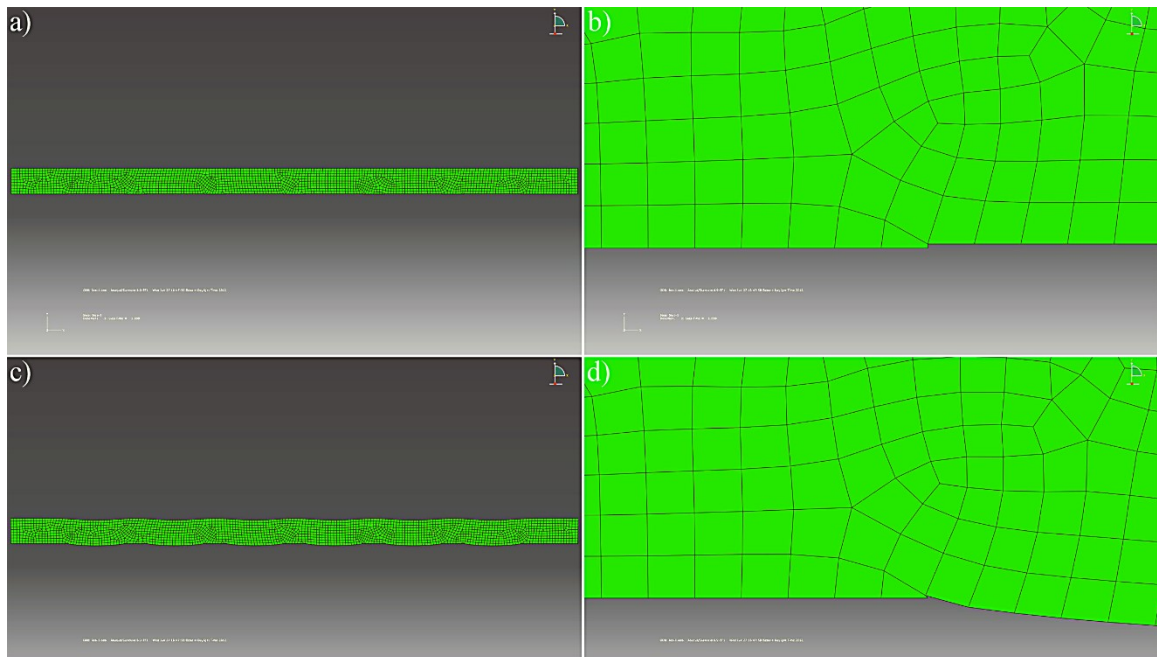


Fig 4.8: a) FEM analysis of modified compression pad of notch device under no compression with 200 μm gap length and 80 μm pedestal length, b) zoomed version of the control condition, c) FEM analysis of modified compression pad of notch device under compression at 7 PSI, pressure needed to barely contact the glass substrate, d) zoomed in version of the compressed condition where one can clearly visualize the buckling

Table 4.2a FEM simulations to determine the gap length and pedestal length

Gap length	Pedestal length	Displacement (μm)	Clearance (μm)	% Clearance
10	10	0.21647	0.69353	76.2120879
10	20	0.208609	0.701391	77.0759341
10	40	0.212688	0.697312	76.6276923
20	10	0.452194	0.457806	50.3083516
20	20	0.423282	0.486718	53.4854945
20	40	0.37877	0.53123	58.3769231
40	10	0.91	0	0
40	20	0.430553	0.479447	52.6864835
40	40	0.823168	0.086832	9.54197802

Table 4.2b. FEM simulations for degenerative loading for chosen gap and pedestal lengths

psi	Clearance (μm)	% Clearance	STDEV
7	0.696668	76.5569	0.003569
8	0.666726	73.2665	0.004040
10	0.607234	66.7290	0.004954
12	0.548264	60.2488	0.005831
14	0.489809	53.8251	0.006674

Degenerative loading response at 10 psi (applied load between 55-95kPa) indicated no collapse of the modified injury pad for a gap length of 10 μm and pedestal length of 20 μm indicating the choice of dimensions for modified injury pad.

Note: Above simulations in table 4.2 a & b were done assuming a notch height of 910nm and the simulations are run at 7 psi, pressure needed to barely make the contact with glass substrate

Table 4.3: FEM simulations for various notch clearances for chosen gap and pedestal lengths

Notch Height (nm)	Clearance (μm)	% Clearance	STDEV
100	0.000000	0.000000	0.000000
200	0.000000	0.000000	0.000000
300	0.020644	0.068814	0.004872
400	0.116279	0.290698	0.004006
500	0.212539	0.425079	0.004519
600	0.308878	0.514796	0.004942
700	0.404952	0.578502	0.004965
800	0.501089	0.626362	0.004903
900	0.597250	0.663611	0.004919
1000	0.693818	0.693818	0.005447

The above table shows the simulation results of clearance between the top of injury pad and glass substrate to a degenerative loading response of 10 psi where the notches are for a gap length of 10 μm and pedestal length of 20 μm . In the case of 100 nm and 200 nm a total collapse is seen and a minimum of 300 nm is needed. Hence 400 nm was chosen as the minimum height required for notches.

4.2.3.3 Valve operation, stability, and notches

As a proof of principle for sustained compression of axons in the device and to evaluate valve performance over extended periods of time we performed experiments using FITC conjugated PLL to pattern the gap zones on glass substrates. Devices in PDMS were fabricated from master molds with a notch clearance height of 500 nm. The devices were assembled, cleaned, plasma treated, and bonded to glass substrates. Bonded devices were filled immediately with molecular grade water and stored at 37 °C until used. The inlet ports for CO₂ gas in control layer were set up and the modified valves were compressed. Once the contact with glass substrate was established, the water was exchanged with FITC-PLL (10 $\mu\text{g}/\text{ml}$) in the chambers.

The valves were subject to compression for a period over 24 hours and prior to decompressing them FITC-PLL from all the chambers was aspirated and the chambers were washed with molecular grade water thrice. Images were taken both with compressed and uncompressed valves (figure 4.9) and a reliable pattern of notches were seen on the glass substrate without any loss in the structural and mechanical integrity of the valves. This proves that axons could be subject to a constant compression injury to model.

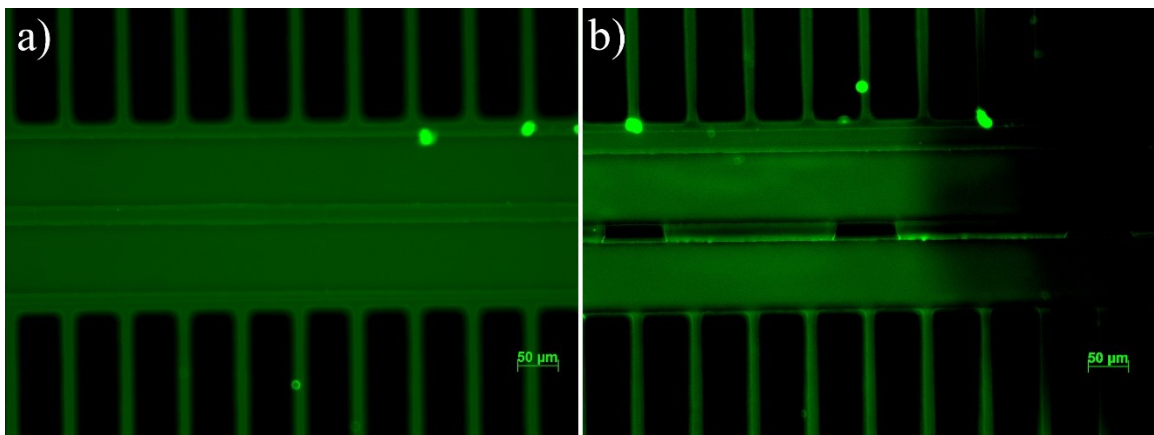


Fig 4.9: a) Uncompressed notch valve: the channels were filled with FITC-PLL and incubated overnight to take the images, b) compressed notch valve: valves were compressed prior to flushing the chambers with FITC-PLL, incubated overnight and washed before release of valve. One can clearly visualize the clear zones where the pedestal made contact with glass substrate for the entire duration of coating.

4.2.3.4 Imaging neurofilaments and microtubules

Cytoskeletal transport network: neurofilaments (NT) and microtubules (MT) of an axon are disrupted during TAI. It is vital to study the disruption of this network during and post injury. In order to visualize these proteins under microscope rat E17 1^o hippocampal neurons were transfected with phosphorylated cytomegalovirus (pCMV)-AC-green fluorescent protein (GFP) plasmids with a C-terminal TurboGFP (Origene, Rockville, MD, USA), encoding an NF-GFP or MT- associated protein tau (Mapt)-GFP fusion gene. To localize the cytoskeletal proteins NT or MT with the membrane of axon CMPTx red cell

tracker (Gibco Life Technologies) was added prior to imaging with high resolution confocal microscopy. MATLAB was used for image processing of the acquired images (figure 4.10). The ability to image individual cytoskeletal components during TAI in combination with modified AIM device provides a powerful tool to study the time course of primary and secondary insults during TAI.

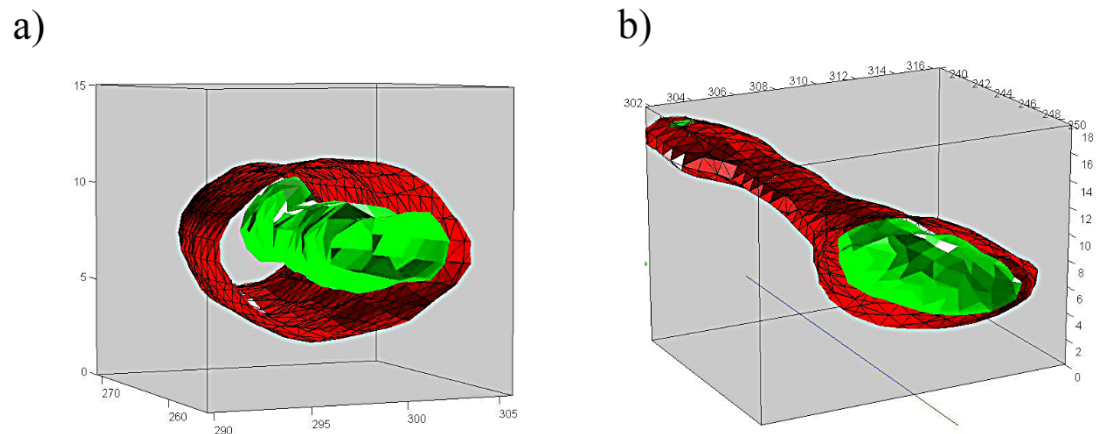


Fig 4.10: a) Confocal images of GFP tagged microtubules (green) with respect to axonal membrane (red) labelled with CMPTx red cell tracker. Microtubules appear to be more localized within the axon with an average diameter around 25nm, b) confocal images of GFP tagged neurofilaments (green) with respect to axonal membrane (red) labelled with CMPTx red cell tracker. Neurofilaments appear to be more dispersed within the axon with an average diameter around 10-12nm. (Axes scale in nm)

4.2.4. Discussions

TAI occurring in the settings of traumatic brain injury and spinal cord injury can be the result of insults of various kind. Amongst those various modes of insults compression is one. In TAI compression can vary from just deformation to complete transection of axon. TAI resulting from compression injury was earlier established and studied in giant squid axons. Giant squid axons are rendered easy to handle because of their large size (>0.5 mm in diameter). Initial experiments with these axons gave insights into

the compression injuries in axons but these studies cannot shed light on the mechanical characteristics of CNS cells. Also, CNS axons are very small in comparison to giant squid axons and very delicate to handle with. It has been widely accepted that changes to the cytoskeletal structure within axons are the primary means for axonal collapse following injury. Actin filaments, intermediate (neuro-) filaments, microtubules, and cross-linking proteins collectively are responsible for the structural properties of the neuronal axon. While the cytoskeletal network contribution has been accepted, the mechanisms by which this structure degrades and the contribution of each cytoskeletal components is not understood. Insight into the structural mechanics of these alterations will lead to a more complete comprehension of neural axon cellular integrity.

Not all injuries lead to complete transection of axons. Some compressive injuries like carpal tunnel syndrome (CTS) [186] are chronic which result in repeated deformation of the axons or nerves under compression. An *in vitro* microfluidic injury platform to model and study repeated compressive injury, with control over the duration of injury being delivered, can effectively reproduce biochemical and mechanical events undergoing during pathologies like CTS. Such platform would serve as a powerful tool for critical study of various pathologies involving repeated compressive injuries. Modification of the injury pad in previously developed AIM platform can potentially address this issue. This modification can facilitate compression of axons to different degrees via displacement control for extended times of up to 16 hours or more. Moreover this method is both quantitative and qualitative. Quantitative in studying the relation of degree of displacement to axonal response, cytoskeletal response and reorganization, and transport disruptions.

The valves designed for TAI platform in AIM device were thus modified to incorporate gaps and pedestals. When the valve is compressed under pressure the pedestals contact the substrate and the gaps between them form notches under which axons can pass. The axons passing through these gaps are compressed to various degrees based on the diameter of the axons and notch clearance. In order to make these changes in valve design an additional layer is added to the master template between layer 2 and layer 3 which defines the notch clearance.

A range of submicron notch height clearance was defined in various master templates. But defining these notches on master templates was very tricky. Notch below 0.75 μm were not observed in master templates. This may be due to adhesion incompatibility between SU8 2000.5 (layer 3), SU8 3005 (layer 1, 2), and SU8 3050 (layer 4) layers. Trial runs in master template fabrication were run with dilutions of SU8 3005 in cyclohexanone to achieve solid ratios of the resist comparable to that in SU8 2000.5 to improve the adhesion compatibility with other layers but this did not seem to have any effect on the formation of notches. The process had to be sufficiently modified by increasing the surface roughness of the layers below notches.

Devices created were tested for formation of notches in PDMS. FITC-PLL in the devices coated the surfaces under the gaps only and not the pedestals indicating that axons can potentially pass under the gap regions and be compressed to various degrees depending on the notch clearance when the valve is compressed. Simultaneously, before any

experiments could be performed in these devices imaging modalities have to be developed or modified. In order to image the sub cellular aspects of axons like cytoskeletal and transport components sufficient imaging modalities like spinning confocal microscopy was used successfully in the already existing TAI platforms. Over all this device can be further integrated with imaging modalities to observe the sub-cellular changes in compressively deformed axons at extended time periods in the lab.

4.2.5. Conclusions

This study aims at modifying existing TAI platform to study chronic and repetitive compressive insults to axons and study the changes in cytoskeleton, transport systems, and axonal fate. This was planned to achieve by incorporating notches in the existing valves using gaps in the valve. Notch heights define the clearance from the substrate on which the axons grow which gives insights into the effect of degree of deformation on the fate of axons after injury. This is a very simple modification to the existing device by adding an additional layer to master template to define notch clearance. Initial experiments show that the modified valves are stable over 16 hours of time and would allow for axon deformation.

Chapter 5

Conclusions

In this chapter I briefly present the results, and contributions resulting from the studies reported in chapters 3 and 4 of this thesis. It also includes the future directions that these results can lead to in order to advance the science and technology directed at solving problems at the heart of the field.

5.1. Contributions from Aim 1:

5.1.1. Technical and Scientific Achievements

In chapter 3, which deals with my aim 1, I have described the study dealing with the role of GDNF family neurotrophic factors GDNF, neurturin, and neublastin, in axonal regeneration, post injury. To study was conducted on rat DRG neurons in simple two chambered, open system microfluidic devices. The open system architecture of the microfluidic device supports better gaseous exchange compared to its closed system counterparts. Open system also supports the reduction in shear forces associated with media exchange/replenishment. To study the influence of microenvironment in axonal regeneration post injury, fluidic isolation between cell body and axonal compartments is a necessity. I achieved this required fluidic isolation by establishing hydrostatic pressure difference between the two chambers that counteracts mass transfer by advection and diffusion phenomena. The established gradient was stable for the entire duration of experiment (over 72 hours). While fluidic isolation is in effect, I demonstrated that GDNF

applied locally to cell body side promotes growth of axon after injury in a better way compared to when applied locally in axonal compartment. This led to a hypothesis that the observed difference in growth rate might be due to the fact that the GDNF signal is to be relayed to cell body via retrograde axonal transport to initiate the influence of GDNF on axonal growth. To test this hypothesis I used retrograde transport blocker Cytochalasin D along with GDNF. The presence of retrograde transport blocker further suppressed the rate of axonal growth post injury conforming my hypothesis..

5.1.2. Dissemination of original research

The work mentioned in chapter 3 is culminating into a publication in a journal soon. While the manuscript is under preparation the results observed in dissociated DRG neurons are being translated at tissue levels *in vitro*.

5.2. Contributions from Aim 2:

5.2.1. Technical and Scientific Achievements

In chapter 4, which deals with my aim 2, I have described two possible directions for further developing existing AIM device to study TAI and carried out preliminary work, which has a great potential to be refined and furthered. One of the possible directions that I considered was to transform the AIM device developed by Hosmane *et al.* [61] into a 3D platform. Such transformation would provide strong relevance to the physiological conditions, for example brain tissue is soft while the axons in AIM are compressed against rigid glass substrate which may not be true reflection of the physiological scenario. Also,

this transformation would eliminate the complexities involved at tissue levels while permitting a study that closely mimics the mechanical nature of a tissue. In order to achieve this I developed an extra layer and named it the ECM layer. This layer had long and wide channels which are out of the regime of microfluidics. The channels were designed in such a way that the aspect ratio of height to width is less, this allows establishment of stable soluble gradients, a phenomenon observed *in vivo*. I established gels in those microchannels which would act as substrates for neurons to grow on. Though this is not a true 3D architecture per se, in essence it would pseudo 3D system that would mimic the mechanical properties of soft tissue. With this experimental plan I set out to culture rat E17 1^o hippocampal cells on the methacrylated hydrogels in these devices. Soon, issues with the compatibility between cell and hydrogels arose. I have attempted several iterations and various combinations of ECM to improve compatibility but nothing seem to work. One interesting thing to note here is that Fan *et al.* [187] were able to achieve good compatibility between methacrylated gelatin hydrogels and rat cortical cells. I tried using cortical cells but they did not show better compatibility either.

The second direction that I was considering was to modify the architecture of injury pad itself, of the AIM platform. The idea was to modify the injury pad such that the axons are subject to partial compression rather than complete transection, when the pad is fully compressed. In other words, the injury is dictated by the displacement caused by the pad rather than the load it delivers. This modality of injury inflection can be extended for prolonged durations so as to establish *in vitro* microfluidic models of pathologies like carpal tunnel syndrome. In order to achieve this, I incorporated an additional layer in the

master template of fluidic layer and termed this layer as the notch layer. With this modification Incorporation of this notch layer required spinning and photolithography of submicron thick layer. Though a challenge in itself, I could successfully achieve clearances in the range 500-1000 nm. This range was chosen assuming that the average diameter of a CNS axon to be 1000 nm. Though actual experiments could not be conducted with this platform the potential that it could offer is quite evident and could be taken up in the near future.

5.2.2. Dissemination of original research

Preliminary results from the first part of the work mentioned in chapter 4 was presented in a poster session of BMES conference 2012, held at Atlanta, Georgia. Likewise, preliminary results leading up to the second part of the work mentioned in chapter 4 was presented in a talk series of Society for Engineering 2012, held at Atlanta, Georgia.

5.3 Future directions

In this concluding section, I try to list few possible future directions to the work mentioned in earlier chapters 3 and 4. These possible future outcomes can broaden the horizons of LOC devices in neuroengineering applications and neuroscience as a whole. I hope that the future of neuroscience is dictated by the miniaturization of tools currently being like the semiconductor revolution to for computers which started out with beasts like ENIAC ending up with smart phones and gadgets in the present day.

5.3.1 Neurotrophic factors and functional nerve regeneration

One of the possible future directions is to employ neurotrophic factors in nerve repair and functional nerve regeneration. Neurotrophic factors are a promising area of research for understanding axonal regeneration. Their role in providing trophic support during development and in maintenance of neurons has long been known, but elucidating their roles in regeneration may prove fruitful in the development of therapies for overcoming neural degeneration and enhancing regeneration post injury.

Understanding axon specific or cell body specific effects of growth factors and being able to distinguish between local effects and retrograde signaling will be necessary for any future therapies. Compartmentalized microfluidic culture devices may be instrumental in these studies, but caution must be exercised to better characterize the devices to ensure true microfluidic separation of chambers. Role of these growth factors can be studied in more complex systems which involve tissue cultures, organotypic cultures and at the ultimate level *in vivo* studies. Initiatives towards *in vivo* study of growth factors like GDNF is already being taken up by couple of groups in rodents in peripheral nervous system [188, 189]

Treatment strategies can combine stable establishment of local gradients of neurotrophic factors by systemic injection along with stimulation of oligodendrocytes or Schwann cell to provide conduits to the regenerating axons. The presence of Schwann cells

and their establishment of stable conduits protects the regenerating axons and they shield the axon from encountering inhibitory cues that will decrease the effective growth rate of axons and nerves. Another challenge that is to be tackled is to keep the distal part of the nerve conduit from degenerating while the proximal part grows in length to reestablish functional connectivity. Once again, local establishment of gradients and neurotrophic cues can be exploited to recruit Schwann cells and debris clearing cells. Microfluidics might soon offer platforms that allow studies involving regeneration and myelination while maintaining stable and sustained gradients in cultures. And these strategies can then be translated *in vivo*.

5.3.2 Secondary Injury and axonal transportation

In TAI, usually a primary insult is followed upon by a much serious and often debilitating secondary injury which involves changes ranging from intracellular $[Ca^{2+}]$ level changes to cytoskeletal reorganizations. These may be associated with a form of memory with these insults in case of prolonged and repeated injuries. Intracellular calcium levels have been shown to be associated with secondary injury mechanisms in various studies [190-192]. These studies were done without compartmentalization of axons from cell body. This implies the need for exploration and tracking of the time course of intracellular $[Ca^{2+}]$ levels in axon independent of cell body during the time course of injury in different injury modalities. With the existing AIM platform and the modifications that I tried to accomplish it might be an achievable feat in near future.

In order to do this, the first and foremost thing that one would want to focus is on modifying the surface chemistry of the hydrogels, to improve the compatibility issues encountered between hydrogels and neurons. Once this is sorted out one could potentially look at the relationship of stiffness of the hydrogel surface to the thresholds of axonal regeneration after injury and subsequently study the intracellular $[Ca^{2+}]$ dynamics. Further, microglia can be incorporated in these gels to improve debris clearance after injury and study the changes in regeneration. Also, comparative studies between stiffness of the hydrogels and intracellular Ca^{2+} concentration changes in the injured axons can be potentially studied. I believe that the monitoring of extracellular field potential during the time course of an injury is an important aspect. As there is the intracellular $[Ca^{2+}]$ levels the membrane potential is potentially altered which will contribute to the opening and closing of several ion channels in the membrane which could be caught in the extra cellular field potentials. Integrating microfluidic devices with multi electrode arrays (MEA) or any other electrodes can facilitate additional information related to axonal injury.

I also believe that the notch device could be combined with the other two devices in various combinations to conduct interesting experiments where axons could be subject to displacement controlled injuries. These studies would shed light at the cytoskeletal reorganization and transport disruption and axonal growth in chronic injuries. I have conducted preliminary experiments on neurofilaments and microtubules in collaboration. These preliminary results were a result of developing a technique to image cytoskeletal elements at great resolutions which can be used to do a time lapse in case of chronic injuries.

5.3.3 Hybrid and *in vivo* microfluidic technologies

I envision that the day when implantable microfluidic devices are a reality is in near future. The miniature size of the microfluidic devices makes them a suitable candidate for *in vivo* monitoring and therapeutic devices. Most commonly used polymer, PDMS for microfluidic devices is biocompatible and flexible which makes it suitable material for implants. Apart from biocompatibility and flexibility, the ability for rapid prototyping, cost effectiveness makes PDMS a powerful material for implantable microfluidic devices for neurological applications.

Before the above mentioned could be successfully achieved one need to make progress in developing hybrid microfluidic platforms to maintain cultures with tissue and organ level organization and sophistication. To achieve the sophistication required for a organ level culture several types of microfluidic platforms mentioned in chapter 1 needs to be integrated. And I believe that this is going to be a major area of research in microfluidics and neuroengineering in the coming years.

Appendix A

Photolithography Protocol

Step	Process Name	Process Parameters	Duration
1	Dehydration Bake	Bake the substrate @200 °C on hot plate (Note: In case of an existing layer of photoresist bake at 95 °C)	10'
2	Plasma Treatment	Treat the substrate with O ₂ plasma @ 350 mTorr and 250 W (Note: If there is already a layer of photoresist on the wafer use a low power of 75 W for 30)	3'
3	Resist Coating	Look up the spin table	Look up the spin table
4	Soft Baking	Bake @ 65 °C -> 95 °C and then cool down to 65 °C (The durations might have to be increased based on the thickness of underlying layers)	Look up the spin table
5	Exposure	Look up the spin table	N/A
6	Post Exposure Bake	Bake @ 65 °C-> 95 °C and then cool down to 65 °C	15'
7	Resist Development	SU8 developer (with gentle agitation) (If the resist layer is thick and the features are of low aspect ratio one could use sonication to speed up the process)	1'-5'
8	Hard Baking	Bake @ 65 °C->95 °C-> 150 °C and cool down to room temperature	12 hrs
9	Cool Down	Cool down to room temperature	~35'

Appendix B

SU8 spin protocols

SU-8	Thickness (μm) [1]		Spin #1	Spin #2	Spin #3	Spin #4	Soft Bake (min) [3]	Dose	PEB (min) [3]
	Real	Expected	[2]	[2]	[2]	[2]	65°C to 95°C	mJ/cm ²	65°C to 95°C
2000.5	0.5	0.4	500 (104) [6s]	2000 (312) [10s]	3500 (520) [37s]	300 (520) [12s]	6 min	400	6 min
2000.5	0.9	0.8	500 (104) [6s]	1250 (255) [34s]	300 (255) [10s]	N/A	6 min	400	6 min
2002	2.5	2.9	500 (104) [6s]	1000 (255) [34s]	300 (255) [10s]	N/A	19 min	450	19 min
3005	10	10	500 (104) [6s]	1000 (255) [32s]	300 (255) [10s]	N/A	19 min	450	19 min
3025	20	20	500 (104) [6s]	2000 (312) [10s]	4000 (520) [37s]	300 (520) [12s]	34 min	500	19 min
3050	160-180	115	500 (104) [6s]	1000 (312) [32s]	300 (255) [10s]	N/A	1 hr 49 min	500	19 min

Appendix C

SU8 Dilution

- 1 SU8 can be diluted to decrease the viscosity in case there is no resist available for spin coating a layer of desired thickness.
- 2 Commonly used solvents for dilution are cyclopentanone or the commercially available SU8 thinner marketed by Microchem.
- 3 Dilutions can be made either by viscosity or the total solid content in the resist.
- 4 Take little less than the measure amount of the solvent in a beaker and keep stirring.
- 5 Add the required amount of desired the photoresist while stirring the solvent continuously.
- 6 Add the remaining solvent, this way you can ensure to wash and dissolve any photoresist sticking to the walls of the beaker.
- 7 Close the beaker with an aluminum foil and keep stirring continuously for 30 min.
- 8 Make sure that the temperature is low so that the evaporation could be minimized and resist of desired viscosity be achieved.

Bibliography

1. Wang, H.C. and Y.B. Ma, *Experimental models of traumatic axonal injury*. J Clin Neurosci, 2010. **17**(2): p. 157-62.
2. Campenot, R.B., *Development of sympathetic neurons in compartmentalized cultures: II. Local control of neurite survival by nerve growth factor*. Developmental Biology, 1982. **93**(1): p. 13-21.
3. Campenot, R.B., *Local control of neurite development by nerve growth factor*. Proceedings of the National Academy of Sciences, 1977. **74**(10): p. 4516-4519.
4. Ivins, K.J., E.T.N. Bui, and C.W. Cotman, *β -Amyloid Induces Local Neurite Degeneration in Cultured Hippocampal Neurons: Evidence for Neuritic Apoptosis*. Neurobiology of Disease, 1998. **5**(5): p. 365-378.
5. Klostermann, S. and F. Bonhoeffer, *Investigations of signaling pathways in axon growth and guidance*. Perspectives on developmental neurobiology, 1996. **4**(2-3): p. 237-252.
6. Natera-Naranjo, O., et al., *Identification and quantitative analyses of microRNAs located in the distal axons of sympathetic neurons*. RNA, 2010.
7. Ng, B.K., et al., *Anterograde Transport and Secretion of Brain-Derived Neurotrophic Factor along Sensory Axons Promote Schwann Cell Myelination*. The Journal of Neuroscience, 2007. **27**(28): p. 7597-7603.
8. Bi, J., et al., *Copb1-facilitated axonal transport and translation of κ opioid-receptor mRNA*. Proceedings of the National Academy of Sciences, 2007. **104**(34): p. 13810-13815.

9. Bi, J., et al., *Axonal mRNA transport and localized translational regulation of κ -opioid receptor in primary neurons of dorsal root ganglia*. Proceedings of the National Academy of Sciences, 2006. **103**(52): p. 19919-19924.
10. Taylor, A.M., et al., *A microfluidic culture platform for CNS axonal injury, regeneration and transport*. Nat Methods, 2005. **2**(8): p. 599-605.
11. Pearce, T.M. and J.C. Williams, *Microtechnology: meet neurobiology*. Lab Chip, 2007. **7**(1): p. 30-40.
12. Wang, J., et al., *Microfluidics: a new cosset for neurobiology*. Lab Chip, 2009. **9**(5): p. 644-52.
13. Park, J.W., et al., *Advances in microfluidics-based experimental methods for neuroscience research*. Lab Chip, 2013. **13**(4): p. 509-21.
14. Gross, P.G., et al., *Applications of microfluidics for neuronal studies*. Journal of the neurological sciences, 2007. **252**(2): p. 135-143.
15. Peyrin, J., et al., *MICROFLUIDIC CHIPS WITH "AXON DIODES" FOR DIRECTED AXONAL OUTGROWTH AND RE-CONSTRUCTION OF COMPLEX LIVE NEURAL NETWORKS*.
16. Cui, B., et al., *One at a Time, Live Tracking of NGF Axonal Transport Using Quantum Dots*. Proceedings of the National Academy of Sciences of the United States of America, 2007. **104**(34): p. 13666-13671.
17. Shi, P., et al., *Synapse microarray identification of small molecules that enhance synaptogenesis*. Nature Communications, 2011. **2**: p. 510.

18. Riviuccio, M.A., et al., *HDAC6 Is a Target for Protection and Regeneration following Injury in the Nervous System*. Proceedings of the National Academy of Sciences of the United States of America, 2009. **106**(46): p. 19599-19604.
19. Dworak, B.J. and B.C. Wheeler, *Novel MEA platform with PDMS microtunnels enables the detection of action potential propagation from isolated axons in culture*. Lab on a Chip, 2009. **9**(3): p. 404-410.
20. Kim, Y.-t., et al., *Neuro-optical microfluidic platform to study injury and regeneration of single axons*. Lab on a chip, 2009. **9**(17): p. 2576-2581.
21. Majumdar, D., et al., *Co-culture of neurons and glia in a novel microfluidic platform*. Journal of neuroscience methods, 2011. **196**(1): p. 38-44.
22. Ziegler, L., et al., *Efficient generation of Schwann cells from human embryonic stem cell-derived neurospheres*. Stem Cell Reviews and Reports, 2011. **7**(2): p. 394-403.
23. Park, J., et al., *Microfluidic compartmentalized co-culture platform for CNS axon myelination research*. Biomedical microdevices, 2009. **11**(6): p. 1145-1153.
24. Hosmane, S., et al., *Circular compartmentalized microfluidic platform: Study of axon-glia interactions*. Lab Chip, 2010. **10**(6): p. 741-7.
25. Yang, I.H., et al., *Compartmentalized microfluidic culture platform to study mechanism of paclitaxel-induced axonal degeneration*. Exp Neurol, 2009. **218**(1): p. 124-8.
26. Chung, K. and H. Lu, *Automated high-throughput cell microsurgery on-chip*. Lab on a Chip, 2009. **9**(19): p. 2764-2766.

27. Chokshi, T.V., A. Ben-Yakar, and N. Chronis, *CO2 and compressive immobilization of C. elegans on-chip*. Lab Chip, 2009. **9**(1): p. 151-157.
28. Guo, S.X., et al., *Femtosecond laser nanoaxotomy lab-on-a-chip for in vivo nerve regeneration studies*. Nature methods, 2008. **5**(6): p. 531-533.
29. Hosmane, S., et al., *Valve-based microfluidic compression platform: single axon injury and regrowth*. Lab Chip, 2011. **11**(22): p. 3888-3895.
30. Li, L., et al., *Spatiotemporally Controlled and Multi-Factor Involved Assay of Neuronal Compartment Regeneration after Chemical Injury in an Integrated Microfluidics*. Analytical Chemistry, 2012.
31. Wu, Z., et al., *Caenorhabditis elegans neuronal regeneration is influenced by life stage, ephrin signaling, and synaptic branching*. Proceedings of the National Academy of Sciences, 2007. **104**(38): p. 15132.
32. Chokshi, T.V., D. Bazopoulou, and N. Chronis, *An automated microfluidic platform for calcium imaging of chemosensory neurons in Caenorhabditis elegans*. Lab Chip, 2010. **10**(20): p. 2758-2763.
33. Vogel, A. and V. Venugopalan, *Mechanisms of pulsed laser ablation of biological tissues*. Chemical Reviews, 2003. **103**(2): p. 577-644.
34. Kilinc, D., et al., *Wallerian-Like Degeneration of Central Neurons After Synchronized and Geometrically Registered Mass Axotomy in a Three-Compartmental Microfluidic Chip*. Neurotoxicity research, 2011. **19**(1): p. 149-161.

35. Ellis, E., et al., *A new model for rapid stretch-induced injury of cells in culture: characterization of the model using astrocytes*. Journal of neurotrauma, 1995. **12**(3): p. 325-339.
36. Fouad, K., V. Dietz, and M.E. Schwab, *Improving axonal growth and functional recovery after experimental spinal cord injury by neutralizing myelin associated inhibitors*. Brain research reviews, 2001. **36**(2-3): p. 204-212.
37. Caroni, P. and M.E. Schwab, *Antibody against myelin associated inhibitor of neurite growth neutralizes nonpermissive substrate properties of CNS white matter*. Neuron, 1988. **1**(1): p. 85-96.
38. Smith, D.H., J.A. Wolf, and D.F. Meaney, *A new strategy to produce sustained growth of central nervous system axons: continuous mechanical tension*. Tissue engineering, 2001. **7**(2): p. 131-139.
39. Kim, Y., et al., *Neuro-optical microfluidic platform to study injury and regeneration of single axons*. Lab Chip, 2009. **9**(17): p. 2576-2581.
40. Bhattacharjee, N., et al., *A neuron-benign microfluidic gradient generator for studying the response of mammalian neurons towards axon guidance factors*. Integr. Biol., 2010. **2**(11-12): p. 669-679.
41. Dertinger, S.K.W., et al., *Gradients of substrate-bound laminin orient axonal specification of neurons*. Proceedings of the National Academy of Sciences, 2002. **99**(20): p. 12542.
42. Millet, L.J., et al., *Guiding neuron development with planar surface gradients of substrate cues deposited using microfluidic devices*. Lab Chip, 2010. **10**(12): p. 1525-1535.

43. Riviuccio, M.A., et al., *HDAC6 is a target for protection and regeneration following injury in the nervous system*. Proceedings of the National Academy of Sciences, 2009. **106**(46): p. 19599-19604.
44. Taylor, A.M., et al., *Microfluidic multicompartiment device for neuroscience research*. Langmuir, 2003. **19**(5): p. 1551-1556.
45. Sretavan, D.W., et al., *Microscale surgery on single axons*. Neurosurgery, 2005. **57**(4): p. 635.
46. Mahto, S.K., H. Song, and S.W. Rhee, *Functional synapse formation between compartmentalized cortical neurons cultured inside microfluidic devices*. BioChip Journal, 2011. **5**(4): p. 289-298.
47. Abu-Rub, M., et al., *Spinal cord injury in vitro: modelling axon growth inhibition*. Drug Discov Today, 2010. **15**(11-12): p. 436-43.
48. Song, H.-j., G.-l. Ming, and M.-m. Poo, *cAMP-induced switching in truning direction of nerver growth cones*. Nature, 1997. **388**(6639): p. 5.
49. Park, T.H. and M.L. Shuler, *Integration of Cell Culture and Microfabrication Technology*. Biotechnology Progress, 2003. **19**(2): p. 243-253.
50. Taylor, A., S. Rhee, and N. Jeon, *Microfluidic Chambers for Cell Migration and Neuroscience Research*, in *Microfluidic Techniques*, S. Minteer, Editor. 2006, Humana Press. p. 167-177.
51. Moraes, C., et al., *Organs-on-a-chip: a focus on compartmentalized microdevices*. Ann Biomed Eng, 2012. **40**(6): p. 1211-27.
52. Whitesides, G.M., *The origins and the future of microfluidics*. Nature, 2006. **442**(7101): p. 368-73.

53. Siddique, R. and N. Thakor, *Investigation of nerve injury through microfluidic devices*. J R Soc Interface, 2014. **11**(90): p. 20130676.
54. Manz, A., N. Graber, and H.M. Widmer, *Miniaturized total chemical analysis systems: A novel concept for chemical sensing*. Sensors and Actuators B: Chemical, 1990. **1**(1–6): p. 244-248.
55. Hu, G. and D. Li, *Multiscale phenomena in microfluidics and nanofluidics*. Chemical Engineering Science, 2007. **62**(13): p. 3443-3454.
56. Squires, T.M. and S.R. Quake, *Microfluidics: Fluid physics at the nanoliter scale*. Reviews of Modern Physics, 2005. **77**(3): p. 977-1026.
57. Atencia, J. and D.J. Beebe, *Controlled microfluidic interfaces*. Nature, 2005. **437**(7059): p. 648-55.
58. Takeuchi, A., et al., *Device for co-culture of sympathetic neurons and cardiomyocytes using microfabrication*. Lab Chip, 2011. **11**(13): p. 2268-75.
59. Majumdar, D., et al., *Co-culture of neurons and glia in a novel microfluidic platform*. J Neurosci Methods, 2011. **196**(1): p. 38-44.
60. Gao, Y., et al., *A versatile valve-enabled microfluidic cell co-culture platform and demonstration of its applications to neurobiology and cancer biology*. Biomed Microdevices, 2011. **13**(3): p. 539-48.
61. Hosmane, S., et al., *Valve-based microfluidic compression platform: single axon injury and regrowth*. Lab Chip, 2011. **11**(22): p. 3888-95.
62. Terry, S.C., J.H. Jerman, and J.B. Angell, *A gas chromatographic air analyzer fabricated on a silicon wafer*. Electron Devices, IEEE Transactions on, 1979. **26**(12): p. 1880-1886.

63. McDonald, J.C. and G.M. Whitesides, *Poly(dimethylsiloxane) as a Material for Fabricating Microfluidic Devices*. Accounts of Chemical Research, 2002. **35**(7): p. 491-499.
64. Qin, D., Y. Xia, and G.M. Whitesides, *Soft lithography for micro- and nanoscale patterning*. Nat Protoc, 2010. **5**(3): p. 491-502.
65. Xia, Y. and G.M. Whitesides, *Soft Lithography*. Angewandte Chemie International Edition, 1998. **37**(5): p. 550-575.
66. McDonald, J.C., et al., *Fabrication of microfluidic systems in poly(dimethylsiloxane)*. ELECTROPHORESIS, 2000. **21**(1): p. 27-40.
67. Kim, E., Y. Xia, and G.M. Whitesides, *Micromolding in Capillaries: Applications in Materials Science*. Journal of the American Chemical Society, 1996. **118**(24): p. 5722-5731.
68. Sparreboom, W., A. van den Berg, and J.C.T. Eijkel, *Principles and applications of nanofluidic transport*. Nat Nano, 2009. **4**(11): p. 713-20.
69. Bocquet, L. and E. Charlaix, *Nanofluidics, from bulk to interfaces*. Chem Soc Rev, 2010. **39**(3): p. 1073-95.
70. Napoli, M., J.C. Eijkel, and S. Pennathur, *Nanofluidic technology for biomolecule applications: a critical review*. Lab Chip, 2010. **10**(8): p. 957-85.
71. Schoch, R., J. Han, and P. Renaud, *Transport phenomena in nanofluidics*. Reviews of Modern Physics, 2008. **80**(3): p. 839-883.
72. Sparreboom, W., A. van den Berg, and J.C.T. Eijkel, *Transport in nanofluidic systems: a review of theory and applications*. New Journal of Physics, 2010. **12**(1): p. 015004.

73. Erickson, D., *Towards numerical prototyping of labs-on-chip: modeling for integrated microfluidic devices*. *Microfluidics and Nanofluidics*, 2005. **1**(4): p. 301-318.
74. Koch, M., A. Evans, and A. Brunnschweiler, *Microfluidic technology and applications*. 2000: Research Studies Press Philadelphia, PA, USA.
75. Zhang, J., *Lattice Boltzmann method for microfluidics: models and applications*. *Microfluidics and Nanofluidics*, 2011. **10**(1): p. 1-28.
76. Hlushkou, D., D. Kandhai, and U. Tallarek, *Coupled lattice-Boltzmann and finite-difference simulation of electroosmosis in microfluidic channels*. *International journal for numerical methods in fluids*, 2004. **46**(5): p. 507-532.
77. Sussman, M. and E. Fatemi, *An efficient, interface-preserving level set redistancing algorithm and its application to interfacial incompressible fluid flow*. *SIAM Journal on scientific computing*, 1999. **20**(4): p. 1165-1191.
78. Harnett, C.K., et al., *Model based design of a microfluidic mixer driven by induced charge electroosmosis*. *Lab on a Chip*, 2008. **8**(4): p. 565-572.
79. Tang, G., et al., *Assessment of Joule heating and its effects on electroosmotic flow and electrophoretic transport of solutes in microfluidic channels*. *Electrophoresis*, 2006. **27**(3): p. 628-639.
80. Mengeaud, V., J. Josserand, and H.H. Girault, *Mixing Processes in a Zigzag Microchannel: Finite Element Simulations and Optical Study*. *Analytical Chemistry*, 2002. **74**(16): p. 4279-4286.

81. Li, H., et al., *Characterization and modeling of a microfluidic dielectrophoresis filter for biological species*. *Microelectromechanical Systems, Journal of*, 2005. **14**(1): p. 103-112.
82. Hung, P.J., et al., *A novel high aspect ratio microfluidic design to provide a stable and uniform microenvironment for cell growth in a high throughput mammalian cell culture array*. *Lab Chip*, 2005. **5**(1): p. 44-8.
83. Smith, J.P., et al., *Microfluidic transport in microdevices for rare cell capture*. *Electrophoresis*, 2012. **33**(21): p. 3133-42.
84. Zhang, J., et al., *A finite element method for transient analysis of concurrent large deformation and mass transport in gels*. *Journal of Applied Physics*, 2009. **105**(9): p. 093522.
85. Engle, E.C., *Human genetic disorders of axon guidance*. *Cold Spring Harb Perspect Biol*, 2010. **2**(3): p. a001784.
86. Takayama, Y., et al., *Formation of one-way-structured cultured neuronal networks in microfluidic devices combining with micropatterning techniques*. *J Biosci Bioeng*, 2012. **114**(1): p. 92-5.
87. Mahto, S.K., H.-s. Song, and S.W. Rhee, *Functional synapse formation between compartmentalized cortical neurons cultured inside microfluidic devices*. *BioChip Journal*, 2011. **5**(4): p. 289-298.
88. Pirlo, R.K., et al., *Biochiplaser cell deposition system to assess polarized axonal growth from single neurons and neuroglia pairs in microchannels with novel asymmetrical geometries*. *Biomicrofluidics*, 2011. **5**(1): p. 13408.

89. Peyrin, J.M., et al., *Axon diodes for the reconstruction of oriented neuronal networks in microfluidic chambers*. Lab Chip, 2011. **11**(21): p. 3663-73.
90. Shi, P., et al., *Combined microfluidics/protein patterning platform for pharmacological interrogation of axon pathfinding*. Lab Chip, 2010. **10**(8): p. 1005-10.
91. Millet, L.J., et al., *Guiding neuron development with planar surface gradients of substrate cues deposited using microfluidic devices*. Lab Chip, 2010. **10**(12): p. 1525-35.
92. Kothapalli, C.R., et al., *A high-throughput microfluidic assay to study neurite response to growth factor gradients*. Lab on a Chip, 2011. **11**(3): p. 497-507.
93. Bhattacharjee, N., et al., *A neuron-benign microfluidic gradient generator for studying the response of mammalian neurons towards axon guidance factors*. Integr Biol (Camb), 2010. **2**(11-12): p. 669-79.
94. De Vos, K.J., et al., *Role of axonal transport in neurodegenerative diseases*. Annu Rev Neurosci, 2008. **31**: p. 151-73.
95. Wiersma-Meems, R., J. Van Minnen, and N.I. Syed, *Synapse formation and plasticity: the roles of local protein synthesis*. Neuroscientist, 2005. **11**(3): p. 228-37.
96. Kim, H.J., et al., *Quantitative Analysis of Axonal Transport by Using Compartmentalized and Surface Micropatterned Culture of Neurons*. ACS Chemical Neuroscience, 2012. **3**(6): p. 433-438.
97. Millet, L.J., et al., *Microfluidic devices for culturing primary mammalian neurons at low densities*. Lab Chip, 2007. **7**(8): p. 987-94.

98. Park, J.W., et al., *Novel microfluidic platform for culturing neurons: culturing and biochemical analysis of neuronal components*. Biotechnol J, 2009. **4**(11): p. 1573-7.
99. Shi, P., et al., *Synapse microarray identification of small molecules that enhance synaptogenesis*. Nat Commun, 2011. **2**: p. 510.
100. Taylor, A.M., et al., *Microfluidic local perfusion chambers for the visualization and manipulation of synapses*. Neuron, 2010. **66**(1): p. 57-68.
101. Hengst, U., et al., *Axonal elongation triggered by stimulus-induced local translation of a polarity complex protein*. Nat Cell Biol, 2009. **11**(8): p. 1024-30.
102. Taylor, A.M., et al., *Axonal mRNA in uninjured and regenerating cortical mammalian axons*. J Neurosci, 2009. **29**(15): p. 4697-707.
103. Park, J., et al., *Multi-compartment neuron-glia co-culture platform for localized CNS axon-glia interaction study*. Lab Chip, 2012. **12**(18): p. 3296-304.
104. ELLIS, et al., *A new model for rapid stretch-induced injury of cells in culture: characterization of the model using astrocytes*. 1995, Larchmont, NY, ETATS-UNIS: Liebert.
105. Li, L., et al., *Spatiotemporally controlled and multifactor involved assay of neuronal compartment regeneration after chemical injury in an integrated microfluidics*. Anal Chem, 2012. **84**(15): p. 6444-53.
106. Taylor, A.M., et al., *A microfluidic culture platform for CNS axonal injury, regeneration and transport*. Nat Meth, 2005. **2**(8): p. 7.

107. Hellman, A.N., et al., *Examination of axonal injury and regeneration in micropatterned neuronal culture using pulsed laser microbeam dissection*. Lab Chip, 2010. **10**(16): p. 2083-92.
108. Kim, Y.T., et al., *Neuro-optical microfluidic platform to study injury and regeneration of single axons*. Lab Chip, 2009. **9**(17): p. 2576-81.
109. Klemic, K.G., et al., *Micromolded PDMS planar electrode allows patch clamp electrical recordings from cells*. Biosensors and Bioelectronics, 2002. **17**(6-7): p. 597-604.
110. Ravula, S.K., et al., *A compartmented neuronal culture system in microdevice format*. J Neurosci Methods, 2007. **159**(1): p. 78-85.
111. Peterman, M.C., et al., *The Artificial Synapse Chip: A Flexible Retinal Interface Based on Directed Retinal Cell Growth and Neurotransmitter Stimulation*. Artificial Organs, 2003. **27**(11): p. 975-985.
112. Coleman, M., *Axon degeneration mechanisms: commonality amid diversity*. Nat Rev Neurosci. **6**(11): p. 10.
113. Coleman, M.P. and V.H. Perry, *Axon pathology in neurological disease: a neglected therapeutic target*. Trends in Neurosciences, 2002. **25**(10): p. 532-537.
114. Hosmane, S., et al., *Toll/interleukin-1 receptor domain-containing adapter inducing interferon-beta mediates microglial phagocytosis of degenerating axons*. J Neurosci, 2012. **32**(22): p. 7745-57.
115. Neumann, H., M.R. Kotter, and R.J. Franklin, *Debris clearance by microglia: an essential link between degeneration and regeneration*. Brain, 2009. **132**(Pt 2): p. 288-95.

116. Vallieres, N., et al., *Systemic injections of lipopolysaccharide accelerates myelin phagocytosis during Wallerian degeneration in the injured mouse spinal cord.* *Glia*, 2006. **53**(1): p. 103-13.
117. Medana, I.M. and M.M. Esiri, *Axonal damage: a key predictor of outcome in human CNS diseases.* *Brain*, 2003. **126**(3): p. 515-530.
118. Ivins, K.J., E.T. Bui, and C.W. Cotman, *Beta-amyloid induces local neurite degeneration in cultured hippocampal neurons: evidence for neuritic apoptosis.* *Neurobiol Dis*, 1998. **5**(5): p. 365-78.
119. Taylor, A.M., S.W. Rhee, and N.L. Jeon, *Microfluidic chambers for cell migration and neuroscience research.* *Methods Mol Biol*, 2006. **321**: p. 167-77.
120. Nam, S.W., et al., *N-Methyl-D-aspartate receptor-mediated chemotaxis and Ca(2+) signaling in Tetrahymena pyriformis.* *Protist*, 2009. **160**(2): p. 331-42.
121. Rhee, S.W., et al., *External force-assisted cell positioning inside microfluidic devices.* *Biomed Microdevices*, 2007. **9**(1): p. 15-23.
122. Kordower, J.H., et al., *Neurodegeneration prevented by lentiviral vector delivery of GDNF in primate models of Parkinson's disease.* *Science*, 2000. **290**(5492): p. 767-73.
123. Boucher, T.J., et al., *Potent analgesic effects of GDNF in neuropathic pain states.* *Science*, 2000. **290**(5489): p. 124-7.
124. Meng, X., et al., *Regulation of cell fate decision of undifferentiated spermatogonia by GDNF.* *Science*, 2000. **287**(5457): p. 1489-93.
125. Zhou, R., et al., *KIF26A is an unconventional kinesin and regulates GDNF-Ret signaling in enteric neuronal development.* *Cell*, 2009. **139**(4): p. 802-13.

126. Vrieseling, E. and S. Arber, *Target-induced transcriptional control of dendritic patterning and connectivity in motor neurons by the ETS gene Pea3*. Cell, 2006. **127**(7): p. 1439-52.
127. Zhou, F.Q., J. Zhong, and W.D. Snider, *Extracellular crosstalk: when GDNF meets N-CAM*. Cell, 2003. **113**(7): p. 814-5.
128. Perrier, J.F., et al., *Dedifferentiation of intrinsic response properties of motoneurons in organotypic cultures of the spinal cord of the adult turtle*. Eur J Neurosci, 2000. **12**(7): p. 2397-404.
129. Zurn, A.D., et al., *Combined effects of GDNF, BDNF, and CNTF on motoneuron differentiation in vitro*. J Neurosci Res, 1996. **44**(2): p. 133-41.
130. Mount, H.T., et al., *Glial cell line-derived neurotrophic factor promotes the survival and morphologic differentiation of Purkinje cells*. Proc Natl Acad Sci U S A, 1995. **92**(20): p. 9092-6.
131. Ernsberger, U., *The role of GDNF family ligand signalling in the differentiation of sympathetic and dorsal root ganglion neurons*. Cell Tissue Res, 2008. **333**(3): p. 353-71.
132. Narantuya, D., et al., *Human microglia transplanted in rat focal ischemia brain induce neuroprotection and behavioral improvement*. PLoS One, 2010. **5**(7): p. e11746.
133. Piltonen, M., et al., *Heparin-binding determinants of GDNF reduce its tissue distribution but are beneficial for the protection of nigral dopaminergic neurons*. Exp Neurol, 2009. **219**(2): p. 499-506.

134. Andereggen, L., et al., *Effects of GDNF pretreatment on function and survival of transplanted fetal ventral mesencephalic cells in the 6-OHDA rat model of Parkinson's disease*. Brain Res, 2009. **1276**: p. 39-49.
135. Lee, R.H., et al., *Differential effects of glial cell line-derived neurotrophic factor and neurturin in RET/GFRalpha1-expressing cells*. J Neurosci Res, 2006. **83**(1): p. 80-90.
136. Hoke, A., et al., *Glial cell line-derived neurotrophic factor alters axon schwann cell units and promotes myelination in unmyelinated nerve fibers*. J Neurosci, 2003. **23**(2): p. 561-7.
137. Liu, G.S., et al., *Peripheral gene transfer of glial cell-derived neurotrophic factor ameliorates neuropathic deficits in diabetic rats*. Hum Gene Ther, 2009. **20**(7): p. 715-27.
138. Zhang, L., et al., *GDNF-enhanced axonal regeneration and myelination following spinal cord injury is mediated by primary effects on neurons*. Glia, 2009. **57**(11): p. 1178-91.
139. Yamasaki, R., et al., *Restoration of microglial function by granulocyte-colony stimulating factor in ALS model mice*. J Neuroimmunol, 2010.
140. Guillot, S., et al., *Local GDNF expression mediated by lentiviral vector protects facial nerve motoneurons but not spinal motoneurons in SOD1(G93A) transgenic mice*. Neurobiol Dis, 2004. **16**(1): p. 139-49.
141. Kaspar, B.K., et al., *Retrograde viral delivery of IGF-1 prolongs survival in a mouse ALS model*. Science, 2003. **301**(5634): p. 839-42.

142. Tomac, A., et al., *Retrograde axonal transport of glial cell line-derived neurotrophic factor in the adult nigrostriatal system suggests a trophic role in the adult*. Proc Natl Acad Sci U S A, 1995. **92**(18): p. 8274-8.
143. Lin, L.F., et al., *GDNF: a glial cell line-derived neurotrophic factor for midbrain dopaminergic neurons*. Science, 1993. **260**(5111): p. 1130-2.
144. Evans, J.R. and R.A. Barker, *Neurotrophic factors as a therapeutic target for Parkinson's disease*. Expert Opin Ther Targets, 2008. **12**(4): p. 437-47.
145. Ramaswamy, S., et al., *Neurturin gene therapy improves motor function and prevents death of striatal neurons in a 3-nitropropionic acid rat model of Huntington's disease*. Neurobiol Dis, 2007. **26**(2): p. 375-84.
146. Liu, W.G., et al., *Dopaminergic neuroprotection by neurturin-expressing c17.2 neural stem cells in a rat model of Parkinson's disease*. Parkinsonism Relat Disord, 2007. **13**(2): p. 77-88.
147. Schmutzler, B.S., S. Roy, and C.M. Hingtgen, *Glial cell line-derived neurotrophic factor family ligands enhance capsaicin-stimulated release of calcitonin gene-related peptide from sensory neurons*. Neuroscience, 2009. **161**(1): p. 148-56.
148. Sah, D.W., et al., *New approaches for the treatment of pain: the GDNF family of neurotrophic growth factors*. Curr Top Med Chem, 2005. **5**(6): p. 577-83.
149. Gardell, L.R., et al., *Multiple actions of systemic artemin in experimental neuropathy*. Nat Med, 2003. **9**(11): p. 1383-9.
150. Vyas, A., et al., *An in vitro model of adult mammalian nerve repair*. Exp Neurol, 2010. **223**(1): p. 112-8.

151. Gordon, T., *The role of neurotrophic factors in nerve regeneration*. Neurosurg Focus, 2009. **26**(2): p. E3.
152. Barati, S., et al., *GDNF gene delivery via the p75(NTR) receptor rescues injured motor neurons*. Exp Neurol, 2006. **202**(1): p. 179-88.
153. Lonka-Nevalaita, L., et al., *Characterization of the intracellular localization, processing, and secretion of two glial cell line-derived neurotrophic factor splice isoforms*. J Neurosci, 2010. **30**(34): p. 11403-13.
154. Li, J., et al., *Autocrine regulation of early embryonic development by the artemin-GFRA3 (GDNF family receptor-alpha 3) signaling system in mice*. FEBS Lett, 2009. **583**(15): p. 2479-85.
155. Park, J., et al., *Microfluidic culture platform for neuroscience research*. Nature Protocols, 2006. **1**(4): p. 2128-2136.
156. Taylor, A.M. and N.L. Jeon, *Micro-scale and microfluidic devices for neurobiology*. Current opinion in neurobiology, 2010. **20**(5): p. 640-647.
157. Hosmane, S., et al., *Circular compartmentalized microfluidic platform: Study of axon–glia interactions*. Lab on a Chip, 2010. **10**(6): p. 741-747.
158. Taylor, A., et al., *A microfluidic culture platform for CNS axonal injury, regeneration and transport*. Nature methods, 2005. **2**(8): p. 599-605.
159. Kilinc, D., et al., *Wallerian-Like Degeneration of Central Neurons After Synchronized and Geometrically Registered Mass Axotomy in a Three-Compartmental Microfluidic Chip*. Neurotoxicity Research: p. 1-13.

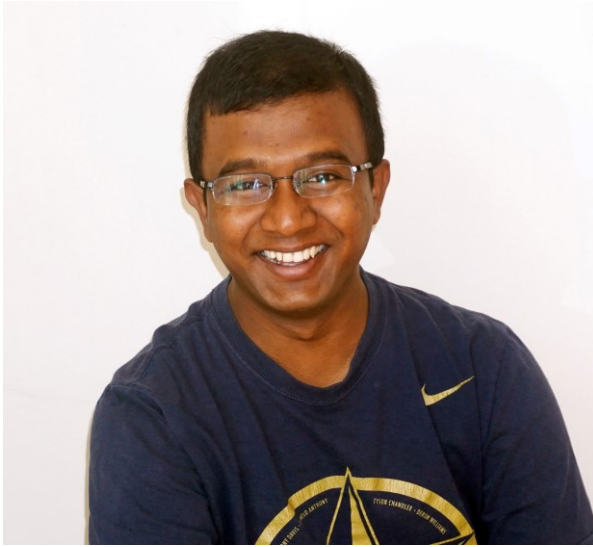
160. Cui, Q., *Actions of neurotrophic factors and their signaling pathways in neuronal survival and axonal regeneration*. Molecular neurobiology, 2006. **33**(2): p. 155-179.
161. Abe, N. and V. Cavalli, *Nerve injury signaling*. Current opinion in neurobiology, 2008. **18**(3): p. 276-283.
162. Ben-Yaakov, K. and M. Fainzilber, *Retrograde Injury Signaling in Lesioned Axons*, in *Cell Biology of the Axon*, E. Koenig, Editor. 2009, Springer Berlin / Heidelberg. p. 327-338.
163. Mills, C., et al., *GDNF selectively promotes regeneration of injury-primed sensory neurons in the lesioned spinal cord*. Molecular and Cellular Neuroscience, 2007. **36**(2): p. 185-194.
164. Höke, A., C. Cheng, and D. Zochodne, *Expression of glial cell line-derived neurotrophic factor family of growth factors in peripheral nerve injury in rats*. Neuroreport, 2000. **11**(8): p. 1651.
165. Tsui, C.C. and B.A. Pierchala, *The Differential Axonal Degradation of Ret Accounts for Cell-Type-Specific Function of Glial Cell Line-Derived Neurotrophic Factor as a Retrograde Survival Factor*. J. Neurosci., 2010. **30**(15): p. 5149-5158.
166. Culpier, M. and C.F. Ibáñez, *Retrograde propagation of GDNF-mediated signals in sympathetic neurons*. Molecular and Cellular Neuroscience, 2004. **27**(2): p. 132-139.
167. Taber, K.H.H., Robin A, *Traumatic Axonal Injury: Atlas of Major Pathways*. The Journal of Neuropsychiatry and Clinical Neurosciences, 2007. **19**(2): p. iv-104.

168. De Stefano, N., et al., *Axonal damage correlates with disability in patients with relapsing-remitting multiple sclerosis. Results of a longitudinal magnetic resonance spectroscopy study*. Brain, 1998. **121**(8): p. 1469-1477.
169. Mattson, M.P., *Pathways towards and away from Alzheimer's disease*. Nature, 2004. **430**(7000): p. 9.
170. Busch, S.A. and J. Silver, *The role of extracellular matrix in CNS regeneration*. Current Opinion in Neurobiology, 2007. **17**(1): p. 120-127.
171. Horn, K.P., et al., *Another barrier to regeneration in the CNS: activated macrophages induce extensive retraction of dystrophic axons through direct physical interactions*. J Neurosci, 2008. **28**(38): p. 9330-41.
172. Johnson, V.E., *Traumatic brain injury and amyloid-[beta] pathology: a link to Alzheimer's disease?* Nature Rev Neuroscience 2010. **11**(5): p. 10.
173. Yung Chia Chen, D.H.S., David F. Meaney, *In-Vitro Approaches for Studying Blast-Induced Traumatic Brain Injury*. J Neurosci, 2009. **26**(6): p. 6.
174. Fouad, K., V. Dietz, and M.E. Schwab, *Improving axonal growth and functional recovery after experimental spinal cord injury by neutralizing myelin associated inhibitors*. Brain Research Reviews, 2001. **36**(2-3): p. 204-212.
175. El-Ali, J., P.K. Sorger, and K.F. Jensen, *Cells on chips*. Nature, 2006. **442**(7101): p. 403-11.
176. Rhee, S.W., et al., *Patterned cell culture inside microfluidic devices*. Lab Chip, 2005. **5**(1): p. 102-7.
177. Gross, P.G., et al., *Applications of microfluidics for neuronal studies*. J Neurol Sci, 2007. **252**(2): p. 135-43.

178. Blake, A.J., et al., *Multilayer PDMS microfluidic chamber for controlling brain slice microenvironment*. Lab Chip, 2007. **7**(7): p. 842-9.
179. Campenot, R.B., *Local control of neurite development by nerve growth factor*. Proc Natl Acad Sci U S A, 1977. **74**(10): p. 4516-9.
180. Chung, B.G., et al., *Human neural stem cell growth and differentiation in a gradient-generating microfluidic device*. Lab Chip, 2005. **5**(4): p. 401-6.
181. Nichol, J.W., et al., *Cell-laden microengineered gelatin methacrylate hydrogels*. Biomaterials, 2010. **31**(21): p. 5536-5544.
182. Du, Y., et al., *Rapid generation of spatially and temporally controllable long-range concentration gradients in a microfluidic device*. Lab on a Chip, 2009. **9**(6): p. 761-767.
183. Banker, G. and K. Goslin, *Culturing nerve cells*. 1998: MIT press.
184. Galbraith, J.A., L.E. Thibault, and D.R. Matteson, *Mechanical and Electrical Responses of the Squid Giant Axon to Simple Elongation*. Journal of Biomechanical Engineering, 1993. **115**(1): p. 13-22.
185. Fournier, A.J., et al., *In vitro and in situ visualization of cytoskeletal deformation under load: traumatic axonal injury*. FASEB J, 2014.
186. Höke, A., *A (heat) shock to the system promotes peripheral nerve regeneration*. Journal of Clinical Investigation, 2011. **121**(11): p. 4231-4.
187. Fan, Y., et al., *Single neuron capture and axonal development in three-dimensional microscale hydrogels*. Lab on a chip, 2012. **12**(22): p. 4724-4731.
188. Deng, L.-X., et al., *A novel growth-promoting pathway formed by GDNF-overexpressing Schwann cells promotes propriospinal axonal regeneration*,

- synapse formation, and partial recovery of function after spinal cord injury*. The Journal of Neuroscience, 2013. **33**(13): p. 5655-5667.
189. Marconi, S., et al., *Human adipose-derived mesenchymal stem cells systemically injected promote peripheral nerve regeneration in the mouse model of sciatic crush*. Tissue Engineering Part A, 2012. **18**(11-12): p. 1264-1272.
190. Wang, J.T., Z.A. Medress, and B.A. Barres, *Axon degeneration: molecular mechanisms of a self-destruction pathway*. The Journal of cell biology, 2012. **196**(1): p. 7-18.
191. Bradke, F., J.W. Fawcett, and M.E. Spira, *Assembly of a new growth cone after axotomy: the precursor to axon regeneration*. Nature Reviews Neuroscience, 2012. **13**(3): p. 183-193.
192. Johnson, V.E., W. Stewart, and D.H. Smith, *Axonal pathology in traumatic brain injury*. Experimental neurology, 2013. **246**: p. 35-43.

Vita



Bhaskar earned his B.Tech. in Biotechnology from the Indian Institute of Technology (IIT), Guwahat, in 2011 where his bachelors' thesis was focused on membrane biophysics. He earned the prestigious Institute's Silver Medal for his outstanding academic performance as the topper from the Department of Biotehnology. In 2011, Bhaskar entered the M.S.E. program in the department of Biomedical Engineering at Johns Hopkins University (JHU). At Hopkins, Bhaskar's research was focused on microfluidic platforms for neuroscience and neuroengineering. During his tenure as a M.S.E. student, Bhaskar has authored one review article, co-authored one research article. He received full scholarship for his M.S.E. at Hopkins.